Identification of leaf rust susceptibility genes in wheat

by

Joseph Fenoglio

B.S., Kansas State University, 2016

A THESIS

submitted in partial fulfillment of the requirements for the degree

MASTER OF SCIENCE

Department of Plant Pathology
College of Agriculture

KANSAS STATE UNIVERSITY
Manhattan, Kansas

2022

Approved by:

Co-Major Professor
David Cook

Approved by:

Co-Major Professor
John Fellers

Copyright

Abstract

Leaf Rust, caused by *Puccinia triticina,* is a major disease of wheat. Leaf rust has proven to be a resilient pathogen, overcoming resistance genes multiple times. Plants have factors, known as susceptibility genes, that facilitate the ability of pathogens to cause disease. Altering susceptibility genes may provide a more durable defense against infection than resistance genes but have yet to be identified for susceptibility to leaf rust in wheat. By characterizing random mutants created through chemical mutagenesis, mechanisms determining wheat susceptibility to leaf rust can be determined. The susceptible wheat variety Thatcher was mutagenized using ethyl methanesulfonate (EMS). Surviving plants were scored for a reduction in pustule size or quantity when challenged with leaf rust. From these plants, three mutant lines (1995, 2048, and 2348) have been obtained. Mutant lines 1995 and 2048 exhibit a constitutive hypersensitive-like response (HR-like). Mutant line 2348 exhibits no evidence of a HR.

Microscopic analysis of the initial 5 days of the infection process revealed the ability of *P. triticina* to form appressoria, early colonization, and pustule development was altered in 1995 and 2048. In 2348, *P. triticina* was less able to progress beyond appressoria formation and intercellular hyphae than in Thatcher. Bulked segregant RNAseq analysis of $F_{2:3}$ pools of tissue originating from a backcross to the wild type parent revealed an induction of the plant defense response in 1995 and 2048. Genotypic studies were conducted to identify regions that may contain the causative mutation. A F_4 mapping population was generated by crossing each mutant line with the hard red winter wheat variety KS061705M11 and utilizing single seed descent. Association mapping identified SNPs within each population that associated with the mutant phenotype. Confidence intervals surrounding each identified SNP were created through haplotype blocking. A second genotyping method, exome capture, identified SNPs in M_8 lines for each mutant. Using the confidence intervals from association mapping, the list of SNPs from exome capture was narrowed. Mutant line 1995 mapped to a 3.89Mb window on 2D, a 7Mb window on 3A, and a 4.85Mb window on 4B. Mutant line 2048 mapped to a 3.89Mb window on 3B and a 4.52Mb window on 4B. These intervals narrow the region of interest for future fine mapping studies that seek to identify the causative mutation.

Table of Contents

List of Figures

List of Tables

Chapter 1 - Identification of leaf rust susceptibility genes in wheat

Introduction

The fungal disease leaf rust, also known as brown rust, is an important pathogen of bread wheat (*Triticum aestivum* L.), rye, barley, and other grass species around the world (Bolton et al., 2008). Leaf rust is caused by *Puccinia triticina* Eriks. It is more prevalent, and widespread than the other two major rusts of wheat, stem rust and stripe rust (Bolton et al., 2008; Kolmer, 1996). When not controlled leaf rust can cause up to 20% losses over a large area, but can be much more severe if infection occurs prior to heading (Bolton et al., 2008; Kolmer, 2020).

When urediniospores land on a host, come into contact with water, and the temperature is optimal (15-20ºC), germination occurs. The germ tube grows thigmotropically towards a stoma. When it reaches a stoma an appressoria is formed, which immediately produces a penetration peg, and substomatal vesical (Roelfs et al., 1992). After penetration into the host, an infection hypha proliferates and a haustorial mother cell (HMC) is formed. From the HMC, a hyphal tip finds a mesophyll cell. The hyphal tip forms a septum at the site of penetration, then penetrates the host cell wall, and invaginates the host cell membrane while differentiating into a haustorium (Allen, 1926; Bolton et al., 2008; Roelfs et al., 1992). The space between the haustorium and the membrane, is known as the extrahaustorial membrane. The haustoria is the primary site of host-pathogen interactions for *P. triticina.* Haustoria are responsible for the uptake of nutrients from the host and the secretion of pathogenicity factors known as effectors (Garnica et al., 2014; Kemen et al., 2005; Petre et al., 2015; Rafiqi et al., 2010; Szabo & Bushnell, 2001). After the first haustorium is established, secondary hyphae are formed from the haustoria mother cell. Secondary hyphae colonize the intercellular space and go on to infect new adjacent cells, form new HMCs and haustoria. As *P. triticina* ages, intercellular hyphae differentiate into uredinia. (Bolton et al., 2008; Garnica et al., 2014; Szabo & Bushnell, 2001).

Uredinia develop and produce dikaryotic urediniospores, which are blown by the wind to infect new plants. *P. triticina* is heteroecious with two hosts within a sexual life cycle (Bolton et al., 2008; Roelfs et al., 1992). Uredinia develop into telia. Telia produce dikaryotic haploid teliospores that are thick walled and allow for the rust to survive during summers. During telia maturation teliospores undergo karyogamy and form a diploid nucleus (Bolton et al., 2008). When conditions are optimal the diploid teliospores undergo meiosis and mature into four haploid basidiospores, these basidiospores then form single cell basidiospores with two haploid nuclei. Mature basidiospores are blown into contact with the sexual (aecial) stage host (Bolton et al., 2008; Roelfs et al., 1992). The alternate host is meadow rue (*Thalictrum speciosissimum*), however the sexual stage is rarely seen in North America due to the absence of meadow rue in the United States (Levine and Hildreth, 1957). In Europe the sexual stage can be found on *T. speciosissimum* (Casulli and Siniscalco, 1987) and *Isopyrum fumaroides* in Siberia (Chester, 1946). The fall sown wheat in the southern United States and Mexico functions as a winter reservoir for *P. triticina*, providing the initial inoculum load for winter wheat (Roelfs et al., 1992). This makes leaf rust a continuous problem (Wegulo & Byamukama, 2012), and due to the constant threat, leaf rust control is extremely important.

The plant immune system provides protection against pathogens. There are two main branches of the plant immune system, pattern triggered immunity (PTI) and effector triggered immunity (ETI) (Jones & Dangl, 2006). Generally, PTI recognizes pathogen associated molecular patterns (PAMPs) and can be broken down further into two classes; PAMPs directly associated with the presence of a pathogen, and are often highly conserved such as chitin or flagellin (Chinchilla et al., 2006; Miya et al., 2007) and those associated with cellular damage caused by pathogen infection (Chassot et al., 2007; Yamaguchi et al., 2010). These PAMPs are recognized by pattern recognition receptors (PRRs) made up of several classes of receptor-like kinases (RLKs) and receptor-like proteins (RLPs). RLKs and RLPs localize to the cell wall surface (Chinchilla et al., 2006; Sun et al., 2013; Yamaguchi et al., 2006). When PRRs recognize PAMPs a defense response is elicited. The characteristics of a PTI defense response are a burst of reactive oxygen species (ROS), influx of Ca^{2+}, production of salicylic acid (SA), callose deposition, activation of mitogen-activated protein kinases (MAPKs), and accumulation of defense proteins (Wang et al., 2019). To bypass PTI, pathogens have developed ways to prevent host recognition and signaling of defense (Zhao et al., 2020).

One way that pathogens bypass host PTI is through the use of effectors, proteins secreted by the pathogen for the purpose of promoting virulence. To avoid host detection, pathogens change, modify, or lose effectors recognized by host receptors. Effector triggered immunity (ETI) recognizes effectors and elicits defense responses (Jones & Dangl, 2006). ETI and PTI defense responses have commonalities. Both branches result in a ROS burst, Ca^{2+} influx, increased SA biosynthesis, MAPK signaling cascade, and increased defense protein expression. However, in general, ETI is elicited more rapidly, and with greater intensity than PTI (Chandra et al., 1996; Draper, 1997; Grant et al., 2000; Su et al., 2018). Hypersensitive response (HR) results in plant cell death at the pathogen infection site (Dietrich et al., 1994; Greenberg et al., 1994). ETI induction occurs when effectors are recognized by host receptors. The most common receptors in ETI are nucleotide binding site-leucine rich repeats (NBS-LRRs) with a coiled-coil binding domain (Shao et al., 2016).

NBS-LRR recognition of effectors follows the gene-for-gene model (Meyers et al., 2005; Shao et al., 2016) based on the initial observations of *Melampsora lini* virulence on flax (*Linum usitatissimum*). It was observed that the capability of *M. lini* to cause disease is determined by two genes. The avirulence (*Avr*) gene in the pathogen, and the resistance (*R*)-gene in the plant (Flor, 1947). The gene-for-gene model can be summarized as follow. When the plant has an *R*-gene and the pathogen has the complimentary *Avr* plant resistance occurs. When the either the *R*-gene or complimentary *Avr* gene is absent pathogens go undetected, and disease occurs. (Flor, 1947).

Breeding programs are constantly searching for broad-spectrum durable resistance. Currently, single *R*-gene based resistance is the primary control method used for leaf rust, but is not broad-spectrum. Due to their gene-for-gene interaction *R*-genes only provide resistance to races of leaf rust that have the complimentary avirulence (*Avr*) gene. *Lr1, Lr10,* and *Lr17* (Feuillet et al., 2003; Ling et al., 2003; Qiu et al., 2007) are examples of genes identified to grant qualitative, race-specific (gene-for-gene) resistance to leaf rust. NBS-LRR resistance, puts high selection pressure on the leaf rust population. Once considered reliable sources of resistance, *Lr9, Lr25* (Huerta-Espino et al., 2008), *Lr14a* (Soleiman et al., 2016), *Lr19* (Bhardwaj et al., 2005; Huerta-Espino & Singh, 1994), and *Lr21* (Kolmer & Anderson, 2011) have been rendered ineffective due to the proliferation of new, virulent races.

The application of selection pressure on leaf rust and rapid selection for the development of new virulent races by heavy use of *R*-gene based resistance, has complicated the control of wheat leaf rust. Pyramiding of major *R*-genes could provide a durable resistance in other rusts (Green & Campbell, 1979; McIntosh & Brown, 1997; Samborski, 1985; Schafer & Roelfs, 1985). The probability of simultaneous mutations that overcome all of the *R*-genes becomes exponential when enough undefeated *R*-genes are deployed. *R*-gene pyramids can be durable, but their development is time consuming and when deployed in insufficient numbers, or with previously defeated *R*-genes their durability is compromised (Bernardo et al., 2013). Fortunately, there may be alternatives to using major *R*-gene resistance for durable prevention of leaf rust infection.

A second class of resistance genes, adult plant resistance (APR) genes, are available for use in wheat. The APR genes *Lr34/Sr57* and *Lr67/Sr55* provide inspiration for the idea that leaf rust control can be granted by resistance genes that do not use NBS-LRR based resistance. APR genes differ from NBS-LRR in that they only grant resistance in the adult plant and are broad spectrum. Additionally, both *Lr34/Sr57* and *Lr67/Sr55* provide leaf rust resistance, as well as stripe rust (*P. striiformis* f.sp. *tritici, Pst*) resistance (Krattinger et al., 2009; Moore et al., 2015). Rather than encoding an NBS-LRR, *Lr34* has been found to encode an ATP-binding cassette (ABC) transporter (Krattinger et al., 2009). *Lr34/Sr57* has a "slow rusting" phenotype, meaning it takes longer for leaf rust to colonize. *Lr34/Sr57* lines also have leaf tip necrosis observed in the flag leaves (Huerta-Espino et al., 2020). *Lr67/Sr55* encodes a hexose transporter mutant variant (Moore et al., 2015), and will be discussed in more detail later in this review. Both of these genes have yet to lose efficacy, suggestting stable race non-specific resistance is possible

The plant immune system is an intricate and dynamic web of recognition and defense signaling that protects the plant from disease. From leaf rust's narrow host range, it can be inferred the pathogen must utilize some host factors to successfully colonize a host. After the infection occurs, the battle between host and pathogen still rages. The pathogen must avoid recognition within the host and be able to successfully utilize host factors to facilitate survival and replication. If the pathogen can avoid detection or successfully modulate defense responses in their favor, the pathogen will be able to feed. By hijacking host metabolic mechanisms fungi can take up nutrients. The pathogens need of host factors brings up an interesting line of thought.

What if these host factors can be altered or deleted so that the pathogen cannot utilize them to survive? This method of preventing disease has been described as a loss of susceptibility, and these host factors are called susceptibility genes (S-genes). Plant S-genes allow for the successful infection by pathogens. Susceptibility genes for leaf rust have not yet been identified in wheat. This review will be discussing S-genes in other systems, to drawn insight on how loss of susceptibility can be exploited in wheat to protect from leaf rust.

Susceptibility

Recent investigations into S-genes have shown that the ability of a pathogen to cause disease is dependent upon the presence of S-genes within the host. Furthermore, when S-genes are knocked out, or altered so that they are unable to be exploited by the pathogen, disease development is reduced, and in some cases prevented. It would seem disadvantageous for a host to retain S-genes that allow pathogens to cause disease, and that plants without them would have been selected for. The proteins encoded by S-genes often have important roles within the host (i.e., glucose transport, negative defense regulation), and altering them can have negative pleiotropic effects. Thus, S-gene efficacy and utility must be evaluated on a case-by-case basis.

Prepenetration S-genes

Perhaps the best known and well-studied S-genes is the *Mildew resistance locus o* (*Mlo*). When *Mlo* is inactivated, either through natural or artificial means, the plant has reduced susceptibility to the powdery mildew (*Blumeria graminis* f. sp *hordei*). Originally identified in barley in the 1930s, *mlo*-based resistance has been found in a wide variety of plants (Kusch & Panstruga, 2017). The *Mlo* gene was isolated and cloned in 1997 (Büschges et al., 1997). *mlo*-based resistance is pertinent to this review because of the obligate biotrophic lifestyle shared by powdery mildew and leaf rust. By searching for a gene that disrupts the interaction between leaf rust and wheat, in a manner similar to how *mlo* disrupts the powder mildew-host interaction, durable protection may be granted.

What is most interesting about *mlo*-based resistance is the non-R-gene mediated, and race non-specific nature of *mlo.* Additionally, *mlo* has been used in European barley for nearly 50 years without losing efficacy (Ge et al., 2020). Susceptibility mutants often have a degree of

negative pleiotropic effects. Usually these are explained by the fact that the susceptibility gene has a role in plant physiology that has been impaired. Early leaf senescence, and increased susceptibility to some nonbiotrophic pathogens are two examples of negative pleiotropic effects due to *mlo* (Ge et al., 2020). Despite the negative effects of *mlo,* other characteristics of *mlo* has made it of particular interest in the study of S-genes.

Resistance granted by *mlo* is classified as prepenetration resistance. Powdery mildew growth is arrested prior to the development of haustoria (Skou, 1982). In barley *mlo* mutants there are a higher number of cell wall appositions, with greater diameter, containing callose at sites of infection (Skou, 1982). This is similar to the response of barley to nonhost pathogens (Douchkov et al., 2016; Kusch & Panstruga, 2017). Additionally, *mlo*-Barley has an increased accumulation of ROS, and faster and increased transcription rates of defense-related proteins, without the presence of a HR (Ge et al., 2020; Piffanelli et al., 2002; Zierold et al., 2005), indicators of a PTI-based defense response.

Defense regulatory S-genes

One recently identified rust susceptibility genes in wheat is *TaBCAT$_1$* (Corredor-Moreno et al., 2021). The presence of a functional *TaBCAT$_1$* renders wheat susceptible to infection by *Pst* and *Puccinia graminis* F.sp. *tritici* (Stem Rust, *Pgt*). Mutants with a disruption of *TaBCAT$_1$* have constitutively increased levels of salicylic acid (SA) leading to a "primed" defense response which reduces susceptibility to disease by preconditioning plants to respond more rapidly to infection (Corredor-Moreno et al., 2021; H. W. Jung et al., 2009). The proper regulation of SA biosynthesis is critical to the appropriate signaling of a defense response. Biosynthesis of SA is involved in a feedback loop that induces the expression of pathogenesis-related (PR) genes, as well as further increasing SA levels (Yalpani et al., 1991) Higher levels of SA early in the infection process thus correspond with a reduction in disease susceptibility (Rahman et al., 2014). *TaBCAT$_1$* is a known branched-chain amino acid aminotransferase and likely functions in branched chain amino acid metabolism (BCAAs). By disrupting *TaBCAT$_1$*, levels of BCAAs and SA accumulate. The necessity of a functional *TaBCAT$_1$* in the plant, for yellow and stem rust to cause disease, underlies the point that *TaBCAT$_1$* is an S-gene.

The genes *TaEIL1* and *TaRac6* have been shown to be positive regulators of susceptibility in wheat-*Pst* interactions (Duan et al., 2013; Zhang et al., 2020). *TaEIL1* codes for a protein with an ETHYLENE INSENSITIVE3 (EIN3) binding domain. EIN3 is implicated in plant defense to pathogen infection, specifically the crosstalk between SA, methyl-jasmonic acid (Me-JA) and ethylene (Eth). When *TaEIL1* was knocked out, *Pst* infection was decreased and the expression of SA and hypersensitive response proteins was increased (Duan et al., 2013). As mentioned above the presence of SA early in the pathogen infection process reduces susceptibility. The need for a functional *TaEIL1* for *Pst* to successfully colonize the host shows that it is a susceptibility gene.

TaRac6 is a wheat small G protein gene recently identified as a *Pst* susceptibility gene (Zhang et al., 2020). *Pst* infection induced transcript accumulation of *TaRac6* was higher in compatible interactions than in non-compatible interactions. The study further states that by silencing *TaRac6,* susceptibility can be lost and *Pst* produces fewer uredinia (Zhang et al., 2020). Reduced growth is attributed to an increase in H_20_2 production, suggesting that *TaRac6* is involved with the negative regulation of H_20_2. Additionally, when expressed in *Nicotiana benthamiana, TaRac6* was shown to inhibit Bax-induced plant cell death. The study reports that *TaRac6* encodes a protein almost identical to HvRacB and OsRac6. Both of which are termed susceptibility proteins and negative regulators of the defense response in their respective system (Zhang et al., 2020). If, in the wheat-*P. triticina* system, a negative regulator of H_20_2 production can be identified and taken advantage of, then protection can potentially be granted.

Post-penetration

After a pathogen successfully colonizes, and manipulates the host defense mechanism, the pathogen must feed. In the case of *P. triticina,* being an obligate biotroph, it can only feed on susceptible living hosts. To do this, feeding structures must be formed (Garnica et al., 2014). The complexity of host metabolism, and the development of feeding structures offer several potential target sites for disrupting the host-pathogen interactions, known as post-penetration susceptibility factors (van Schie & Takken, 2014).

One major type of metabolic post-penetration susceptibility genes are those involved with sugar transport. By manipulating sugar transporters pathogens are able to improve their access to

nutrients (Huai et al., 2019). Some of the most well studied sugar transport susceptibility genes are those in the SWEET family. The rice *OsSWEET11, OsSWEET13,* and *OsSWEET14* genes have been shown to be bacterial hemibiotroph *Xanthamonas oryzae* pv. *oryzae* (*Xoo*) susceptibility genes (Zhou et al., 2015), and are targets of transcription activator like effectors (TALEs). When the host is infected, SWEET gene expression is increased and renders the plant susceptible to infection by *Xoo* (Cox et al., 2017; Zhou et al., 2015). In a genome wide search for SWEETs in wheat, using OsSWEET and Arabidopsis SWEET (AtSWEET) sequences, 59 wheat SWEET (TaSWEET) genes were identified (Gao et al., 2018). Within this group, 5 TaSWEETs were shown to have increased expression when exposed to *Pgt* (Gao et al., 2018), but have not been shown to be targets of any *Pgt* effectors. Additionally, TALEs like those in bacteria, have yet to be identified in fungi. However, the hemibiotrophic life styles of *Xanthamonas spp.* (Maeda et al., 2016) and biotrophic lifestyle of *Puccinia spp.* both insinuate the need to modulate the host metabolism in order to acquire nutrients. Thus, the upregulation of TaSWEETs in wheat when exposed to *Pgt*, which is similar to what has been observed in the Rice-*Xoo* interaction, may hint at the need for SWEET genes for leaf rust susceptibility.

SWEET genes aren't the only sugar transporters that have been identified as susceptibility genes for rusts. The genes *TaSTP6* and *TaSTP13* both contribute to wheat susceptibility to *Pst* (Huai et al., 2019, 2020). One study by Huai et al. (2019) found that in wheat, *TaSTP6* is upregulated when infected by *Pst*, and when wheat and *TaSTP6* transgenic *Arabidopsis* were treated with abscisic acid (ABA). By knocking down *TaSTP6* expression wheat *Pst* resistance was increased. Interestingly, transgenic *Arabidopsis* lines susceptibility to powdery mildew (PM) increased (Huai et al., 2019). Additionally, there was increased accumulation of glucose in the transgenic Arabidopsis lines, indicating a role in glucose transport. By analyzing the transient expression of *TaSTP6* in *Nicotiana benthamiana* leaves and wheat protoplasts, it was revealed that TaSTP6 is localized to the plasma membrane (Huai et al., 2019). *TaSTP6* was then expressed in *Saccharomyces cerevisiae* to further elucidate the function of TaSTP6 as a hexose/H^+ symporter. With the data supporting the role of TaSTP6 as a sugar transporter, the induction of TaSTP6 expression during *Pst* and ABA exposure, and reduced susceptibility to *Pst* when TaSTP6 is knocked down, the authors propose that TaSTP6 is a susceptibility gene with a role in supplying sugar into haustoria invaded cells. (Huai et al., 2019).

TaSTP13 was shown to be transporter of several different monosaccharides and is localized in the plasma membrane (Huai et al., 2020). Plants infected with *Pst* had higher levels of *TaSTP13* expression in their leaves. When *TaSTP13* expression was suppressed, there was lower levels of *Pst* infection. This shows that *TaSTP13* increases wheat *Pst* susceptibility (Huai et al., 2020). What is even more interesting is the relationship between *TaSTP13* and the leaf rust resistance gene *Lr67.* As discussed, earlier *Lr67* is an APR wheat leaf rust resistance gene. Lr67 lines with *Lr67* exhibit a slow rusting phenotype, with pleiotropic leaf tip necrosis. *Lr67* is a natural mutant of *TaSTP13* and although there is the undesirable leaf tip necrosis, *Lr67* provides a partial resistance to several haustoria forming biotrophs such as leaf rust, stripe rust, stem rust, and powdery mildew. So, it shows that there is a natural case of an altered *TaSTP13* reducing susceptibility to leaf rust (Huai et al., 2020).

Conclusion

The molecular interactions between leaf rust and wheat determining host susceptibility are just beginning to be understood. Currently there are no known leaf rust susceptibility genes in wheat, but there are at least two *Lr* genes (*Lr34* and *Lr67*) with similarities to susceptibility genes. These genes provide inspiration for future studies that aim to identify susceptibility genes to *P. triticina* in wheat. As discussed previously genes involved in structural defense, defense response and immune system regulation, and sugar transport are just a few examples of the plethora of potential susceptibility genes.

S-genes have proven to be difficult to identify, especially those that reduce susceptibility to obligate biotrophs. Often, when new R-genes are needed researchers search for them in wild populations and close relatives of agricultural plants, such as *Aegilops spp.* (Olivera et al., 2018). For S-genes this is unlikely to be a viable option. S-genes are often the result of a loss of function mutation in normal plant physiology. However, *mlo* and *Lr67* do provide a counter argument to this point as they were found to both be naturally occurring (Moore et al., 2015; Piffanelli et al., 2002). Regardless, the identification of novel S-genes granting disease protection has proven difficult. The development of reliable methodology to identify S-genes is critical to their successful deployment.

One tool that has shown useful in the development and identification of susceptibility genes has been the use of random mutagenesis, more specifically, a TILLING approach. Target Induced Local Lesions In Genomes (TILLING) is a reverse genetics approach towards identification of novel genes of interest through high throughput mutation discovery in target genes (McCallum et al., 2000). By taking a similar initial approach to induce random mutations across the wheat genome and selecting for reduced disease development, it may be possible to induce and identify mutations that would not normally be selected for in nature that grant reduced susceptibility to *P. triticina.*

The genetics of R-genes and S-genes make an approach using ethyl methanesulfonate (EMS) of particular interest. Ethyl methanesulfonate induces random mutations with a preference for guanine to adenine conversions. These random mutations can cause gain or loss of function. Random mutations that result in a gain of function are less likely to occur than loss of function mutations. As seen in *mlo,* S-genes mutants granting disease reduction are commonly due to loss of function mutations.

Leaf rust susceptibility in wheat is dependent upon susceptibility genes. By treating wheat seeds from the susceptible line Thatcher with EMS, a S-gene that determines the capability of *P. triticina* to cause infection in wheat can be mutated, resulting in a loss of susceptibility. Three mutant lines, 1995, 2048, and 2348, were generated through EMS mutagenesis. The objectives of this study were to (1) characterize the mutant line phenotype; (2) genetically map EMS induced SNPs to candidate genome regions in each mutant; (3) reduce quantity and size of candidate regions through comparative analysis and provide a SNP list for future fine mapping studies.

Chapter 2 - Characterization of mutant phenotype through RNAseq analysis and cytology

Introduction

The origins of wheat (*Triticum aestivum*) date back 8000-10,000 years to Southeastern Turkey, Northern Syria, Northern Iraq, and Western Iran. It was in this region that the domestication of Emmer wheat (*Triticum turgidum*) occurred (Luo et al., 2007; Ozkan et al., 2002) as a result of a natural hybridization event between *T. urartu* and an unknown lineage of *Aegilops speltoides* (Huang et al., 2002; Petersen et al., 2006). As humans migrated, and agriculture spread, *T. turgidum* naturally hybridized with *Aegilops tauschii* (Huang et al., 2002; Kihara, 1944; Mcfadden & Sears, 1946) and birthed *T. aestivum*.

Since the initial development in the Fertile Crescent, wheat has become an important food source for many peoples across the world. Worldwide, wheat is considered a staple crop for nearly 35% of the population, and occupies nearly 17% of all cultivated land (IDRC, 2010). Additionally, the Food and Agriculture Organization (FAO) of the United Nations predicts both global production and utilization will top 850 million tonnes in 2022 (FAO, 2022), an increase of nearly 100 million metric tonnes from 2021. According to the USDA, wheat is an economically important crop in the United States, which is the third largest exporter in terms of global total production. In the U.S., wheat is third in planted acreage and production behind corn and soybeans (USDA ERS, 2022). The national and global importance of wheat, both economically and as a food source, indicates the need to prevent yield losses.

One significant cause of wheat yield loss is disease, especially those caused by the rust fungi *Puccinia graminis* f.sp. *tritici* (*Pgt*), *P. striiformis* f.sp. *tritici* (*Pst*), and *P. triticina* Eriks (*Pt*) (Roelfs et al., 1992). Leaf rust, caused by *P. triticina*, can cause up to 20% losses over large areas when uncontrolled and is more globally widespread than *Pgt* and *Pst* (Bolton et al., 2008; Kolmer, 2020). One method of protecting wheat from leaf rust is to breed for and deploy major

resistance (*R*)-genes. Major *R*-genes recognize effectors that are secreted by the pathogen to facilitate disease. Major *R*-genes code for nucleotide binding site-leucine rich repeats (NBS-LRRs; Meyers et al., 2005; Shao et al., 2016). When major *R*-genes recognize effectors, a strong defense response is elicited known as the hypersensitive response (HR)(Dietrich et al., 1994; Greenberg et al., 1994). When major *R*-genes cannot recognize effectors, disease occurs. This *R*-gene-effector interaction is highly specific and follows a gene for gene model (Flor, 1947). To protect wheat from leaf rust in this manner, constant identification and introgression of new *R*-genes is necessary, due to their selective nature for the most virulent members of a pathogen population. An alternative to the use of major *R*-genes is slow rusting adult plant resistance (APR) genes. APR genes, only confer resistance to rusts at the adult stage of the plant, and their defense response tends to be less intense. However, the protection that is granted is more durable. Some durable APR genes of note are *Lr34*, *Lr67*, *Sr2,* and *Yr36* (Fu et al., 2009; Huerta-Espino et al., 2020; Krattinger et al., 2009; Mcintosh et al., 1995).

Lr34 encodes an ATP-binding cassette (ABC)-hexose transporter variant (Krattinger et al., 2009), and grants the "slow rusting" phenotype (Huerta-Espino et al., 2020). *Lr67* encodes a hexose transporter mutant variant (Moore et al., 2015). *Lr34* and *Lr67* both prevent leaf rust from establishing successful interactions. *Lr34* expression in barley, resulted in the constitutive expression of defense pathways (Chauhan et al., 2015), pathogenesis related (PR) proteins, salicylic acid (SA), and secondary metabolites (Chauhan et al., 2015). *Lr67* also has increased expression of PR proteins when expressed in barley (Milne et al., 2019). Unfortunately, leaf tip necrosis can be associated with *Lr34* and *Lr67* (Chauhan et al., 2015; Milne et al., 2019).

Reduction of susceptibility to disease is another and relies upon the prevention of the pathogen from utilizing host factors that are normally required to facilitate disease. For example, the recently discovered wheat rust susceptibility gene, $TaBCAT_{1,}$ is required for infection by stem rust and stripe rust. $TaBCAT_1$ has been shown to be crucial to the proper activation of SA-dependent systemic acquired response (SAR) (Corredor-Moreno et al., 2021). Wheat mutants with a disruption of $TaBCAT_1$ have constitutively increased levels of SA leading to a "primed" defense response. By disrupting $TaBCAT_{1,}$ levels of branched chain amino acids (BCAAs) accumulate and levels of SA, and SA-dependent defense responses increase. The increase accumulation of BCAAs and SA in the knockout mutants correlates with a reduction in stem and

stripe rust colonization (Corredor-Moreno et al., 2021). This provides evidence for the presence of alternatives to traditional *R*-gene based resistance, and the possibility of identifying more genes that modulate leaf rust susceptibility in wheat.

The plant immune system is a network of tightly regulated pathways and the use of lesion mimics has proved extremely useful. Plants with the lesion mimic phenotype exhibit constitutive expression of defense mechanisms such as callose deposition, reactive oxygen species, pathogenesis-related (PR) proteins, and phytoalexins, as well as, exhibiting cell death and enhanced resistance to pathogens (Y.-H. Jung et al., 2005). Several examples of lesion mimics have been identified in rice. Rice *spl11* causes the development of spontaneous lesions and grants broad spectrum resistance to rice blast (*Magnaporthe oryzae*) and bacterial blight (*Xanthamonas oryzae* pv *oryzae*, *Xoo*) (Yin et al., 2000; Zeng et al., 2004). The level of pathogen resistance in *spl11* mutants is related to the levels of defense-related gene expression, and intensity of lesion development (Yin et al., 2000). *Spl11* encodes a protein with a U-box domain and six armadillo (ARM) repeats, and functions as an E3 ubiquitin ligase (Zeng et al., 2004). The rice mutant line *hpil* forms lesions two weeks after germination (Yong et al., 2021). When inoculated with *M. oryzae* and *Xoo* these individuals were highly resistant compared to wild type variety. Within *hpil* mutants, PR proteins were upregulated in uninoculated, lesion forming leaves, indicating the induction of defense responses in the absence of a pathogen (Yong et al., 2021).

Few lesion mimic examples exist in wheat. Those that have been identified are members of the *lm* gene series and provide enhanced disease resistance (Anand et al., 2003; Li & Bai, 2009; Liu et al., 2021; Yao et al., 2009). *lm,* grants enhanced resistance to *P.* triticina. *lm3* was shown to provide resistance to powdery mildew (Wang et al., 2016). *lm4* was shown to enhance resistance to *Pst* (Liu et al., 2021). Kamlofski et al. (2007) reported the presence of a lesion mimic phenotype in an ethyl methanesulfonate (EMS) mutagenized line of Sinvalocho M.A., providing reduced leaf rust disease development, but the causative mutation has yet to be identified. Although lesion mimics can provide protection from disease, their agronomic importance is low due to the undesirable nature of spontaneous cell death. But the importance of lesion mimics to understanding the plant immune system and plant cell death cannot be understated.

To induce random mutations that could potentially disrupt a leaf rust susceptibility gene, wheat seeds of the variety Thatcher were treated with EMS. Mutated plant seedlings were challenged with *P. triticina* to evaluate disease severity. Plants with reduced disease severity were selected for and selfed. Three of these mutant lines, 1995, 2048, and 2348, were chosen for further evaluation. To characterize the phenotypes of these mutant lines, bulked segregant RNAseq analysis and evaluation of the initial time course of leaf rust infection through microscopic analysis were conducted. Bulked segregant RNAseq analysis will provide insight into the differences in the expression profile between mutant and wild type individuals in each mutant. Time course microscopy will provide evidence for the point at which the host-pathogen interaction is being disrupted in the mutant lines. These two assays will elucidate the effect that the causative mutation has on the establishment of successful host-pathogen interactions.

Materials and methods

Development of Mutant Lines

The hard red spring variety Thatcher (USDA-NSGC Cltr 10003, Clark, 1935) was used for mutagenesis. Ten seeds from a source of Thatcher were inoculated with *Puccinia triticina* Eriks, race BBBDB (virulent to *Lr14a*, *Lr50*) according to Bruce et al., (2014) to verify susceptibility. A single plant in which *P. triticina* was highly virulent on, was bagged at the time of flowering and allowed to self-fertilize. Twenty seeds of the subsequent generation were grown and self-fertilized in the same manor. A total of 5000 seed were used for mutagenesis. Seeds were treated according to Williams et al, (1992) and Simmons et al., (2006) with the following modifications. Lots of 300 were placed in 100 ml of ddH2O for 8 hours and placed on an orbiting shaker at 75 rpm at room temperature. A concentration of 0.3-0.4 % ethyl methanesulfonate in ddH2O (EMS, Sigma catalog M0880, St. Louis, MO), leading to a 20-30% lethality, was used to treat seeds (Williams et al, 1992; Simons et al., 2006) for 16 hours on the same shaker. Seeds were then rinsed for two hours in tap water, planted in root trainers containing MetroMix 360 (Sun-gro, Vancouver, CA), and transferred to a greenhouse, 18-22 ^{o}C, 16h/8h day/night cycle of artificial sodium pressure lighting 250 µE (Neugebauer, 2018). Surviving plants were bagged and allowed to self-fertilize. Twelve M_2 family seeds from each line were screened at the 2-3 leaf stage with the *P. triticina* race BBBDB as above and visually

rated using a 0-4 scale (0- no infection, ";" fleck - small hypersensitive response, 1-2 small moderate uredinia pustules, 3-4 moderate to large pustules; Long and Kolmer, 1989). Lines with a reduction of infection (0-2 infection type) were identified, self-fertilized and carried out to the M_6 generation. Verification of phenotype occurred at each generation by inoculation with *P. triticina*. In total, 2,500 M_2 families were evaluated for changes in susceptibility. M_6 plants at the 2-3 leaf stage were scored for leaf rust infection type ten days post infection using leaf rust race BBBDB.

Bulked Segregant RNAseq Analysis

Bulk Tissue

M_6 mutant lines were backcrossed to Thatcher and F_1 individuals were allowed to self. Twelve seeds from each $F_{2:3}$ families were planted in root trainers containing MetroMix360 (Sun-gro, Vancouver, CA) as described above and placed in a Percival growth chamber 20ºC with 16 h/8 h day/night cycles. At the two to three leaf stage, seedlings were inoculated with *P. triticina* race BBBDB as above and homozygous families with phenotypes similar to the mutant and wildtype were identified. Three bulks of mutant and three bulks of wild type were made by pooling tissue from three families for each bulk. Two cm fragments were cut from the mid-section of the fourth leaf of one plant from each of the families in the bulk, 13 days post inoculation. Tissue was frozen in liquid nitrogen and stored at -80ºC.

RNAseq analysis

Total RNA was extracted from frozen tissue using the Invitrogen *mir*Vana miRNA isolation kit (AM1561, Fisher Scientific) according to the plant protocol. RNA was sent to Genewiz (South Plainfield, NJ) and Genohub for Illumina 150-bp paired end cDNA sequencing with a goal of 20-30 million reads per sample. Paired end sequencing files were analyzed using CLC Genomics Workbench v21 (Qiagen, Redwood City, CA). Reads were filtered with maximum distance of 1 Kb, removal of failed reads and trimmed. RNA-seq analysis within CLC follows a methodology based on Mortazavi et al. (Mortazavi et al., 2008). The IWGSC Chinese Spring cDNA list v1.1 (Alaux et al., 2018) was used as reference for gene expression. Reads were mapped against the reference set using batch function. Expression levels of the top 50

genes with the highest coefficient of variation (ratio of standard deviation to the mean expression value) were compared using the heat map function in CLC and grouped with Euclidean distance (parameter value) and complete linkage. A list of genes with expression levels > 1.5x fold difference were characterized by gene ontology (GO) for possible function. Sequences for >1.5x differentially expressed genes were imported into OmicsBox v2.0 and analyzed using the GO slim function (Conesa et al., 2005; Conesa & Götz, 2008; Götz et al., 2008, 2011).

Microscopy

Time course assays were used to determine mutant infection phenotypes. Each M_6 mutant and Thatcher had five seeds planted in 14 7.5x7.5cm pots filled with MetroMix 360 (Sun-gro, Vancouver, CA). For each wheat line, seven pots were inoculated with *P. triticina* race BBBDB suspended in Soltrol 170 isoparafin as described above, the remaining seven were mock inoculated with Soltrol only. All plants were treated at the 2-3 leaf stage and placed in a dew chamber as described previously. Beginning with Day 0, the mid-section of the second leaf of each of the five plants per treatment were collected. This was repeated each day through day 6. Tissue was placed in 10 ml of Farmer Fixative (3:1 v/v 100 methanol:acetic acid Dugyala et al., 2015) and placed at 4ºC overnight. The solution was drained and replaced with 10 ml of Farmers Fixative and stored until staining. Tissue was stained with Uvitex 2B according to Dugyala (2015).

Stained tissue was viewed on a Zeiss Axio Imager M2 epifluorescence upright microscope. For visualizing fungal staining with Uvitex 2B a Zeiss 96 HE filter set was used with excitation set to PP 390/40 and emission set to BP 450/40. Imaging of tissue was conducted on the center of the tissue with the midrib down. Three pieces of tissue from each day were observed. For each piece of tissue, 20 observations of the *P. triticina* infection process were taken at random. No scale existed previously for the scoring of *P. triticina* spore infection types (IT) during the infection process. A scale was developed using a method similar to that used by Henningsen et al. (2021) for the characterization of the infection of *P. graminis* f.sp. *tritici* on wheat. Progression of infection based on descriptions by Roelfs (1992) was utilized. Spores were scored from 0-6 (0) no germination; (1) ability to germinate, (2) find stoma and form appressoria, (3) develop intercellular hyphae and haustoria, (4) begin forming small colonies, (5)

mature into large hyphal colonies, and (6) form pustules of uredinia. Two repetitions of planting, inoculating, tissue collection, staining, and scoring were completed at separate times, under near identical conditions. Statistical analyses were conducted in Rstudio (Rstudio Team, 2022). A three-way analysis of variance (ANOVA) was conducted to determine significance of results and interactions between variables using the packages dplyr (Wickham et al., 2022), tidyverse (Wickham et al., 2019), and rstatix (Kassambara, 2021). Significant interactions were further analyzed using a post-hoc Tukey's Honestly Significant Difference (HSD) test using α=.05. The frequency of each IT score at each day was analyzed for significant deviation from the wild type IT frequencies using a z-test.

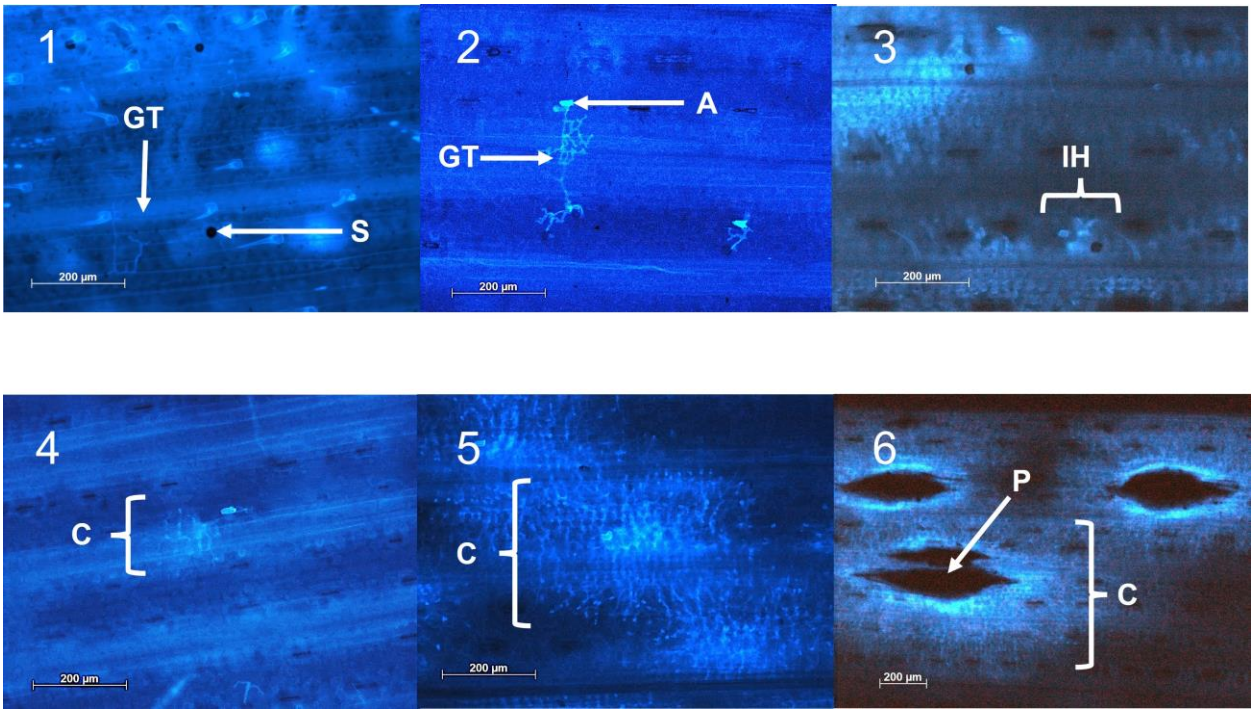

Figure 2.1

Examples of *P. triticina* microscopic infection types on wheat variety Thatcher. Infection types were scored as follows: 0) (not depicted) spore has failed to germinate, 1) spore (S) successfully formed a germ tube (GT), 2) spore successfully germinated and formed appressorium (A), 3) spore has begun to develop intercellular hyphae (IH) and haustorium, 4) spore has successfully formed small colonies (C), 5) colonies have matured and enlarged, 6) colonies have erupted and formed pustules (P) of urediniospores.

Results

Mutant Phenotypes

Of the 2,500 M_2 families that were evaluated for changes in susceptibility, 25 lines were identified that had some level of reduced infection based on pustule size, pustule number, increased plant reaction and subsequent lack of fungal infection. Three lines 1995, 2048, and 2348 were identified for further characterization (Figure 2.2). Wild type Thatcher was scored as infection type (IT) "3-3+". 1995 was found to have small to moderate sized chlorotic regions along the leaf in both non inoculated and inoculated leaves and found in all the leaves of the plant. At 12 days post inoculation (dpi), the number of pustules as well as size of pustules were reduced (Figure 2.2). Mutant 2048 had similar lesions in the leaves, but they tended to be more defined along the leaf. Pustule numbers and sizes were also reduced when compared to wild type. Mutant 2348 on the other hand did not have lesions. Oil only mock inoculated leaves were similar to wild type phenotype. At 12 dpi the pustules present on line 2348 were rated at 1-2 IT (Figure 2.2)

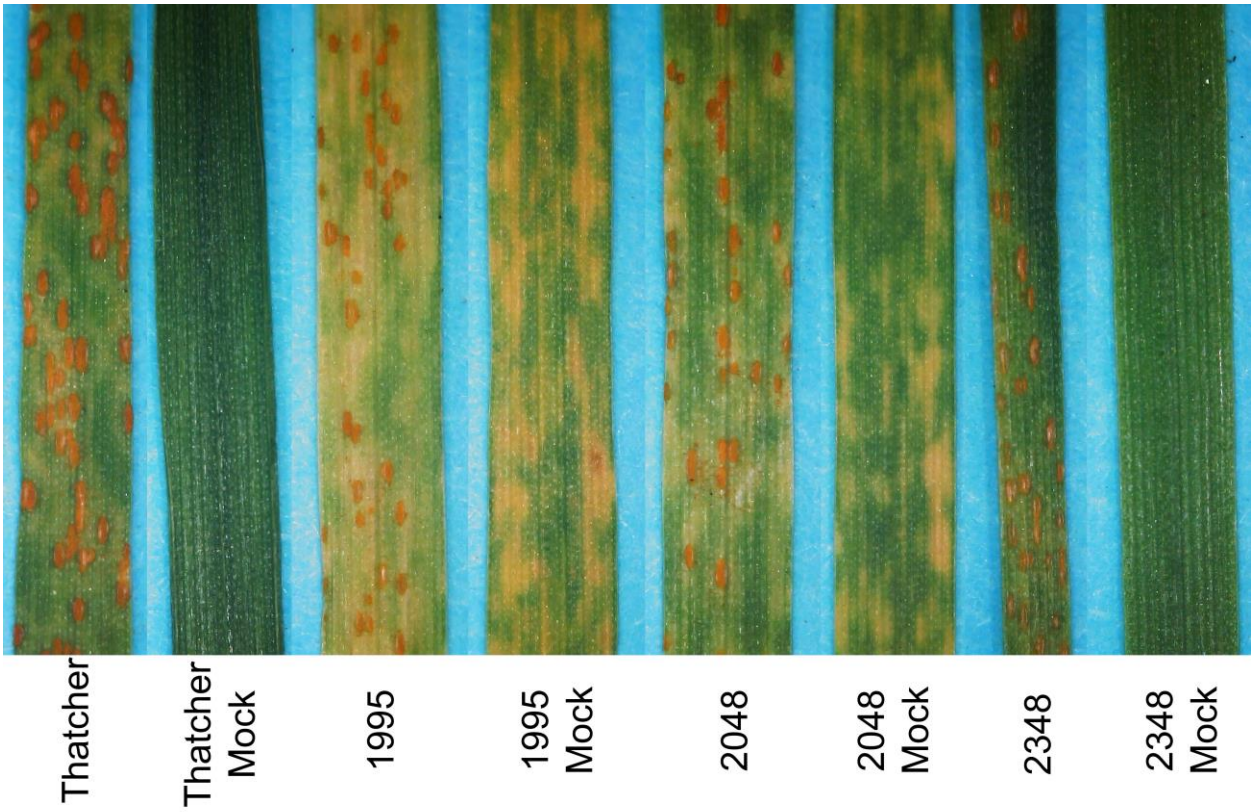

Figure 2.2

Phenotypes of Thatcher and EMS mutant M_6 lines 1995, 2048, and 2348. Lines were inoculated with *P. triticina* race BBBDB and scored at 12dpi. The second seedling leaf from both *P. triticina* race BBBDB inoculated and oil only mock inoculation are being shown.

Microscopy

1995

Mock inoculated wild type Thatcher and mock inoculated mutant 1995 were compared to tissue inoculated with *P. triticina* race BBBDB in a time course study to characterize the reduction of fungal infection. In the wild type, germination of BBBDB spores was evident by day 1 (Figure 2.5B) germ tubes could be observed growing thigmotropically towards a stoma. Once a stoma was reached appressoria could be seen being formed. A low number of spores observed progressed to the formation of early intercellular hyphae and haustoria (Figure 2.3). By 3dpi, few spores were seen at the germination stage. Spores have successfully formed appressorium, begun to form hyphae in the subdermal intercellular tissue, and haustoria as

indicated by bright staining (Figure 2.3 & Figure 2.5C). By 5 dpi, a well-defined cluster of fungal tissue could be seen at each infection point (Figure 2.5D). In 1995, infection appeared to be similar in the first three days of infection (Figure 2.5A-C, I-K). In 1995, at 1dpi, there is a larger quantity of spores that have germinated but are unable to form appressoria (Figure 2.3). At 3dpi fewer spores have successfully progressed beyond appressoria formation to form intercellular hyphae compared to the wild type (Figure 2.3& Figure 2.5C, K). By day 5, fungal colony sizes were reduced (Figure 2.5D, L), fewer colonies were produced, and there was a greater presence of spores unable to proliferate past the initial stages of infection when compared to wild type (Figure 2.3). Figure 2.3 shows that at 5dpi there was a greater number of spores in thatcher that were able to form large colonies than in 1995. Statistical analysis of infection type scores over these periods indicates that there is a significant difference in the infection process attributed to the difference between Thatcher and 1995 at both 1dpi ($F(1, 228)=5.266$, $p=0.023$) and 3dpi ($F(1, 228)=11.975$, $p=0.000644$). Full ANOVA tables for each day post infection can be found in Appendix A supplemental Figure 1. These differences were shown to be significant and due to the differences between 1995 and Thatcher ($F(1, 228)=40.867$, $p=9.10\text{x}10^{-10}$).

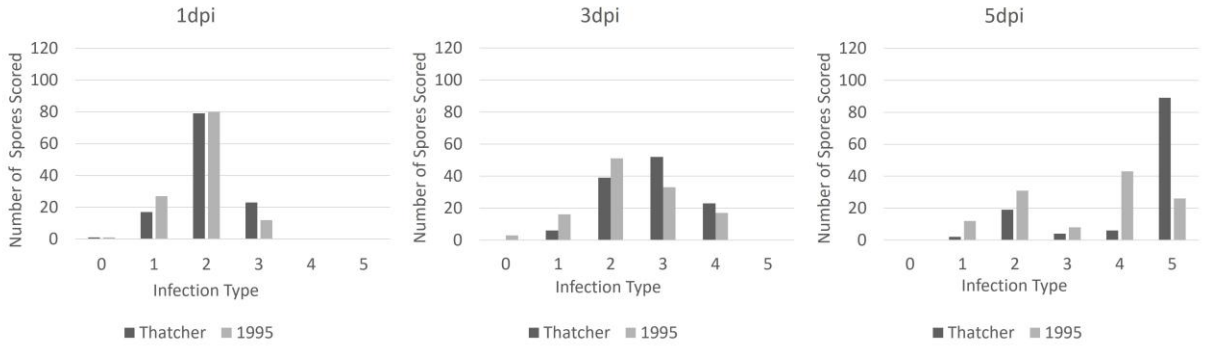

Figure 2.3

Total counts of each infection type (IT) score for Thatcher and 1995 at 1dpi, 3dpi, and 5dpi. At 1dpi there are more spores at IT 1 compared to thatcher ($p=0.00887$), the same quantity at IT 2 ($p=0.84658$) and fewer spores at IT 3 ($p=0.0107$). At 3dpi 1995 has more spores at IT 1 ($p=0.000028$) and IT 2 ($p=0.01954$), fewer spores at IT 3 ($p=0.000467$) and no change in quantity of spores at IT 4 ($p=0.16407$) compared to Thatcher. At 5dpi 1995 has fewer spores at IT 5 ($p<0.00001$), and a greater number of spores at IT 1 ($p<0.00001$), 2 ($p=0.002693$), 3 ($p=0041931$), and 4 ($p<0.00001$) compared to Thatcher

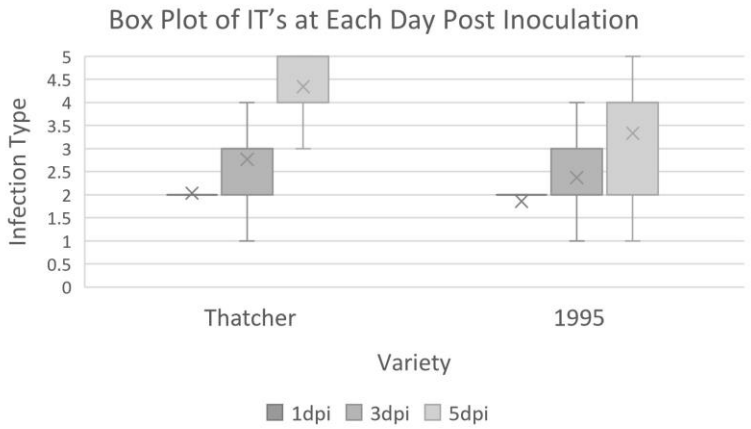

Figure 2.4

Box plot of the infection types at days 1, 3, and 5 post inoculation on Thatcher, and mutant line 1995. Average infection scores are indicated by (x). Each box contains 50% of the infection type scores, whiskers extend to the 10th and 90th percentiles.

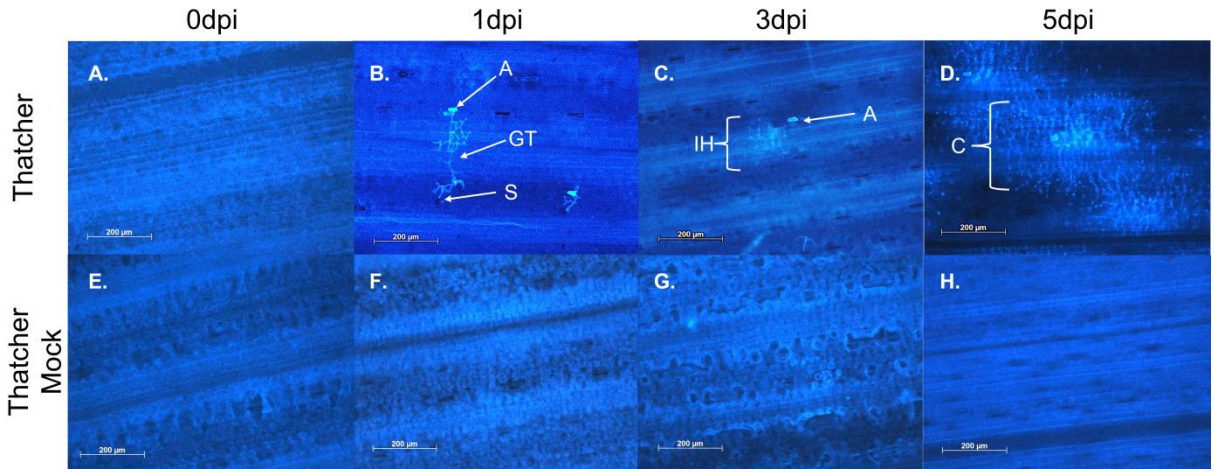

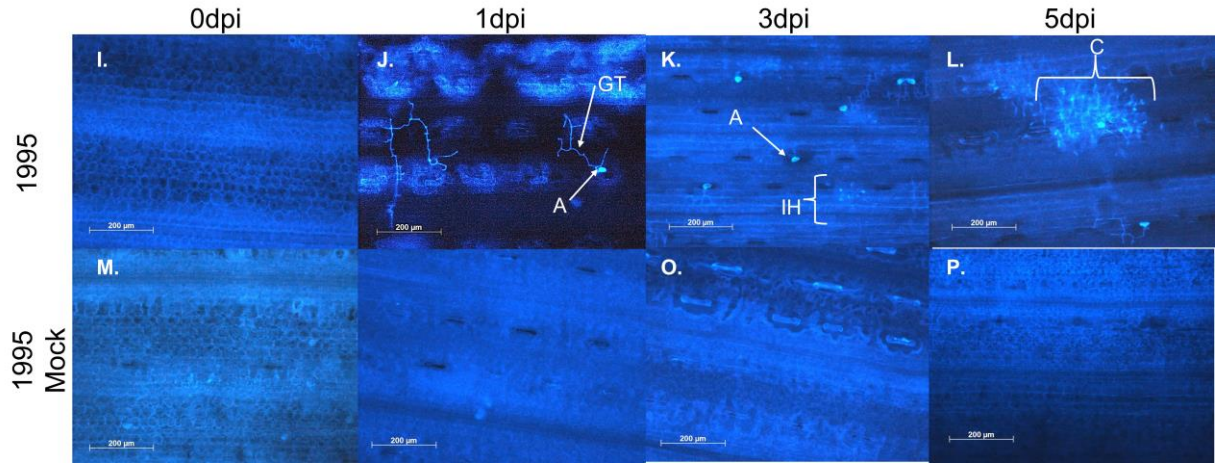

Figure 2.5

The infection process of *P. triticina* in Thatcher, and 1995. Mock samples were inoculated with soltrol 170 only (**E.-H. & M.-P.).** Spores (S) germinating at 1dpi with germ tube (GT) and appressorium (A) (**B., J.**). At 3dpi, germinated spores proliferating from appressorium to form infection hyphae (IH) and haustoria (H) (**C.,K.**). Development of fungal colonies (C) at 5dpi with increased number of haustoria and hyphae compared to 3dpi (**D., L.**).

2048

In the time course assay for mutant 2048, comparisons were drawn against the wild type Thatcher. Full ANOVA tables for each day post infection can be found in Appendix A supplemental figure 2. A significant difference in the infection types, attributed to differences in variety ($F(1, 228)=18.335$, $p=2.73x10^{-5}$), between Thatcher and 2048 is observed as early as 1dpi. An increased number of spores at the germination stage was observed in 2048, along with a reduction in the number of spores that have formed appressoria and progressed to IT 3 (Figure 2.6). At 3dpi there is a significant ($F(1, 228)=4.625$, $p=.033$) difference in the *P. triticina* infection types between 2048 and Thatcher. Compared to Thatcher, in 2048 there is a greater number of spores that have not progressed beyond appressoria formation (Figure 2.6 & Figure 2.8C, K), and fewer spores able to produce intercellular hyphae and haustoria (Figure 2.6). At 5dpi large colonies have begun to develop in both Thatcher and 2048 (Figure 2.8D, L). However, a significant difference ($F(1, 228)=13.558$, $p=.000289$) in infection types for each line was observed. A greater number of spores at infection types 1 and 2 were observed in 2048 (Figure 2.6). There were more spores with infection type 4 in 2048, than in Thatcher. Additionally, there

was a reduction in the total number of spores forming large colonies in 2048 (Figure 2.6). Both of these points indicate a reduction in the ability of *P. triticina* to form large colonies in 2048.

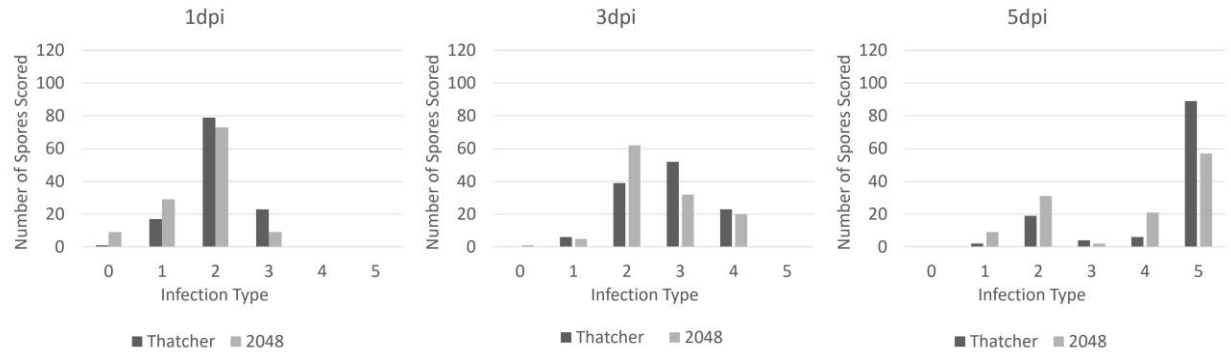

Figure 2.6

Total counts of each infection type (IT) score for Thatcher and 2048 at 1dpi, 3dpi, and 5dpi. At 1dpi there are more spores at IT 0 ($p<0.00001$), and 1 ($P=0.003471$) compared to thatcher, the same quantity at IT 2 ($p=0.238172$), and fewer spores at IT 3 ($p=0.001166$). At 3dpi 2048 has no difference in the number of spores at IT 1 ($p=0.67534$) or IT 4 ($p=0.48658$), a greater number at IT 2 ($p<0.00001$), and fewer spores at IT 3 ($p=0.00023$) than Thatcher. At 5dpi 2048 has fewer spores at IT 5 ($p<0.00001$), and a greater number of spores at IT 1 ($p<0.00001$), IT 2 ($p=0.002693$), and IT 4 ($p<0.00001$) compared to Thatcher.

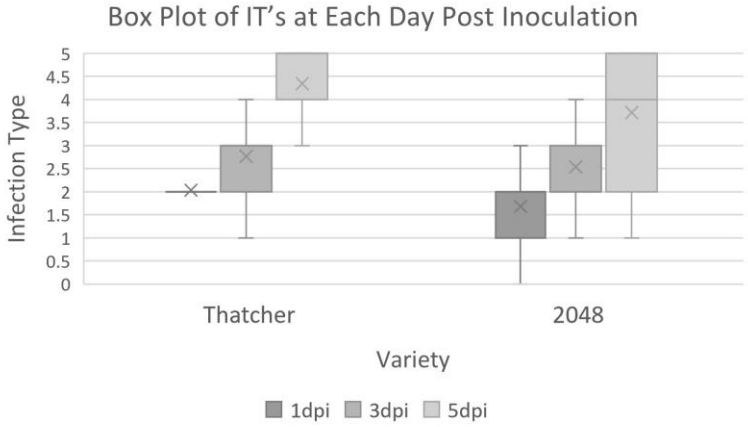

Figure 2.7

Box plot of the infection types at days 1, 3, and 5 post inoculation on Thatcher, and mutant line 2048. Average infection scores are indicated by (x). Each box contains 50% of the infection type scores, whiskers extend to the 10th and 90th percentiles.

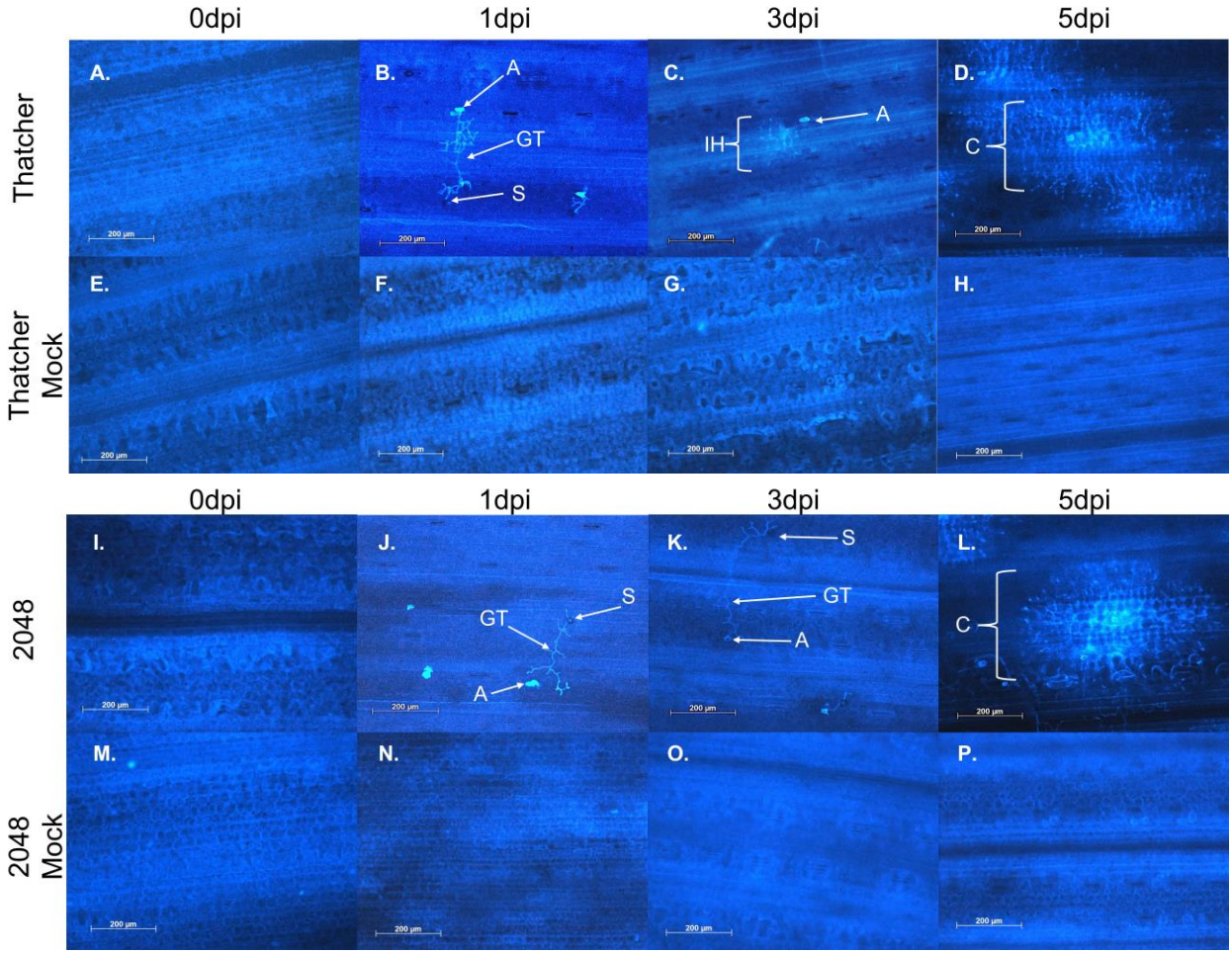

Figure 2.8

The infection process of *P. triticina* in Thatcher, and 2048. Mock samples were inoculated with soltrol 170 only (**E.-H. & M.-P.**). Spores (S) germinating at 1dpi with germ tube (GT) and appressorium (A) (**B., J.**). At 3dpi, germinated spores proliferating from appressorium to form infection hyphae (IH) and haustoria (H) (**C., K.**). Development of fungal colonies (C) at 5dpi with increased number of haustoria and hyphae compared to 3dpi (**D., L.**)

2348

Full ANOVA tables for each day post infection can be found in Appendix A supplemental figure 3. Differences in infection types, attributable to the differences in variety between 2348 and Thatcher, were seen at 1dpi ($F(1, 228)= 4.018$, $p=0.046$). At 1dpi spores on 2348 were able to produce germ tubes, find stoma, and produce appressoria normally (Figure 2.11, J). However, fewer spores were observed that had begun to form intercellular hyphae (Figure 2.9). At 3dpi, a significant difference ($F(1, 228)= 18.335$, $p=2.73x10^{-5}$) between infection types in Thatcher and 2348 was observed. Both Thatcher and 2348 have begun to develop intercellular hyphae, and progress to form small colonies (Figure 2.11C, K). The formation of small colonies in 2348 and Thatcher was similar (Figure 2.8). However, in 2348 there are fewer spores beginning to form intercellular hyphae, and a greater number of spores at the formation appressoria (Figure 2.9). At 5dpi large colonies have developed in Thatcher (Figure 2.11D). In 2348 some spores have begun to form large colonies (Figure 2.11L), but on average there are fewer spores that have successfully formed large colonies compared to Thatcher (Figure 2.9). The quantity of spores forming small colonies and beginning to form intercellular hyphae is similar between Thatcher and 2348 (Figure 2.9). There is a greater quantity of spores at the appressoria formation stage in 2348 at 5dpi than in Thatcher. These differences between the infection types due to variety is significant at $F(1, 228)=56.818$, $p=1.12x10^{-12}$.

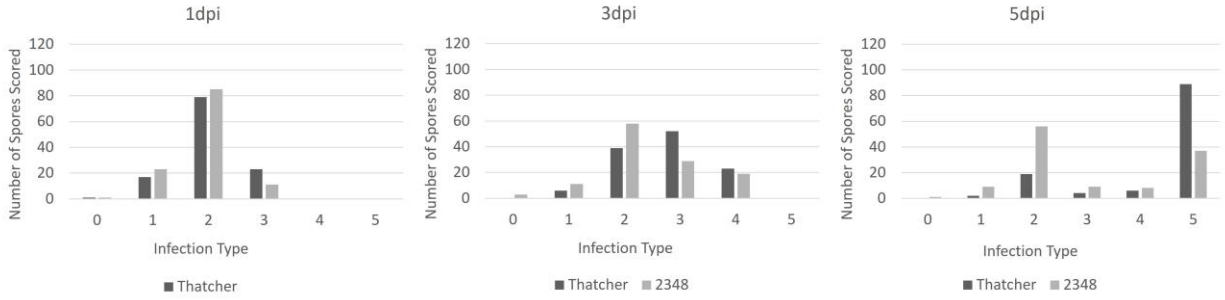

Figure 2.9

Total counts of each infection type (IT) score for Thatcher and 2348 at 1dpi, 3dpi, and 5dpi. At 1dpi there is no difference in the quantity of spores at IT 0, IT 1 (p=.11625), or IT 2 (p=.23813) compared to Thatcher. A reduction in the quantity of spores at IT 3 (p=.005384) was observed. At 3dpi 2048 has more spores at IT 1 (p=.03623) and IT 2 (p=.000213), fewer spores at IT 3 (p=.000023) and no change in quantity of spores at IT 4 (p=.35357) compared to Thatcher. At 5dpi 2048 has fewer spores at IT 5 (p<.00001), and a greater number of spores at IT 1 (p<.00001), 2 (p<.00001), 3 (p=.011), and no change in quantity of spores at IT 4 (p=.40219) compared to Thatcher.

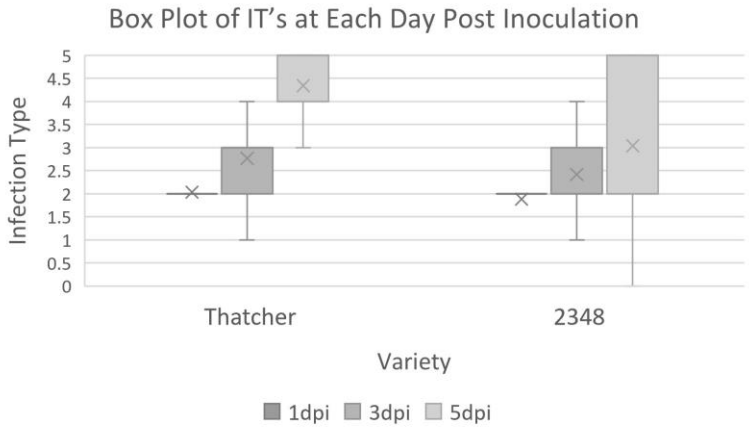

Figure 2.10

Box plot of the infection types at days 1, 3, and 5 post inoculation on Thatcher, and mutant line 1995. Average infection scores are indicated by (x). Each box contains 50% of the infection type scores, whiskers extend to the 10^{th} and 90^{th} percentiles.

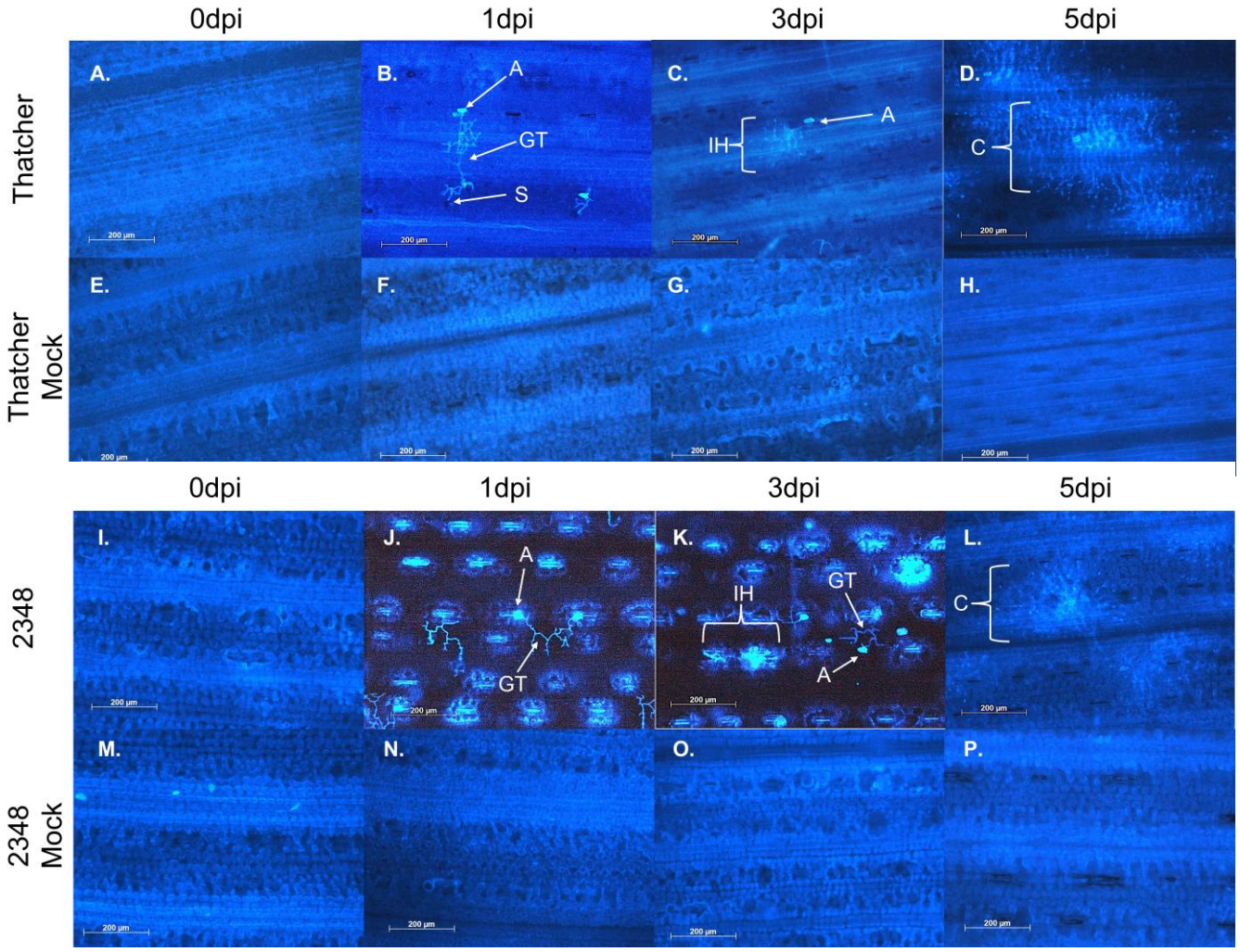

Figure 2.11

The infection process of *P. triticina* in Thatcher, and 2348. Mock samples were inoculated with soltrol oil only (**E.-H. & M.-P.**). Spores (S) germinating at 1dpi with a germ tube (GT) and appressorium (**B., J.**). At 3dpi, germinated spores proliferating from appressorium to form infection hyphae (IH) and haustoria (H) (**C., K.**). Development of fungal colonies (C) at 5dpi with increased number of haustoria and hyphae compared to 3dpi (**D., L.**).

RNAseq Analysis

Gene expression was compared between the mutants and wild type Thatcher by Illumina sequencing of mRNA. A bulking approach was used to identify common gene expression patterns that would be found associated with the mutant. Since the F2:3 families were derived by

backcrossing the mutant to the wild type, the genetic backgrounds should be the same except for segregating mutant loci. Total number of reads for the 1995 experiment ranged from 110.4 million paired end reads to 132.2 million. After trimming and alignment to the Chinese Spring reference v1.1 cDNA set, unique reads ranged from 29.3 million reads to 35.8 million reads with total expression reads evaluated 43.5 million reads to 52.8 million reads. For 2048, total paired end reads ranged from 30 to 70 million, while total reads used in the analysis ranged from 11-27.6 million paired reads. For 2348, total reads ranged from 74-92.4 million paired end reads while 27-37 million reads were used for expression analysis. Individual values can be seen in supplemental Figure 1.

Heat mapping of gene expression

1995

Gene expression tracks generated from CLC RNAseq expression analysis were heat mapped. Pools were independently sorted by CLC into two groups. Sorting is based on relatedness of expression and cannot be forced. The pools were separated into a mutant group and a wild type group with the corresponding parent. Based on the relative expression values, heat shows a clear distinction in the gene expression between wild type and mutant phenotypes. Among the top 50 differentially expressed genes, 25 were involved in the plant defense response, and 25 were involved in photosynthesis (Figure 2.9). Genes involved with plant defense had greater expression in the mutant pools, compared to the wild type pools. Whereas the genes involved with photosynthesis had increased expression in wild type pools, compared to the mutant pools.

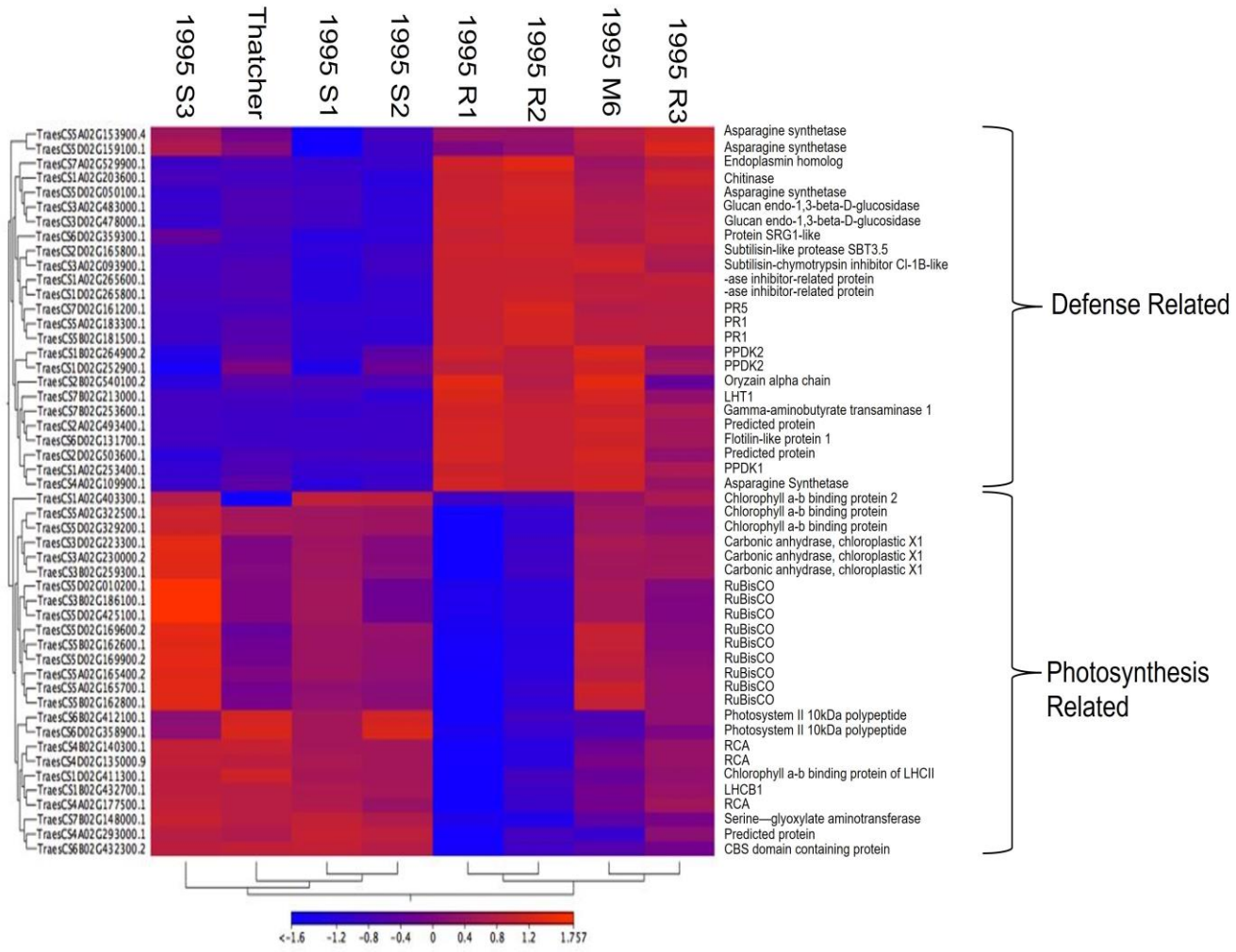

Figure 2.12

Top 50 differentially expressed genes in 1995. Clustering of genes is dependent upon relatedness of sample expression profiles. Pool phenotypes are indicated by S (wild type) and R (mutant). Predicted genes are displayed to the right of the heat map and have their biological roles as assigned by Gene Ontology (GO).

2048

2048 gene expression tracks were heat mapped in the same manner as in 1995. Two groups were obtained, one with mutant pools and one with wild type pools. The heat map shows a clear distinction in the gene expression between the wild phenotype and the mutant phenotype. Two major groups are present. Among the top 50 differentially expressed genes The genes

involved with plant defense had greater expression in mutant pools and parent line, compared to wild type pools and parent lines (Figure 2.10).

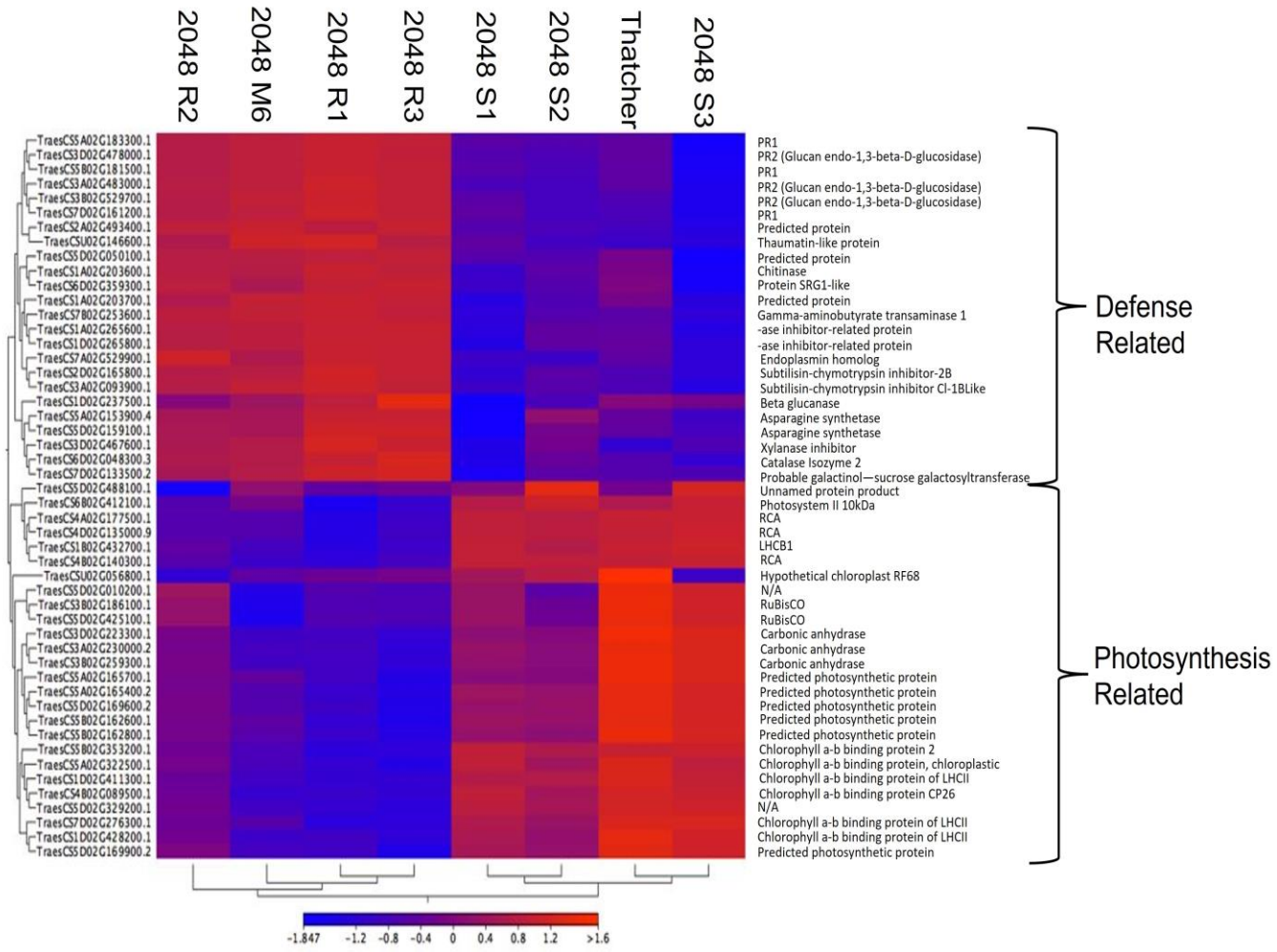

Figure 2.13

Top 50 differentially expressed genes in 2048. Clustering of genes is dependent upon relatedness of sample expression profiles. Pool phenotypes are indicated by S (wild type) and R (mutant). Predicted genes are displayed to the right of the heat map and have their biological roles as assigned by Gene Ontology (GO).

2348

For 2348, gene expression tracks obtained as discussed previously, were heat mapped for the top 50 differentially expressed genes (Figure 2.11). As mentioned, CLC independently sorts these tracks into groups based on their relatedness. In the top 50 heat map for 2348, Four groups were generated. These four groups did not separate based on their phenotypes as 1995 and 2048 did. The 2348 parent paired with 2348 wild type pool 3 and thatcher paired with mutant pool 3, this is contrary to expected results of 2348 parent grouping with the mutant pools, and thatcher grouping with wild type pools. Wild type pool 1 and 2 grouped together, and mutant pool 1 and 2 grouped together.

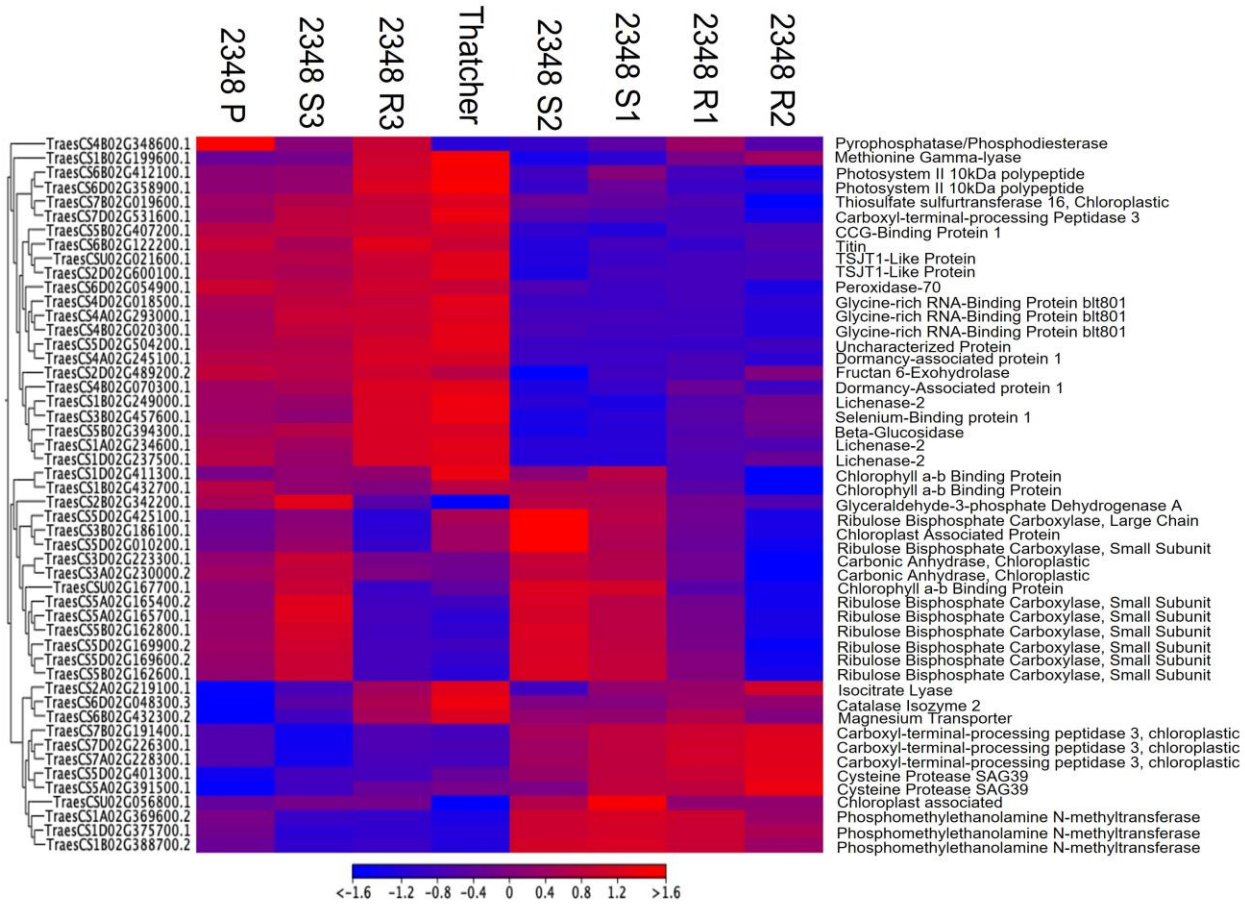

Figure 2.14

Top 50 differentially expressed genes in 2348. Obtained from CLC v21. Clustering of genes is dependent upon relatedness of sample expression profiles. Pool phenotypes are indicated by S (wild type) and R (mutant). Predicted genes are displayed to the right of the heat map.

Pathway involvement of differentially expressed genes

1995

Differential expression of genes between mutant pools and wild type pools was analyzed. The differential expression discussed in this section refers to the expression values of genes in mutant pools in relation to their expression in susceptible pools, unless otherwise stated. Within the top 250 differentially expressed genes the three pathways with the most genes in them were "defense" (35%), "photosynthesis" (26%), and "undetermined" (18%). Additionally, there was an increase in expression of a small number of genes that were involved in the regulation of salicylic acid (SA) production, and a systemic defense response. Several negative regulators of the plant immune system were down regulated.

Once GO terms were obtained, the biological function was further investigated. Figure 2.12 contains a list of the genes, proteins, and their biological functions in the defense response. Several indicators of a pathogen induced defense response were present. Proteins involved in defense against fungi were identified. Among these proteins were pathogenesis-related (PR) protein 1, PR5, and chitinase. Indicators of a systemic acquired defense (SAR) were also present.

Table 2.1

Differential expression of predicted genes with roles in defense 1995

Differentially expressed gene	BLASTn predicted gene	Biological function from GO term	Differential expression value (R vs S)
TraesCSU02G060600	putative disease resistance RPP13-like protein 1	ADP and ATP binding; NBS-LRR for *Peronospora parasitica* in *Arabidopsis thaliana*	7.11x
TraesCS2B02G097800	MLO-like protein 1	calmodulin binding, defense modulation, leaf cell death	208.86x
TraesCS3A02G483000	Glucan endo-1,3-beta-D-glucosidase	Carbohydrate metabolic process	307.15x
TraesCS3B02G529700	Glucan endo-1,3-beta-D-glucosidase	Carbohydrate metabolic process	588.74x
TraesCS3D02G478000	ribulose bisphosphate carboxylase/oxygenase activase	defense against bacteria, response to JA	259.97x
TraesCS3D02G475200	ribulose bisphosphate	defense against bacteria,	50.61x

	carboxylase/oxygenase activase	response to JA	
TraesCS1D02G431200	Glucan endo-1,3-beta-glucosidase 13	Defense, Carbohydrate metabolysis, cell wall organization	35.51x
TraesCS5A02G018200	pathogenesis-related protein 5	Defense, fungal	25.99x
TraesCS5A02G183300	Pathogenesis-related protein 1	Defense, SAR indicator	311.99x
TraesCS5B02G181500	Pathogenesis-related protein 1	Defense, SAR indicator	334.91x
TraesCS7D02G161200	Pathogenesis-related protein 1	Defense, SAR indicator	128.60x
TraesCS1A02G203600	chitinase	Defense, fungal	657.72x
TraesCS1D02G207000	chitinase	Defense, fungal	38.55x
TraesCS4A02G296300	alpha-amylase/trypsin inhibitor	inhibits alpha-amylase activity	445.41x
TraesCS4D02G015800	putative lipid-transfer protein DIR1	Lipid transport, SAR	9.63x
TraesCS7A02G558500	thaumatin-like protein	local root response to colonization by non-pathogenic PGPR	717.94x
TraesCSU02G146600	thaumatin-like protein	local root response to colonization by non-pathogenic PGPR	773.38x
TraesCSU02G008300	serine/threonine-protein kinase PBL13-like isoform X1	Negative regulation of immune response	310.44x
TraesCS1A02G146000	Hypersensitive-induced response protein 1	Positive regulator of HR-like cell death, Interacts with NBS-LRRs	288.62x
TraesCS2B02G519100	agmatine coumaroyltransferase	synthesis of antifungal derivatives in barley	160.91x
TraesCS1A02G173800	benzyl alcohol O-benzoyltransferase	transferase activity, upregulated during HR after pathogen infection	65.08x
TraesCS1B02G164200	Hypersensitive-induced response protein 1	Positive regulator of HR-like cell death, Interacts with NBS-LRRs	650.07x
TraesCS4D02G350500	cell wall invertase	Defense response, Systemic Acquired Response (SAR)	33.97x
TraesCS4B02G264500	aminotransferase ALD1 homolog	Upregulated by PAD4, induces SAR	1954.06x
TraesCS2A02G394900	protein DMR6-LIKE OXYGENASE 1	converts SA to DHBA; negative regulator of defense; susceptibility to downy mildew	-285.45x
TraesCS7D02G536900	2-oxoglutarate-Fe(II) type oxidoreductase	Dioxygenase activity	168.52x
TraesCS2A02G395000	Naringenin,2-oxoglutarate 3-dioxygenase	flavonoid biosynthetic process; response to UV-B	245.05x
TraesCS6D02G359300	protein SRG1-like	leaf senescence	69.85x
TraesCS4B02G382300	cytochrome P450 716B1-like	Oxidoreductase activity	152.90x
TraesCS5B02G209100	cytochrome P450 71A1-like	Oxidoreductase activity	140.52x
TraesCS2D02G392800	protein DOWNY MILDEW RESISTANCE 6-like	Negatively regulates defense associated gene expression; required for susceptibility to downy mildew	187.19x
TraesCS5A02G469800	B2 protein	Adverse temperature tolerance	4.20x
TraesCS2A02G219100	isocitrate lyase	glyoxylate cycle; salt tolerance	1.28x

TraesCS2B02G244600	isocitrate lyase	glyoxylate cycle; salt tolerance	3.25x
TraesCS2D02G224200	isocitrate lyase	glyoxylate cycle; salt tolerance	3.50x
TraesCS2B02G244600	isocitrate lyase	glyoxylate cycle; salt tolerance	3.25x
TraesCS5D02G328100	chaperone protein ClpD1, chloroplastic	Heat stress response	2.45x
TraesCS2A02G389900	glutamate dehydrogenase 2, mitochondrial	Glutamate biosynthesis/catabolism; ox-red process	2.81x
TraesCS2B02G409300	glutamate dehydrogenase 2, mitochondrial	Glutamate biosynthesis/catabolism; ox-red process	3.70x
TraesCS2D02G388800	glutamate dehydrogenase 2, mitochondrial	Glutamate biosynthesis/catabolism; ox-red process	9.3x

2048

The top four largest groups were “photosynthesis” (25%), “defense” (26%), “amino acid metabolism” (9%), and “undetermined” (19%). Similar to 1995, regulation of SA, systemic defense response, and negative regulators of the plant immune system were all involved. 2048 did have unique pathways that were altered. Gene expression in jasmonic acid biosynthesis and ethylene synthesis were both altered.

Several genes involved in defense against microbes were upregulated in 2048. (Figure 2.13) Transcripts with the following GO terms were up regulated: -ase inhibitor related proteins, catalase isozyme 2, chitinases, glucan endo-1,3-β-D-glucosidase, pathogenesis related (PR) protein 1, PR4, PR5, ribulose bisphosphate carboxylase/oxygenase activase A, thaumatin-like proteins, wall associated receptor kinase 2, xylanase inhibitor proteins, and downy mildew resistance 6-like protein.

Five genes that express proteins involved in jasmonic acid (JA) biosynthesis were seen to have increased expression (Figure 2.14).

Table 2.2

Differential expression of predicted genes with roles in defense in 2048

Differentially expressed gene	BLASTn Predicted gene	Biological function from GO term	Differential expression value (R vs S)

TraesCS7D02G269400	ABC transporter G family member 45	ATPase, ATP binding	1111.23x
TraesCS6A02G041700	Catalase isozyme 2	Protect cell from toxicity of H2O2	31.22x
TraesCS6B02G056800	Catalase isozyme 2	Protect cell from toxicity of H2O2	2.48x
TraesCS6D02G048300	Catalase isozyme 2	Protect cell from toxicity of H2O2	2.28x
TraesCS3D02G518200	cationic peroxidase SPC4-like	Removal of H2O2, response to/stress Pathogen attack	14.02x
TraesCS1A02G203600	chitinase	Defense/stress response	10.62x
TraesCS1D02G207000	chitinase	Defense/stress response	6.01x
TraesCS3D02G260300	endochitinase	breakdown chitin	51.49x
TraesCS3A02G483000	glucan endo-1,3-beta-D-glucosidase	Carbohydrate metabolic process	31.92x
TraesCS3B02G528500	glucan endo-1,3-beta-D-glucosidase	Carbohydrate metabolic process	95.99x
TraesCS3B02G529700	glucan endo-1,3-beta-D-glucosidase	Carbohydrate metabolic process	121.06x
TraesCS3D02G478000	glucan endo-1,3-beta-D-glucosidase	Carbohydrate metabolic process	28.07x
TraesCS3D02G476500	glucan endo-1,3-beta-D-glucosidase	Carbohydrate metabolic process	9.54x
TraesCS3D02G475200	glucan endo-1,3-beta-D-glucosidase	Carbohydrate metabolic process	12.56x
TraesCS5A02G183300	Pathogenesis-related protein 1	Defense, SAR indicator	48.18x
TraesCS5B02G181500	Pathogenesis-related protein 1	Defense, SAR indicator	43.20x
TraesCS7D02G161200	Pathogenesis-related protein 1	Defense, SAR indicator	128.46x
TraesCS3A02G517100	pathogenesis-related protein 4	Defense response to bacteria & fungus	17.84x
TraesCS5A02G018200	pathogenesis-related protein 5	Defense response, SAR	8.78x
TraesCS3A02G399000	putative calreticulin	multifunctional; defense against biotrophic pathogens	2.68x
TraesCS3B02G432000	putative calreticulin	multifunctional; defense against biotrophic pathogens	1.94x
TraesCS6B02G091100	S-(+)-linalool synthase, chloroplastic-like	monoterpene biosynthesis	38.66x
TraesCS7A02G558500	thaumatin-like protein	local root response to colonization by non-pathogenic PGPR	46.16x
TraesCS5B02G063600	wall-associated receptor kinase 2	ATP binding, protein kinase, ~susceptibility to fungal pathogens	7.09x
TraesCS3D02G467600	xylanase inhibitor	defense response	11.30x
TraesCS4D02G142000	xylanase inhibitor protein 1	defense response to fungus	4.36x
TraesCS2D02G392800	protein DOWNY MILDEW RESISTANCE 6-like	Negatively regulates defense associated gene expression; req for sus to downy mildew, *P. syringae*, and *P. capsici* in *Arabadopsis*	64.70x

TraesCS5A02G469800	B2 protein	Adverse temperature tolerance	3.10x
TraesCS5A02G321300	chaperone protein ClpD1, chloroplastic	Heat stress response	1.69x
TraesCS5B02G321800	chaperone protein ClpD1, chloroplastic	Heat stress response	3.60x
TraesCS5D02G328100	chaperone protein ClpD1, chloroplastic	Heat stress response	4.23x
TraesCS7B02G253600	gamma-aminobutyrate transaminase 1, mitochondrial	Stress response	1737.60x
TraesCS4B02G059300	glutathione transferase	multifunctional	2.70x
TraesCS7A02G134100	probable galactinol--sucrose galactosyltransferase 6	carbohydrate metabolic process	4.17x
TraesCS7B02G035200	probable galactinol--sucrose galactosyltransferase 6	carbohydrate metabolic process	2.80x
TraesCS7D02G133500	probable galactinol--sucrose galactosyltransferase 6	carbohydrate metabolic process	3.70x

Discussion

This study seeks to identify wheat susceptibility genes to leaf rust. By creating random mutations in wheat, and then selecting for reduced disease development, plants were generated that have random mutations in genes involved in disease protection. By further characterizing the phenotype, and mapping the causative mutations, insight can be obtained into how the mutation affects plant pathogen interaction and the possibility of new mechanisms of resistance or the identification of susceptibility genes.

Mutant lines 1995, 2048, and 2348 all exhibit a reduction in pustule size and number when compared to the unmutated parent Thatcher. 1995 and 2048 exhibit a hypersensitive-like response even in the absence of *P. triticina.* This is a similar phenotype to lesion mimic plants. However, establishing molecular evidence of a hypersensitive response (HR) in the mutant lines is necessary. Additionally, although lesion mimics are not of significant agronomic interest, the study of lesion mimics has shown to be useful in furthering the understanding of the plant immune system. Lesion mimics have provided insight into the molecular workings of the plant immune system, its regulation, and signaling (Bruggeman et al., 2015; Johal et al., 1995; Y.-H. Jung et al., 2005; Lorrain et al., 2003; Moeder & Yoshioka, 2008; Takahashi et al., 1999). The study of lesion mimicry in wheat and barley has also provided useful information on the defense against rusts (Anand et al., 2003; Kamlofski et al., 2007; Liu et al., 2021; Wright et al., 2013;

Zhang et al., 2019). Further investigation into the phenotype and genotype of both 1995 and 2048 could provide valuable insight into the plant immune system and the interactions between wheat and leaf rust.

RNAseq analysis allows for a snapshot of host gene expression during pathogen infection. By obtaining a list of differentially expressed genes, their general biological function, and a more specific pathway involvement can be assigned. From this a more accurate understanding of a phenotype can be obtained. RNAseq analysis of lesion mimics has provided an expression profile in a variety of crops. These studies show an increased expression of genes involved in the hypersensitive response to pathogens (Mu et al., 2021). For 1995 and 2048, it is clear that lesions are forming in the absence of leaf rust, and when challenged with leaf rust, disease was less severe. What remained unclear was if the plant was expressing a defense response that primed the plant against infection. With RNAseq, the expression profile, and presence or absence of a defense response can be determined.

1995

Macroscopic morphological characterization of 1995 shows a reduction in pustule size and quantity, indicating that there is a reduction in the ability of *P. triticina* to cause disease. Cytological examination was conducted to determine at which point during the infection process *P. triticina* is being interrupted by the mutant phenotype. Because 1995 exhibits the formation of spontaneous lesions, it was hypothesized that there is a constitutive hypersensitive-like response that results in the expression of PR genes. The constitutive expression of PR genes due to an HR-like response would expose spores to the plant defense response immediately after inoculation and result in a reduced ability of the fungus to colonize at all stages of infection.

The cytological examination of 1995 shows that there is a reduced colonization by *P. triticina* as early as 1dpi, as indicated by a greater number spores able to form germ tubes but failing to form appressoria. Reduction in hyphal colonization is apparent at days 3 and 5 post inoculation. At 3dpi there are a greater number of spores on 1995 that are unable to form appressoria and more spores unable to progress past appressoria formation compared to Thatcher. This point is driven home by the presence of fewer spores forming early intercellular hyphae and small colonies. At 5 dpi, in Thatcher, nearly all of the spores have progressed to form

large mats of hyphae. In 1995 this is not the case as indicated by the greater number of type 4 infections and lower number of type 5 infections compared to Thatcher. There are a greater number of spores unable to form appressoria or move past appressoria formation. Spores that have produced appressoria are progressing past initial intercellular hyphae development and produce colonies. However, there are a greater number of small colonies, and fewer large colonies at 5dpi in 1995 than in Thatcher.

Spontaneous formation of lesions, in 1995 suggest the dysregulation of cell death. The presence of colonies in 1995 indicates that there is indeed living tissue for the fungus to colonize. The microscopic visualization of a restriction of fungal growth, indicated by reduction in colony size at 5dpi, in living tissue indicates that the plant is expressing a defense response. In this case 1995 has what visually appears to be a constitutive hypersensitive like-responses. Lesion mimics have a similar phenotype. However, to determine whether the mutant lines are lesion mimics, there must be molecular evidence that supports the induction of a hypersensitive-like defense response. The regulation of normal plant defense responses is complex. There are many different possible points of dysregulation that could cause the lesion mimic phenotype. The lesion mimic phenotype is characterized by upregulated defense response genes and/or the dysregulation of normal SA/JA crosstalk (Yin et al., 2000).

In 1995, from the RNAseq data, there is clearly greater expression in defense related genes within resistant pools than in susceptible. These genes code for proteins with a wide variety of functions. Putative lesion mimic mutant 1995 has similar expression patterns of several proteins in common with other confirmed lesion mimics. Upregulation of PR1, PR5, thaumatin-like proteins, glucosidases, and chitinases are commonly seen in lesion mimics (Anand et al., 2003, 2004; Yin et al., 2000) and indicate that a HR is occurring. The increased expression of a peroxidase in 1995 combined with the evidence of reduced expression of a negative regulator of the plant defense response, further indicate that a defense response is occurring. The presence of proteins regulating the SAR, a cell wall invertase, an ALD1 homologue, and DIR1, further indicate that this defense response is systemic (Champigny et al., 2011; Herbers et al., 1996; Zhang et al., 2008). Lesion mimics have upregulated systemic defense responses (Yin et al., 2000). A DMR6-like protein and DMR6-like oxygenase 1, which are involved with the biosynthesis of SA and negatively regulates the plant defense (Thomazella

et al., 2021; Zeilmaker et al., 2015) are also downregulated. These two proteins are involved in the suppression of SA biosynthesis. SA in high levels initiates a feedback loop resulting in the overexpression of PR proteins (Anand et al., 2003). When SA is produced in high levels a SAR occurs. This shows further dysregulation of the normal plant defense and systemic acquired response. Additionally, high levels of SA can provide inherent defense to fungal pathogens and may be responsible for reduced growth of *P. triticina* in 1995. Decreased expression of photosynthesis related genes was observed in 1995 and is expected if the lesions that are forming in 1995 are resulting in cell death. Fewer viable cells result in less photosynthesis and expression of photosynthesis-related genes.

The evidence provided by RNAseq analysis of 1995 during infection with leaf rust supports the claim that 1995 is a lesion mimic. Microscopy data shows that the lesion mimic phenotype is resulting in the reduction of leaf rust infection, and colony formation. It is likely that the causative mutation in 1995 occurs within a gene regulating a normal plant defense response. The observed phenotype could be due to a mutation that results in reduced expression of a negative regulator of defense, or an increased expression of a positive regulator of defense.

2048

Similar to 1995, it was hypothesized that the causative mutation in 2048 resulted in the induction of a constitutive HR-like phenotype. If a constitutive HR-like response is present, then there will be increased expression of defense related genes. Additionally, due to the exposure of spores to defense gene products, a reduction in the ability of *P. triticina* to infect 2048 at all stages of infection will be observed. 2048 had a reduced ability to form infection structures as early as 1dpi. This reduction was primarily seen in the greater number of spores unable to form appressoria. At 3dpi there is a reduction in the ability of *P. triticina* to progress beyond appressoria formation in 2048, as indicated by a lower quantity of spores forming intercellular hyphae. However, there are an equal number of small colony forming spores between the two varieties. By 5dpi the majority of spores in Thatcher have advanced to form large colonies. In 2048 there is a reduction in the quantity of spores forming large colonies, but an increase in the spores forming small colonies. These results indicate that there is an overall reduced ability of the fungus to form appressoria at early stages, and intercellular hyphae at all stages of infection.

Based on the formation of spontaneous lesions in 2048, and the reduction in infection at all days post infection, it is likely that there is constitutive expression of defense related genes contributing to 2048's phenotype.

The presence of a constitutive HR-like response, as seen in 2048, is often the result of dysregulation of the plant defense response (Anand et al., 2003; Takahashi et al., 1999; S. Wang et al., 2017; Yuchun et al., 2021; Zeng et al., 2004) Constitutive expression of defense genes such as PR1, PR4, PR5, and SA, and the presence of cell death would explain the reduced ability of *P. triticina* to cause infection. The expression of PR genes and SA biosynthesis would protect the plant, and the presence of cell death would reduce the overall availability of viable cells for *P. triticina* to infect. It is likely, that both of these factors are contributing to reduced disease. To further characterize the phenotype of 2048, and determine if PR proteins are expressed, RNAseq analysis was conducted to obtain a snapshot of the mutant expression profile.

The RNAseq expression profile of 2048 is similar to that of 1995. However, there are key differences. In both 2048 and 1995 thaumatin-like proteins, PR1, and PR5 have increased expression. In 2048 PR4 also has increased expression. PR4 is involved in the defense against pathogens and development of a systemic required response (SAR) (Guevara-Morato et al., 2010; Stanford et al., 1989). Additionally, 2048 had lower levels of DMR6, indicating the dysregulation of the defense response.

In 2048 expression of proteins regulating the biosynthesis of JA was increased but not in 1995. Increased expression of 3-ketoacyl-CoA thiolases, and a plastid-lipid-associated protein 2 were seen. The dysregulation of SA/JA biosynthesis is a contributing factor to the development of lesion mimics (Bruggeman et al., 2015). Typically, JA is thought of as antagonistic to SA. SA is considered to be more important to plant protection from biotrophic pathogens, whereas JA is typically considered more important to response to wounding by herbivorous pests and necrotrophic pathogens (Tamaoki et al., 2013). However, it has been shown that JA is important in the modulation of ozone-induced HR-like cell death (Rao et al., 2000). If, a gene regulating JA biosynthesis has been upregulated it would be possible for a lesion mimic phenotype to develop that is entirely JA dependent. Having genes involved in SA biosynthesis, and genes involved in JA biosynthesis being increased in mutant pools compared to wild type pools, seems

contradictory, since they are antagonistic towards each other. However, Tamoaki (2013), found that treatment of rice with JA, doubled the expression of nearly one-fifth of SA regulating genes. So, even if the causative mutation results in JA biosynthesis, the lesion mimic may be the result of the accumulation of SA

The RNAseq data suggests that a hypersensitive response is occurring. Microscopic observations show a reduced ability of *P. triticina* to form early infection structures, and reduced ability to form intercellular hyphae later in the infection process. These two points, along with the presence of lesions in the absence of pathogens supports the conclusion that the causative mutation in 2048 is within a gene regulating the plant immune system. Resulting in a lesion mimic mutant with reduced susceptibility to *P. triticina*.

2348

Both macroscopically and microscopically, a reduction in colonization by *P. triticina* was observed in 2348. Analysis of the fungal infection process over the course of the initial six days of infection showed a reduction in the ability of *P. triticina* to cause disease in 2348 as early as 1dpi. Examination of the quantity of individual IT scores (Figure 2.8) at 3- and 5-days post inoculation shows that in 2348 there is a reduction in the ability of spores to progress past the formation of appressoria. In Thatcher, the composition of IT types at each day post inoculation, shows that there is a transition from predominantly low infection scores at 1dpi, to predominantly high infection scores at 5dpi, with most spores being able to form large colonies. However, in 2348 this trend is not seen. The quantity of spores at appressoria formation stagnates at IT 2 at 3dpi. Interestingly, at 3dpi there is a similar number of spores able to begin forming small colonies, and some ability of spores to form intercellular hyphae in 2348. Then at 5dpi large colonies begin to be formed in 2348. The number of spores at the appressoria stage at 5dpi is similar to that in 3dpi. However, the quantity of spores forming small colonies and intercellular hyphae in 2348 at 5dpi is similar to that in Thatcher. This point shows that the spores that were able to form early intercellular hyphae and small colonies are able to form large colonies. This indicates that the mutation in 2348 results in a reduction in the ability of *P. triticina* to successfully transition from the formation of appressoria to the development of intercellular hyphae and haustoria. A reduction in the ability of *P. triticina* to form intercellular

hyphae and haustoria could additionally account for the observed reduction in pustule size at the macroscopic level.

RNAseq expression analysis was inconclusive for 2348. The pooled samples and parents did not separate based on their phenotypes as 1995 and 2048 did. The 2348 parent paired with 2348 wild type pool 3 and thatcher paired with mutant pool 3, this is contrary to expected results of 2348 parent grouping with the mutant pools, and thatcher grouping with wild type pools. Likely, this is explained by incorrect phenotyping of infection types, and the unintentional inclusion of heterozygous individuals in pooled tissue. Due the aberrant differential expression data, the RNAseq data for 2348 is not currently useful in pathway analysis. Although RNAseq analysis was not able to be conducted on mutant line 2348, this line remains of interest as a potential susceptibility mutant. The disruption of *P. triticina'*s ability to form intercellular hyphae and haustoria, without the induction of a hypersensitive like response indicates a disruption in plant-microbe interactions that is not dependent upon the expression of an R-gene. Additionally, because the enhanced protection from *P. triticina* is observed at the seedling stage, it is unlikely that the responsible mutation occurred within an APR gene. To obtain a better understand the phenotype in 2348 expression studies must be conducted. Either by attempting the perform bulked segregant RNAseq analysis again, or by measuring expression levels of known defense genes via qPCR.

Conclusion

Based on the phenotyping and RNAseq data for 1995 and 2048 the conclusion can be drawn that both mutants are lesion mimics. However, it would seem, based on the differences in RNA expression data in 1995 and 2048, that the causative mutations likely occur in a different gene for each mutant. Further, it can be inferred that the causative mutation in 1995 and 2048 occurs in a gene regulating the activation or suppression of the plant defense response. Although lesion mimics are generally not agriculturally significant, mapping the mutation for each of these mutants will reveal useful information on the regulation of the plant defense response.

Microscopic analysis of the infection process by *P. triticina* on mutant line 2348 revealed a disruption in the ability of *P. triticina* to progress beyond appressoria formation and form intercellular hyphae. Due to the indications of 2348 being a susceptibility mutant, there is an

opportunity to provide breeders with a durable tool to combat *P. triticina* infection in wheat. However, the causative mutation has yet to be mapped.

As phenotypic analysis of mutant lines 1995, 2048, and 2348 was being conducted, a mapping study was set up to identify candidate mutations within each mutant line. Mapping the causative mutation in 1995, 2048, and 2348 will allow future projects to clone, and develop markers for the introgression of the causative mutations into varieties that are adapted to regional agriculture. To map the causative mutation in 1995, 2048, and 2348 the identification of SNPs within the mutant lines and associating the SNPs with the mutant phenotype. By using multiple methods of SNP identification, the number of SNPs associating with the mutant phenotype can be reduced to only those consistent between methodologies.

Chapter 3 - Genotyping mutant lines and mapping candidate genes

Introduction

Disease is a significant cause of agricultural losses. In wheat, disease caused by the rust fungi *Puccinia graminis* f.sp. *tritici, P. striiformis* f.sp. *tritici,* and *P. triticina* Eriks (Roelfs et al., 1992) are of particular interest. Although it is often overshadowed by *Pgt* and *Pst,* leaf rust, caused by *Puccinia triticina,* is more globally widespread than *Pgt* and *Pst.* Additionally, *P. triticina* infection can cause up to 20% loss over large areas when uncontrolled (Bolton et al., 2008; Kolmer, 2020). Protecting wheat from *P. triticina* is critical to preventing losses. One method of protecting wheat from leaf rust is to deploy major resistance (*R*) genes. The majority of known *R*-genes follow the gene-for-gene model, that states, *R*-genes recognize the products of a specific *avr*-gene that is present in the pathogen. When *R*-genes are able to detect the corresponding *avr*-gene product the plant elicits a defense response. If the *avr*-gene product is unable to be detected by the corresponding *R*-gene, disease occurs (Flor, 1947). These *R*-genes most commonly code for nucleotide binding site-leucine rich repeats (NBS-LRRs)(Meyers et al., 2005; Shao et al., 2016), and *avr* genes most commonly encode effectors (Saur et al., 2019). *R*-gene based defense generally results in the expression of a qualitative HR response (Dietrich et al., 1994; Greenberg et al., 1994). This HR response puts selection pressure on pathogen populations to overcome the *R*-gene, leading to a loss of efficacy. To protect wheat from leaf rust constant development of major *R*-genes is necessary. Another method of leaf rust control is the use of slow rusting adult plant resistance (APR) genes. APR genes confer resistance to rusts at the adult stage of the plant. Rather than eliciting an HR response, the APR induced defense response tends to be less intense that results in a delayed development of rust. Although this protection is less intense it seems to be more durable.

Reduction of susceptibility to disease is a way to protect a plant from disease by preventing the pathogen from utilizing host factors that are normally required by the pathogen to facilitate disease. Attempting to reduce susceptibility is an intriguing method of leaf rust

protection. The use of susceptibility (S) genes may provide a more durable form of protection than the use of *R*-genes. Currently, there aren't any leaf rust S-genes genes that have been identified. Studies in stem and stripe rust (Huai et al., 2020; Q. Zhang et al., 2020) have shown that knocking out S-genes results in reduced disease development. By inducing random mutations and selecting for reduced disease development new S-genes may be identified. Prior to this experiment, mutant lines with reduced disease severity were generated. Seeds were treated with ethyl-methanesulfonate to induce random mutations, and then selected for reduced disease severity when plants were exposed to leaf rust. These plants were then selfed to the M_8. Three of these mutant lines, 1995, 2048, and 2348, were used in this study. The intention of this study is to map candidate SNPs for the purpose of identifying the causative SNP, and understanding the genetic mechanism that controls the mutant phenotype.

By utilizing the Chinese spring wheat genome (Alaux et al., 2018), Illumina next-generation sequencing (NGS) (Illumina Inc., CS, USA), genotype-by-sequencing (GBS) (Poland et al., 2012), and exome capture (Krasileva et al., 2017) mapping can be can be conducted. In this study we utilize a bi-parental mapping population genotyped using a two-restriction enzyme GBS to perform association mapping and quantitative trait loci (QTL) mapping.

Association mapping detects correlations between the genotypes of markers within the mapping population and the phenotypes of the mapping population based on linkage disequilibrium. Previous analysis of the sorting ratios during the generation of the mutant lines revealed that the mutant phenotypes in the mutant lines for this study are the result of single gene effect. By using the F_4 generation, heterozygosity within the mapping population should be limited and the population should be approaching a 1:1 ratio for homozygous dominance and homozygous recessiveness. Association mapping has higher probabilities of obtaining false positives than QTL mapping (Pritchard et al., 2000). The removal of heterozygosity in the mapping population decreases probability of erroneous association of SNPs to the mutant phenotype and therefore reduces false positives.

To further increase the confidence of mapping results, QTL mapping and exome capture results can be combined with association mapping. QTL mapping identifies genomic locations that associate with the phenotype based on linkage information from the mapping population. A

genetic map can then be generated for regions with high association for the mutant phenotype. QTL analysis determines how each of these significant loci contribute to the overall phenotype. Using phenotype effect data for the significant traits it can be determined if the phenotype is the result of a single major-effect loci or several minor-effect loci. Using the significant loci's regions of confidence can be obtained and use for comparison with other mapping data to narrow the candidate region containing the causative SNP.

Exome capture utilizes probes to selectively sequence the protein coding regions of a genome. The wheat genome is highly repetitive, is large (~17Gb), and is comprised of >95% non-coding DNA (IWGSC, 2014). The use of exome capture greatly reduces the amount of genetic information that is sequenced while retaining that which is of the most interest. This reduces the amount of time, and resources needed to obtain genotyping information. Additionally, the Curio Genomics variant analysis browser makes analysis of genotyping data simple and efficient. By combining SNP results from exome capture with SNP data obtained through mapping studies and keeping the common regions, a list of high confidence candidate SNPs can be generated.

Materials and Methods

Generating Mapping Lines

The generation of mutant lines are described in Chapter 2. F_4 plants were generated for use in genotyping-by-sequencing (GBS) by initially crossing mutant M_6 lines to hard red winter wheat line KS061705M11. This initial cross was performed by Dr. Mary Guttieri in the Hard Winter Wheat Genetics Research Unit (HWWGRU) of the USDA Agriculture Research Service (ARS). Using two plants from each cross, 96 seeds per plant were then planted in root trainers containing MetroMix 360 (Sun-gro, Vancouver, CA). These seeds were then placed in vernalization at 10ºC for six weeks. While in vernalization the plants had 12hr exposure to light. After six weeks, the seedlings were placed in a growth chamber at 20ºC with 12hr light exposure. At the 2-3 leaf stage of growth these plants were inoculated with *P. triticina* isolate TNRJ in a 10mg urediniospores/per 3mL suspension of Soltrol 170 that was sprayed through an atomizer at 40psi. After inoculation the plants were placed in a dew chamber at 20ºC with 100%

humidity for 16 hours (Bruce et al., 2014). These plants were then removed from the dew chamber and returned to the growth chamber. Ten days after inoculation plants were scored for the phenotype of interest. In crosses to 1995 and 2048, plants were phenotyped for spontaneous formation of a hypersensitive-like response. In crosses to 2348, reduction in pustule quantity and size was scored for using the following scale. visually rated using a 0-4 scale (0- no infection, ";" fleck - small hypersensitive response, 1-2 small moderate uredinia pustules, 3-4 moderate to large pustules; Long and Kolmer, 1989). Plants rated 0-2 were deemed resistant, and those rated 3-4 were deemed susceptible. These plants were then transplanted into larger pots. Transplanted plants were placed in a greenhouse at 18-22ºC with 16h/8h day/night cycle of artificial sodium pressure lighting 250 µE (Neugebauer, 2018). Plants were bagged and allowed to self-fertilize. Then, utilizing single seed descent, this process was repeated out to the F_4 generation. In the F_4 populations there was a total of 97 and 134 individuals for lines 1995 and 2048 respectively.

Tissue Collection and DNA extraction

At each generation, at the 2-3 leaf stage, three 2cm segments of tissue were collected and placed in a 96 deep well plate. Tissue from each plant was kept in separate wells. After tissue collection, plants were dehydrated using a Labconco Free Zone 6 freeze dryer (Kansas City, MO) set at 0psi and -4ºC. Tissue was sent to the USDA Genotyping Lab at the USDA HWWGRU at Kansas State University for DNA extraction, quantification, and normalization. DNA was extracted using a 2% cetyltrimethylammonium bromide (CTAB) and chloroform:isoamyl (24:1 v/v) alcohol methodology (Saghai-Maroof et al., 1984), with a modification using 4mM tris 2-carboxyethyl phosphine (TCEP) instead of 2-mercaptoethanol with an added 40µg of RNase (Amresco, Solon, OH) (A. Bernardo et al., 2020). DNA was then quantified with a Quant-iT PicoGreen dsDNA HS assay kit (ThermoFisher, Waltham, MA) on a FLUOstar Omega fluorescence plate reader (BMG LABTECH, Cary, NC). Once quantified, DNA was normalized to 20 ng/µL with 10mM Tris using the Mantis liquid handling system from Formulatrix (Bedford, MA) (A. Bernardo et al., 2020).

Genotyping-by-sequencing

Extracted DNA was genotyped according to Poland et al. (2012). Genomic DNA from F_4 tissue was digested in a 10µL reaction volume of restriction master mix containing 2µL of 10X

Buffer 4, 0.4µL of *HF-PstI* and *MspI* (New England BioLabs Inc., Ipswich, MA 01938), and 7.2µL of H_2O per sample. The digestion reaction was performed for 2 hours at 37ºC and then at 65ºC for 20 minutes. In the same tube a ligation reaction was performed. 5µL of adapters and 15µL of ligation master mix were added to the digestion product. Ligation master mix contained 2µL of NEB buffer4, 4µL of ATP at 10mM, 0.5µL of T4 DNA ligase, and 8.5µL of H_2O per sample. The ligation reaction was completed at 22ºC for 2 hours and then held at 65ºC for 20 minutes. To multiplex the samples, and generate a single library, 5µL from each ligation sample was pooled into a single tube. This pool was cleaned up using the QIAquick PCR Purification Kit (QIAGEN, Hilden, Germany). 200uL of pooled ligation DNA was combined with 1mL of buffer PB. This mixture was then added to a column and spun down. The DNA was resuspended in 60uL. This pool was PCR amplified with a 30 second denaturation at 95ºC. Amplification was done with 18 cycles of 30 seconds at 95ºC followed by 30 seconds at 62ºC and then 30 seconds at 68ºC. Extension was then conducted at 72ºC for 5 minutes. PCR products were sequenced using an Illumina NextSeq 2000. Sequences were analyzed using the Tassel5 GBS v2 Pipeline (https://bitbucket.org/tasseladmin/tassel-5-source/wiki/Tassel5GBSv2Pipeline). Tags were identified from fastQ input files. Sequences were trimmed. The full set of reads was examined for unique tags and collapsed into a matrix of presence/absence for each sample. This generated a list of SNPs for each individual in the mapping lines. This list was then used in association mapping via TASSEL5 v5.2.79, as well as in QTL mapping and linkage map generation with QTL ICIMapping v4.2

Association mapping

The .hmp file generated in GBS was imported into TASSEL5 v5.2.79, generating a genotype file. Phenotypes of each individual in the population were imported into TASSEL5. Phenotypes were designated as “0” for absence of the mutation and “1” for the presence of the mutation. Genotype file and phenotype file were merged using TASSEL5’s “union join” function. The merged list was analyzed for genotype association with the mutant phenotype using a general linear model (GLM). GLM evaluates each trait by marker combination for association with the mutant phenotype. For GLM, no statistics file, genotype effect file, BLUEs file, ANOVA file or site state file was used. Max P value was set to 1.0. The number of permutations was locked at 0 and minimum class size was 0. The options “Run permutations”,

“Bi-allelic sites only”, “output site states”, and “append effect estimates to stats” were not used. GLM analysis generated a list of SNPs and statistics for each marker. From the statistics list, a Manhattan plot was obtained that plotted the p-values for the association of each SNP to the mutant phenotype. Parameters for Manhattan plotting are set by TASSEL5. SNPs obtained from GBS were converted from their genotyped alleles to an A/B/H code indicating which parent the allele was inherited from. The excel sheet, ”2_Parent_Cross_using_REF_PIPELINE_DATA,_GBS_tag_stats_and_conversion.xlsx” obtained from the HWWGU website (https://hwwgenotyping.ksu.edu/protocols/GBS_protocols/USDA_Bioinformatics_Server_Training/4._Ref_pipeline/) was used for converting SNPs to A/B/H format. Using this format, SNPs were organized into haplotype blocks in excel to find confidence windows of SNPs associating with the mutant phenotype.

Exome Capture

Five seeds from the parent line Thatcher and mutant lines 1995, 2048, and 2348 at the M_8 generation were planted in small pots containing MetroxMix 360 (Sun-gro, Vancouver, CA). These pots were then placed in a growth chamber at 20C with 24hr of light. At the 2-3 leaf stage of growth these plants were inoculated with *P. triticina* isolate BBBDB in a 10mg urediniospores/per 3mL suspension of Soltrol 170 that was sprayed through an atomizer at 40psi. After inoculation the plants were placed in a dew chamber at 20C with 100% humidity for 16 hours (Bruce et al., 2014). These plants were then removed from the dew chamber and returned to the growth chamber. At 6 days post inoculation tissue from each of the five plants per line was collected and placed into 1.5mL microcentrifuge tubes. Tissue was then placed in a -80C freezer until ready to be extracted.

DNA from M_8 plants was isolated using a modified version of Schwessinger and McDonald’s (2017) method for obtaining high quality DNA for long read sequencing. Modifications to the protocol were as follows. 50µL of 10mg/ml RNAse A was added to the ground tissue and isolation buffer solution. This solution was mixed for 1 hour at room temperature. Proteinase K was added to this mixture, and the solution was mixed again for 1 hour. All mixing was conducted using a rotator genie set to the slowest speed. 15mL of

phenol/chloroform/isoamyl alcohol was used to separate DNA from proteins and lipids and rotated for 5 minutes. Extracted DNA was resuspended in 500µL of 0.1 Tris HCL pH 8.5 (Qiagen EB). To clean up extracted DNA 50µL of 5M Sodium Acetate pH 5.2 and 500µL of 100% Isopropanol was added to resuspended DNA and gently mixed by inversion. This suspension was spun at 8000g for 30 minutes. To wash, 1mL of 70% EtOH was added. EtOH was eluted and the sample was air dried. 200µL of 0.1 Tris HCL pH 8.5 (Qiagen EB) was then added and quality was checked. 80µL of MagPure beads was added to the DNA, rotated for 5 minutes, and then placed on magnets. DNA/bead mixture was washed twice with fresh 70% ethanol. Ethanol was removed, samples were air dried, and DNA was resuspended in 50µL of 0.1 Tris HCL pH 8.5 (Qiagen EB). DNA was then quantified.

Extracted DNA was sent to Arbor Biosciences for sequencing and exome capture. Analysis of exome capture data was conducted using the Curio Genomics variant analysis browser. To identify SNPs of interest, the exome of each mutant and Thatcher was compared to the IWGSC Chinese spring wheat reference sequence v2.1 (Alaux et al., 2018). To filter out the SNPs due to differences in Chinese spring wheat and Thatcher, only SNPs not shared between Thatcher and the mutant lines were retained. SNPs present only in the mutant lines were then filtered for homozygosity and read depth of at least five reads. These SNPs were filtered to retain only transition mutations (G to A, and C to T), due to the preferential nature of EMS to induce these mutations. The remaining SNPs were then compared to the regions of interest obtained through association mapping. A final filtering of SNPs was done according to their shared nature between mutants.

Results

Generating mapping populations

The first step in mapping was to create a mapping population. The total number of individuals decreased during each generation due to losses during the vernalization step. Previously 1995 was observed to be a single recessive gene and have a 3:1 (non-mutant:mutant) sorting ratio when backcrossed to the wild type Thatcher. From the initial 192 seeds planted in

the 1995xKS061705M11 F_2 generation, a total of 97 individuals were retained in the F_4. For 97 seeds, the expected sorting ratio for an F_4 population with a single recessive gene is 55:42. The 1995xKS061705M11 yielded 43 individuals negative for the mutant phenotype, and 54 positive for the mutant phenotype at the F_4. These results show there is no significant difference ($p=0.1142$) at $\alpha=.05$, between the expected and observed ratio. The F_4 generated from 2048xKS061705M11 had a total of 134 individuals. Previously, when 2048 was backcrossed to Thatcher, a 3:1 ratio of non-mutant to mutant phenotypes was observed. Indicating that the mutation in 2048 is the result of a single recessive mutant allele. The expected sorting ratio for 134 individuals with a single recessive gene at the F4 is 75:59 for non-mutant:mutant. The cross 2048xKS061705M11 yielded 74 that were negative for the mutant phenotype and 60 individuals positive for the mutant phenotype at the F_4. There is no significant difference ($p=0.902153$) at $\alpha=.05$ from the expected sorting ratio and previous observations. In the 2348xKS061705M11 F_4 generation a total of 99 individuals were retained. In backcrosses of 2348 to Thatcher, a 3:1 sorting ratio for non-mutant to mutant phenotype is observed. Indicating a single recessive gene is responsible for the mutant phenotype. The expected sorting ratio for 99 individuals at the F4 population with a single recessive gene is 56:43. The 2348xKS0617M11 F_4 population yielded 46 individuals positive for the mutant phenotype, and 53 individuals negative for the mutant phenotype. These results are consistent ($p=0.27159$) with the expected results.

Genotyping-by-sequencing

GBS generated a list of SNPs present in the 97 individuals used in 1995 and the 134 individuals in 2048. 2348 was unable to be sequenced and genotyped due to low DNA quality after extraction. For 1995, 8426972 SNPs were identified. In 2048, 10032192 SNPs were identified. The SNPs were input into TASSEL5 for association mapping, and ICIM for QTL mapping.

Association mapping with TASSEL5

1995

By utilizing the GLM function in TASSEL5 and then generating a Manhattan plot, the SNPs that associate with the mutant phenotype were mapped to a chromosomal location. In

1995, chromosomes 2D, 3A, 4B, 5D, and 7B had regions containing SNPs with high association with the phenotype of interest (Figure 3.1A). The SNPs within these regions had P-values<$1x10^{-5}$ For association with the mutant phenotype. Within these regions there was a total of 17 SNPs (Figure 3.1B). The SNP at position 1323477 on chromosome 4B had the highest association with the mutant phenotype seen in 1995. The next highest association could be found on chromosome 7B at positions 354384484, 354384494, and 354384525. All three of these locations had the same p-value of $4.91x10^{-6}$. However, these SNPs were not located within an annotated gene in the available reference genome. The third highest association could be seen at position 572043332 on chromosome 2D, and the fourth highest association could be seen at positions 515096559 and 515096574 on chromosome 3A. These seven SNPs have the clearest association with the phenotype of interest. All 17 SNPs were utilized to define intervals of confidence.

An interval on chromosome 2D was identified flanking the marker 2D_572043332 from 569,000,000-572,890,000bp. On chromosome 3A the interval falls between 511,000,000-519,000,000bp, however genotyping returned few allele calls for markers within this interval, reducing the overall capability of accurate association. The SNP at 1323477 on chromosome 4B was within a block of inheritance that encompassed the additional SNPs identified as significant on chromosome 4B. This interval extends from 450,000-5,300,000bp. No interval was identified on chromosome 5D from the SNPs of significance. Sorting allele calls based on inheritance did not yield any marker blocks. Chromosome 7B markers 7B_354384484, 7B_35484494, and 7B_354384525 fall within an interval between 353,000,000-356,000,000bp. Also, on Chromosome 7B is a window from 721,000,000-721,500,000 that encompasses SNPs at loci 721220443 and 724220453.

A.

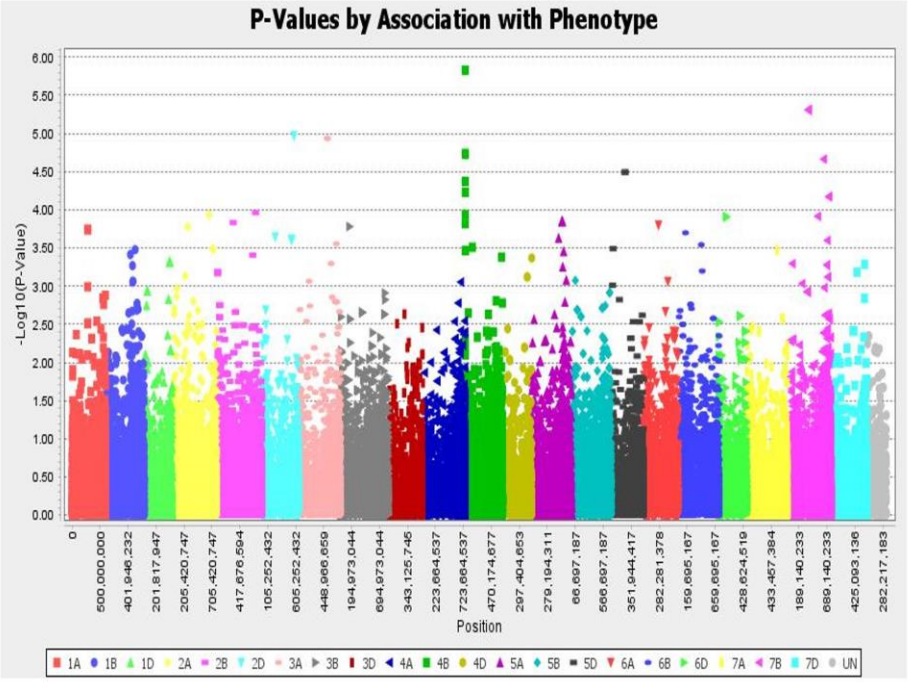

B.

Chromosome	SNP Position	p-value
4B	1323477	$1.48x10^{-6}$
7B	354384484	$4.91x10^{-6}$
7B	354384494	$4.91x10^{-6}$
7B	354384525	$4.91x10^{-6}$
2D	572043332	$1.07x10^{-5}$
3A	515096559	$1.16x10^{-5}$
3A	515096574	$1.16x10^{-5}$
4B	3071155	$1.85x10^{-5}$
4B	3071156	$1.85x10^{-5}$
7B	627366832	$2.12x10^{-5}$
5D	241133666	$3.21x10^{-5}$
5D	241133685	$3.21x10^{-5}$
4B	2134332	$2.26x10^{-5}$
4B	2134366	$2.26x10^{-5}$
4B	4756780	$5.88x10^{-5}$
7B	721220453	$6.72x10^{-5}$
7B	721220443	$6.72x10^{-5}$

Figure 3.1

A) Manhattan plot for SNP association with mutant phenotype in 1995xKS061705M11 F_4 populations for level of association with the mutant phenotype. Each Chromosome is represented by an individual color and shape combination indicated in the key at the bottom of the graph. B) List of SNPs with significant association (P-values<$1x10^{-10}$).

2048

Utilizing the GLM results and Manhattan plot function in TASSEL5 the SNPs associating with disease resistance were identified in 2048 (Figure 3.2A). Chromosome 4B has the greatest levels of association with the mutant phenotype (Figure 3.2B). A 12 SNP group in chromosome 4B can be seen to have high association with p-values<$1x10^{-11}$. The remaining five SNPs with high association come from chromosomes other than 4B. The next two SNPs with the highest association to the mutant phenotype were on Chromosome 7B. One at position 703572334 and the other at position 703572367. Chromosome 3B had one SNP at position 547446552 that high a p-value=$4.7x10^{-10}$. Chromosome 6B had one two SNPs with high association to the phenotype of interest at positions 82883296 and 82883335, both with a p-

value=5.6x10^{-10}. All 17 SNPs identified as significant were used in defining intervals of confidence.

One interval was identified on chromosome 4B, 884,672-5,401,027bp. This window encompassed all 12 SNPs identified on 4B in association mapping. On chromosome 7B one interval was identified between 703,400,000-703,600,000. Marker 3B_547446552 was flanked by an interval from 547,200,000-548,800,000. SNPs identified on 6B did not correlate with a block of alleles inherited from the resistant parent. No confidence interval was determined.

A.

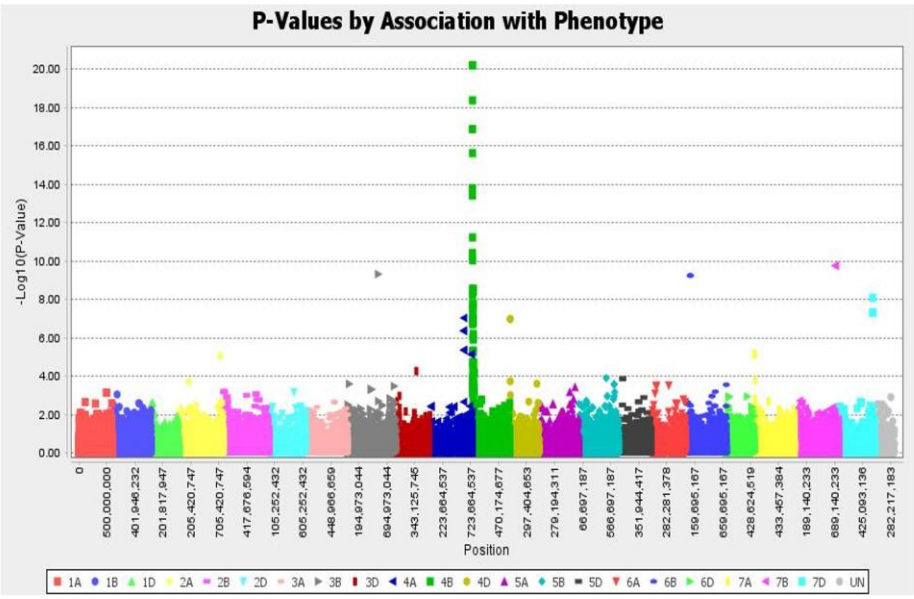

B.

Chromosome	SNP Position	p-value
4B	5400998	6.25x10^{-21}
4B	5401027	6.25x10^{-21}
4B	4756780	4.18x10^{-19}
4B	3071155	1.32x10^{-17}
4B	3071156	1.32x10^{-17}
4B	5038895	2.4x10^{-16}
4B	1323477	1.66x10^{-14}
4B	1386663	3.83x10^{-14}
4B	4687017	5.8x10^{-12}
4B	2212383	3.74x10^{-11}
4B	1359663	6.02x10^{-11}
4B	5891778	9.2x10^{-11}
7B	703572334	1.7x10^{-10}
7B	703572367	1.7x10^{-10}
3B	547446552	4.7x10^{-10}
6B	82883296	5.6x10^{-10}
6B	82883335	5.6x10^{-10}

Figure 3.2

A) Manhattan plot of SNPs from 2048xKS061705M11 F_4 populations for level of association with the mutant phenotype. Each Chromosome is represented by an individual color and shape combination indicated by the key at the bottom of the graph. B) List of SNPs with significant association (P-values<1x10^{-10}).

Exome capture

For both 1995 and 2048 M8 lines, 230,266,029 total genomic positions were analyzed for SNPs in exonic regions. In 1995 90.87% (209,252,532 positions) of genomic positions were covered, and in 2048 94.35% (217,249,315 positions) were covered. 42,268,464 overlapping reads were sequenced in 1995. This accounted for 5,524,905,849 overlapping bases and an

average read depth of 23.99 reads. In 2048 80,345,401 overlapping reads were sequenced, with a total of 10,538728,987 overlapping bases and an average read depth of 45.77 reads. After filtering for SNPs present only due to the treatment of seeds with EMS, Thatcher had 188,170 variants, 1995 had 328,696, and 2048 had 298,282. Each mutant was analyzed for the presence of SNPs in the regions of significance identified through association remapping.

A total of nineteen SNPs of interest in 1995 were found through exome capture using the windows identified in association mapping to narrow the regions of interest (Figure 3.7). The window from 1-5,300,000bp on chromosome 4B had the highest association with the mutant phenotype in 1995. Within this window five SNPs identified by exome capture were determined to be of interest. The window with the next highest association with the mutant phenotype in 1995 occurred on Chromosome 7B from 352,000,000-356,000,000bp. No SNPs were identified within this region using exome capture. Four SNPs were identified in 1995 by exome capture within the window on Chromosome 2D within 569,000,000-572,890,000bp. The window on Chromosome 3A from 511,000,000-519,000,000 had ten SNPs of interest. One SNP was identified on chromosome 7B between 721,000,000-721,500,000, however this SNP is shared with 2348, and is thus considered not of interest.

Table 3.1

SNPs of interest captured by exome sequencing in 1995 that are present in windows identified by association mapping. SNPs marked with an asterisk (*) indicate that the mutation is shared between 1995 and 2048. Putative gene names were obtained from transcripts of the IWGSC reference genome for Chinese Spring Wheat v1.1. Putative GO terms are the results of analysis of gene ontology terms as assigned by AmiGO2 in the IWGSC wheat reference genome browser.

Chromosome	Region	Position	Mutation Type	Putative Gene	Putative GO term
2D	569,000,000-572,890,000bp	569,132,768	G→A	TraesCS2D02G463300	Protein kinase activity
		569,783,877	G→A	N/A	N/A
		569,986,559	G→A	N/A	N/A
		572,789,585	G→A	TraesCS2D02G467900	Aminomethyltransferase activity
3A	511,000,000-519,000,000bp	513,308,167	C→T	TraesCS3A02G284300	DNA binding
		513.550,954	C→T*	TraesCS3A02G284600	Structural constituent of cell wall
		514,216,981	G→A	TraesCS3A02G285700	Mn ion binding
		517,845,633	C→T	N/A	N/A

		518,020,097	C→T*	TraesCS3A02G289400	DNA binding
		518,020,128	C→T*	TraesCS3A02G289400	DNA binding
		518,020,130	C→T*	TraesCS3A02G289400	DNA binding
		518,026,873	C→T	TraesCS3A02G289400	DNA binding
		518,028,227	C→T	TraesCS3A02G289400	DNA binding
		518,980,685	C→T	N/A	N/A
4B	450,000-5,300,000bp	1,153,783	G→A	N/A	N/A
		3,161,112	C→T	N/A	N/A
		3,348,491	C→T	TraesCS4B02G004800	Defense Response
		3,828,677	G→A*	TraesCS4B02G005600	Extracellular Region
		5,045,240	G→A	N/A	N/A

A total of thirty-four SNPs of interest in 2048 were found through exome capture using the windows identified in association mapping (Figure 3.8). The window from 1-5,402,000bp on chromosome 4B had the highest association with the mutant phenotype in 2048. Within this window, thirty-two SNPs identified by exome capture were determined to be of interest. The window with the next highest association with the mutant phenotype in 2048 occurred on Chromosome 7B from 703,400,000-703,600,000bp. No SNPs were identified within this region using exome capture. The window on Chromosome 3B from 547,200,000-548,800,000 had one SNPs of interest.

Table 3.2

SNPs of interest captured by exome sequencing in 2048 that are present in windows identified by association mapping. SNPs marked with an asterisk (*) indicate that the mutation is shared between 1995 and 2048. Putative gene names were obtained from transcripts of the IWGSC reference genome for Chinese Spring Wheat v1.1. Putative GO terms are the result of analysis of gene ontology terms as assigned by AmiGO2 in the IWGSC wheat reference genome browser.

Chromosome	**Region**	**SNP position**	**Mutation Type**	**Putative Gene**	**Putative GO Term**
3B	547,200,000-548,800,000bp	547,899,094	G→A	N/A	N/A
4B	884,000-5,402,000bp	930,790	C→T	N/A	N/A
		1,135,209	C→T	TraesCS4B02G002100	Cellular component organization
		1,292,877	G→A	TraesCS4B02G002600	Nucleotide binding
		1,305,531	C→T	TraesCS4B02G002600	Nucleotide binding

		1,305,717	G→A	TraesCS4B02G002600	Nucleotide binding
		1,339,169	C→T	TraesCS4B02G002700	ATP binding
		1,339,206	C→T	TraesCS4B02G002700	ATP binding
		1,353,798	G→A	N/A	N/A
		1,362,286	C→T	N/A	N/A
		1,407,919	G→A	N/A	N/A
		1,407,993	G→A	N/A	N/A
		2,024,126	G→A	TraesCS4B02G003500	Nucleic acid binding
		2,024,154	C→T	TraesCS4B02G003500	Nucleic acid binding
		2,413,523	C→T	TraesCS4B03G003900	Cysteine-type endopeptidase activity
		2,998,349	C→T	N/A	N/A
		3,057,216	C→T	N/A	N/A
		3,057,238	C→T	N/A	N/A
		3,127,181	G→A	N/A	N/A
		3,128,071	G→A	N/A	N/A
		3,191,318	C→T	N/A	N/A
		3,191,388	G→A	N/A	N/A
		3,604,373	C→T	N/A	N/A
		3,828,677	G→A*	TraesCS4B02G005600	Extracellular region
		3,876,103	C→T	TraesCS4B02G006000	Monooxygenase activity
		3,881,336	G→A	TraesCS4B02G006100	Defense response
		4,544,593	C→T	TraesCS4B02G006800	Acetyl-CoA biosynthetic process from pyruvate
		4,544,596	C→T	TraesCS4B02G006800	Acetyl-CoA biosynthetic process from pyruvate
		4,546,291	G→A	TraesCS4B02G006800	Acetyl-CoA biosynthetic process from pyruvate
		4,546,335	G→A	TraesCS4B02G006800	Acetyl-CoA biosynthetic process from pyruvate
		4,760,926	G→A	N/A	N/A
		4,760,956	G→A	N/A	N/A
		5,043,742	G→A	N/A	N/A

Discussion

The EMS mutant lines 1995, and 2048 exhibit spontaneous development of a hypersensitive like response, which is indicative of a lesion mimic phenotype. Lesion mimics have been used for several decades to provide insight into the molecular workings of the plant immune system, its regulation, and signaling (Bruggeman et al., 2015; Johal et al., 1995; Y.-H. Jung et al., 2005; Lorrain et al., 2003; Moeder & Yoshioka, 2008; Takahashi et al., 1999). The study of lesion mimicry in wheat has also provided useful information on the defense against rusts (Anand et al., 2003; Kamlofski et al., 2007; Liu et al., 2021; Wright et al., 2013; Zhang et al., 2019). The causative mutation for the mutant phenotypes in 1995 and 2048 need to be identified and, be investigated for potential causal genes. For the identification of lesion mimics, regions associating with the mutant phenotype that contain genes involved in the host defense response are of particular interest.

TASSEL5 uses a least squares fixed effects linear model to calculate p-values for the association of each marker and sample combination with the sample phenotype. In the 1995xKS0617M11 F_4 population, 18 SNPs on five chromosomes associated with the mutant phenotype. Although the SNPs seen in 2D, 3A, 5D, and 7B do not have as high of association with the phenotype of interest as the region in 4B, of these SNPs were used to find confidence intervals from haplotype blocking. Haplotyping these SNPs provide confidence intervals from 569,000,000-572,890,000bp on chromosome 2D, 511,000,000-519,000,000bp on chromosome 3A, 450,00-5,300,000bp on chromosome 4B, 353,000,000-356,000,000 on 7B, and 721,000,000-721,500,000 on Chromosome 7B. These windows provide a confidence window for extracting SNPs identified by exome capture.

The second genotyping method, exome capture, utilizes probes specific for exonic regions of the genome to sequence coding DNA within the genome. This greatly reduces the size of the genome being sequenced and thus the amount of data being provided. The reduction in data is useful. It limits the amount of processing needed, but still provides information on the regions of greatest interest to most studies (Bayer et al., 2019). Using the windows of significance identified from association studies in TASSEL5 done with 1995 and 2048 GBS data, the presence of SNPs within coding regions of the genome can be examined. Because 1995

and 2048 have similar phenotypes, it is possible responsible the responsible mutation is shared between them, thus SNPs shared between 1995 and 2048 were retained during exome capture analysis, as well as the SNPs present only in each respective mutant line. However, if SNPs were shared between 2348 and 1995 or 2048, these SNPs were determined to be unable to be responsible for the mutant phenotype due to the differences in phenotyping.

In 1995 a total of nineteen SNPs of interest in 1995 were identified using the windows identified in association mapping. The interval from 450,000-5,300,000bp on chromosome 4B contained five SNPs of interest. The intervals on Chromosome 7B from 352,000,000-356,000,000bp and 721,000,000-721,500,000 contained no SNPs. Four SNPs were identified on Chromosome 2D within 569,000,000-572,890,000bp. Chromosome 3A from 511,000,000-519,000,000 had ten SNPs of interest.

The IWGSC Jbrowse window, with the Chinese spring wheat reference genome v1.0 (Alaux et al., 2018) was searched by SNP position to identify genes in which SNPs occurred. Several SNPs identified by exome capture did not locate to any genes in the reference genome. Considering that exome capture only sequences coding DNA, this poses a conundrum. However, an easy explanation exists. The mutant lines originated from Thatcher, and the only reference genome for wheat comes from Chinese spring wheat. This may cause differences in genome composition. Because SNPs present in mutant lines are reported by position in exome capture, variations in the reference genome may cause inaccuracies when trying to correlate the positions of SNPs from exome capture to positions in the reference genome.

From the exome capture SNPs identified in 1995, eight candidate genes were identified on three chromosomes. As mentioned previously, of particular interest in 1995 are genes that could potentially contribute to a lesion mimic like phenotype, especially defense genes. In 1995 only one SNP was identified in a defense response gene, TraesCS4B02G004800. This SNP occurred on chromosome 4B at 3,348,491bp. The nearest SNPs identified by association mapping were at 3,071,155 and 3,071,156. Their p-value for association was 1.85×10^{-5}. The sequence for TraesCS4B02G004800 was analyzed with the BLASTn algorithm (Zhang et al., 2000) and revealed a similarity to a predicted *Triticum aestivum* disease resistance RPP13-like protein 1 (query coverage=69%, percent identity=100%). Although defense response genes are

of primary interest, they are not the only potential contributors to a lesion mimic like phenotype. Interestingly one gene on 2D contained a SNP, TraesCS2D02G463300, with protein kinase activity. The plant defense response is tightly regulated, and the disruption of regulators may result in a lesion mimic phenotype. Protein kinases are known to play important roles in regulating the plant defense response. Several rice lesion mimics have been identified with mutated protein kinases (Yuan et al., 2007; Yuchun et al., 2021). Further, the SNP on 2D identified by exome capture correlates with an interval from association mapping with a p-value of $1.07x10^{-5}$, the third highest association with the mutant phenotype in 1995. These two genes are interesting in their potential to cause the mutant phenotype. However, no clear conclusions can be drawn without conducting downstream experiments. To fine map the causative mutation in 1995 the confidence intervals from association mapping, containing SNPs from exome capture will be used. These intervals are 569,000,000-572,890,000bp in chromosome 2D, 411,000,000-519,000,000bp in chromosome 3A, and 450,000-5,300,000bp on chromosome 4B.

By comparing SNPs from exome capture of 2048 to the intervals identified by association mapping of 2048xKS0617M11 F_4 mapping population, 34 SNPs were identified. Chromosome 3B had one SNP within interval 547,200,000-548,800,000. This SNP did not correlate with a gene annotated by the Chinese spring reference genome v1.1 (Alaux et al., 2018). The remaining 33 SNPs were found within the intervals 884,672-3,029,539bp and 3,029,552-5,401,027bp on chromosome 4B. As mentioned with 1995, genes with roles in plant defense against pathogens are of particular interest, due to their potential roles in a lesion mimic phenotype. Because 2048 also exhibits a lesion mimic like phenotype, SNPs occurring within defense response genes remain of interest. The SNP at 3,881,336, within gene TraesCS4B02G006100 on chromosome 4B, was the only SNP from exome capture identified as being within a defense gene. Regions of 4B in both 1995 and 2048 associated with disease. Additionally, the confidence interval identified from GLM studies in 1995 and 2048 have some overlap. Interestingly, the known lesion mimic gene *lm2* also maps to chromosome 4B (Yao et al., 2009). The sequence of TraesCS4B02G006100 was analyzed using BLASTn (Zhang et al., 2000). BLASTn revealed a 91% similarity with *Yr28* (max score=4724, query cover=73%). Due to the lack of mapping resolution in a small population, the exact location of the causative mutation cannot yet be determined. So, moving forward with fine mapping studies, the possibility of the causative mutation residing within *Lm2* must be considered. The remaining

SNPs were analyzed for their occurrence in genes with potential roles in a dysregulated immune system. None of the identified genes had clear roles in regulating the immune system. Identification of the causative mutation still remains. As mentioned in the previous paragraph, fine mapping will further narrow the list of candidate mutations to a smaller region on the genome. The intervals from association mapping containing SNPs from exome capture, 547,200,000-548,800,000 on chromosome 3B and 884,672-5,401,027 on chromosome 4B will be utilized moving forward.

Conclusion

In this study mutant lines 1995, 2048, and 2348 crossed to the hard red winter wheat variety KS061705M11, and then taken out to the F_4 generation using single seed descent. The F_4 populations were then genotyped using a two-restriction enzyme GBS methodology. SNP data from GBS was used in a GLM association study. Regions with high association to the mutant phenotypes were extracted. Moving forward, comparisons between SNPs identified in GLM association studies and SNPs identified in exome capture found SNPs that were shared between the two methodologies. In 1995 there were 19 SNPs of interest identified. These SNPs occurred in a 3.89Mb window on 2D, a 7Mb window on 3A, and a 4.85Mb window on 4B. In 2048 there were 32 SNPs of interest identified. These occurred in a 3.89Mb window on 3B and a 4.52Mb window on 4B. These SNPs and regions will be candidates for future experiments.

Further fine mapping of causative mutations is necessary to identify the causative mutation for the phenotype of each mutant. Populations for fine mapping are currently being reared. With the data provided in this study the region being examined in fine mapping can be narrowed down significantly. Once mapping is complete, markers can be created for the use in cloning projects to confirm the role of the gene in the mutant phenotype. By mapping the candidates in each mutant and cloning the causative mutation, further understanding of the plant defense system and disease resistance in wheat can be achieved.

Chapter 4 - Conclusion

This project sought to map potential wheat susceptibility genes to *P. triticina.* Susceptibility genes have functions in normal plant physiology that pathogens exploit for the purpose of establishing and sustaining disease. By rendering susceptibility genes unable to be utilized by the pathogen, they may provide an alternative to conventional major *R*-gene based resistance. Major *R*-genes select for the development of virulent races within the pathogen population. Based on evidence from susceptibility genes such as *mlo* it is thought that susceptibility genes may provide a more durable defense. To identify potential susceptibility genes for *P. triticina* in wheat, a reverse genetics approach was utilized.

Seeds from the spring wheat variety Thatcher were treated with ethyl methanesulfonate to induce random mutations. Ten days after inoculation with *P. triticina* mutants were selected for disease reduction and selfed. This process was repeated to the M_6 generation to create non-segregating lines. This project used three of these mutant lines in phenotypic characterization assays and gene mapping studies.

Mutant line 1995 exhibits a hypersensitive like response in the absence of pathogens. This phenotype is similar to that observed in lesion mimics. Lesion mimic plants constitutively express plant defense responses, resulting in spontaneous formation of lesions and cell death. This phenotype often results in the reduction of disease when the plants are exposed to biotrophic pathogens such as *P. triticina*. To further evaluate the mutant, microscopic assays were conducted over the initial course of infection. These studies revealed a reduction in the ability of *P. triticina* to infect mutant line 1995 at all stages of the infection process. RNA expression analysis was conducted to characterize the phenotype of mutant lines. In 1995 increased expression of pathogenesis related (PR) proteins, salicylic acid associated genes, and peroxidases was observed. This indicates the presence of a defense response. RNAseq data combined with the presence of spontaneous lesion development supports the conclusion of a lesion mimic phenotype in 1995. The presence of a lesion mimic phenotype provides insight into the potential biological role of causative mutations. Because lesion mimicry is the result of a dysregulated defense response it is likely that the causative mutation in 1995 will have a role in plant defense or defense regulation. Mapping studies were then conducted to provide a chromosomal region that associated with the mutant phenotype. In 1995 there were 19 SNPs of

interest identified. These SNPs occurred in a 3.89Mb window on 2D, a 7Mb window on 3A, and a 4.85Mb window on 4B.

The same approach was taken for mutant. Microscopic examination and RNAseq analysis of 2048 revealed similar results to those seen in 1995. The ability of *P. triticina* to infect was reduced at each stage of infection. RNA expression analysis showed an increased expression of PR proteins and SA, indicating the presence of a defense response. One major difference in 2048 however, was the increase in expression of genes involved in jasmonic acid (JA) biosynthesis. JA has roles in host defense against bacterial pathogens, and dysregulation of JA biosynthesis as been observed in other lesion mimics. Thus, it is likely that 2048 is a lesion mimic mutant, and the causative mutation will have roles in either plant defense or plant defense regulation. Mapping studies revealed 32 SNPs of interest. These occurred in a 3.89Mb window on 3B and a 4.52Mb window on 4B.

In 2348 microscopic analysis of the time course of infection revealed early appressoria formation was not different between 2348 and Thatcher, but the quantity of spores that produced intercellular hyphae and colonies was reduced. No hypersensitive response was observed in 2348. The lack of an HR, and the reduction of intercellular hyphae formation suggests that the phenotype is not the result of an *R*-gene based response. Because the candidate mutation it is not likely in a *R*-gene, and the mutation is inherited recessively, it is likely that the candidate mutation is in a susceptibility gene. However, this study was not able to characterize the RNA expression of this mutant or perform mapping studies.

The results presented in this study provide a base for future experiments that can more finely map the candidate mutations. In order to do fine mapping larger mapping populations are currently being reared in the greenhouse. Larger populations will yield better resolution and decrease the size confidence intervals obtained. Once candidate genes are identified, their role in the mutant phenotype can be analyzed through gene cloning, or gene knockout of a wild type plant. Identifying the causative mutation will provide insight into the molecular interactions between wheat and *P. triticina*, as well as provide a potential new source of protection from leaf rust for use by wheat breeders.

References

Alaux, M., Rogers, J., Letellier, T., Flores, R., Alfama, F., Pommier, C., Mohellibi, N., Durand, S., Kimmel, E., Michotey, C., Guerche, C., Loaec, M., Lainé, M., Steinbach, D., Choulet, F., Rimbert, H., Leroy, P., Guilhot, N., Salse, J., … International Wheat Genome Sequencing Consortium. (2018). Linking the International Wheat Genome Sequencing Consortium bread wheat reference genome sequence to wheat genetic and phenomic data. *Genome Biology*, *19*(1), 111. https://doi.org/10.1186/s13059-018-1491-4

Allen, R. F. (1926). A Cytological Study of *Puccinia triticina* Physiologic Form 11 on Little Club Wheat. *Journal of Agricultural Research*, *33*(3), 201-222. plates.

Anand, A., Lei, Z., Sumner, L. W., Mysore, K. S., Arakane, Y., Bockus, W. W., & Muthukrishnan, S. (2004). Apoplastic extracts from a transgenic wheat line exhibiting lesion-mimic phenotype have multiple pathogenesis-related proteins that are antifungal. *Molecular Plant-Microbe Interactions: MPMI*, *17*(12), 1306–1317. https://doi.org/10.1094/MPMI.2004.17.12.1306

Anand, A., Schmelz, E. A., & Muthukrishnan, S. (2003). Development of a lesion-mimic phenotype in a transgenic wheat line overexpressing genes for pathogenesis-related (PR) proteins is dependent on salicylic acid concentration. *Molecular Plant-Microbe Interactions: MPMI*, *16*(10), 916–925. https://doi.org/10.1094/MPMI.2003.16.10.916

Bayer, M., Morris, J. A., Booth, C., Booth, A., Uzrek, N., Russell, J. R., Waugh, R., & Hedley, P. E. (2019). Exome Capture for Variant Discovery and Analysis in Barley. In W. A. Harwood (Ed.), *Barley: Methods and Protocols* (pp. 283–310). Springer. https://doi.org/10.1007/978-1-4939-8944-7_18

Bernardo, A., Amand, P. S., Le, H. Q., Su, Z., & Bai, G. (2020). Multiplex restriction amplicon sequencing: A novel next-generation sequencing-based marker platform for high-throughput genotyping. *Plant Biotechnology Journal*, *18*(1), 254–265. https://doi.org/10.1111/pbi.13192

Bernardo, A. N., Bowden, R. L., Rouse, M. N., Newcomb, M. S., Marshall, D. S., & Bai, G. (2013). Validation of Molecular Markers for New Stem Rust Resistance Genes in U.S. Hard Winter Wheat. *Crop Science*, *53*(3), 755–764. https://doi.org/10.2135/cropsci2012.07.0446

Bhardwaj, S. C., Prashar, M., Kumar, S., Jain, S. K., & Datta, D. (2005). *Lr19* Resistance in Wheat Becomes Susceptible to *Puccinia triticina* in India. *Plant Disease*, *89*(12), 1360–1360. https://doi.org/10.1094/PD-89-1360A

Bolton, M. D., Kolmer, J. A., & Garvin, D. F. (2008). Wheat leaf rust caused by *Puccinia triticina*. *Molecular Plant Pathology*, *9*(5), 563–575. https://doi.org/10.1111/j.1364-3703.2008.00487.x

Bruce, M., Neugebauer, K., Joly, D., Migeon, P., Cuomo, C., Wang, S., Akhunov, E., Bakkeren, G., Kolmer, J., & Fellers, J. (2014). Using transcription of six *Puccinia triticina* races to identify the effective secretome during infection of wheat. *Frontiers in Plant Science, 4*. https://www.frontiersin.org/article/10.3389/fpls.2013.00520

Bruggeman, Q., Raynaud, C., Benhamed, M., & Delarue, M. (2015). To die or not to die? Lessons from lesion mimic mutants. *Frontiers in Plant Science, 6*. https://doi.org/10.3389/fpls.2015.00024

Büschges, R., Hollricher, K., Panstruga, R., Simons, G., Wolter, M., Frijters, A., Daelen, R. van, Lee, T. van der, Diergaarde, P., Groenendijk, J., Töpsch, S., Vos, P., Salamini, F., &

Schulze-Lefert, P. (1997). The Barley *Mlo* Gene: A Novel Control Element of Plant Pathogen Resistance. *Cell*, *88*(5), 695–705. https://doi.org/10.1016/S0092-8674(00)81912-1

Casulli, F. and Siniscalco, A. (1987). *Thalictrum flavum* L. as an alternate host of *Puccinia recondita* f. sp. *tritici* in southern Italy. *7th congress of the Mediterranean Phyopathology Union, Granada, Spain.*

Champigny, M. J., Shearer, H., Mohammad, A., Haines, K., Neumann, M., Thilmony, R., He, S. Y., Fobert, P., Dengler, N., & Cameron, R. K. (2011). Localization of DIR1 at the tissue, cellular and subcellular levels during Systemic Acquired Resistance in *Arabidopsis* using DIR1:GUS and DIR1:EGFP reporters. *BMC Plant Biology*, *11*(1), 125. https://doi.org/10.1186/1471-2229-11-125

Chandra, S., Martin, G., & Low, P. (1996). The Pto kinase mediates a signaling pathway leading to the oxidative burst in tomato. *Proc Natl Acad Sci U S A*, *93*, 13393–13397.

Chassot, C., Nawrath, C., & Métraux, J.-P. (2007). Cuticular defects lead to full immunity to a major plant pathogen. *The Plant Journal*, *49*(6), 972–980. https://doi.org/10.1111/j.1365-313X.2006.03017.x

Chauhan, H., Boni, R., Bucher, R., Kuhn, B., Buchmann, G., Sucher, J., Selter, L. L., Hensel, G., Kumlehn, J., Bigler, L., Glauser, G., Wicker, T., Krattinger, S. G., & Keller, B. (2015). The wheat resistance gene *Lr34* results in the constitutive induction of multiple defense pathways in transgenic barley. *The Plant Journal*, *84*(1), 202–215. https://doi.org/10.1111/tpj.13001

Chester, K.S. (1946). The Nature and Prevention of Cereal Rusts as Exemplified in the Leaf Rust of Wheat. Waltham, MA: *Chronica Botanica*

Chinchilla, D., Bauer, Z., Regenass, M., Boller, T., & Felix, G. (2006). The *Arabidopsis* Receptor Kinase FLS2 Binds flg22 and Determines the Specificity of Flagellin Perception. *The Plant Cell*, *18*(2), 465–476. https://doi.org/10.1105/tpc.105.036574

Conesa, A., & Götz, S. (2008). Blast2GO: A comprehensive suite for functional analysis in plant genomics. *International Journal of Plant Genomics*, *2008*, 619832. https://doi.org/10.1155/2008/619832

Conesa, A., Götz, S., García-Gómez, J. M., Terol, J., Talón, M., & Robles, M. (2005). Blast2GO: A universal tool for annotation, visualization and analysis in functional genomics research. *Bioinformatics*, *21*(18), 3674–3676. https://doi.org/10.1093/bioinformatics/bti610

Corredor-Moreno, P., Minter, F., Davey, P. E., Wegel, E., Kular, B., Brett, P., Lewis, C. M., Morgan, Y. M. L., Macías Pérez, L. A., Korolev, A. V., Hill, L., & Saunders, D. G. O. (2021). The branched-chain amino acid aminotransferase TaBCAT1 modulates amino acid metabolism and positively regulates wheat rust susceptibility. *The Plant Cell*, *33*(5), 1728–1747. https://doi.org/10.1093/plcell/koab049

Cox, K. L., Meng, F., Wilkins, K. E., Li, F., Wang, P., Booher, N. J., Carpenter, S. C. D., Chen, L.-Q., Zheng, H., Gao, X., Zheng, Y., Fei, Z., Yu, J. Z., Isakeit, T., Wheeler, T., Frommer, W. B., He, P., Bogdanove, A. J., & Shan, L. (2017). TAL effector driven induction of a SWEET gene confers susceptibility to bacterial blight of cotton. *Nature Communications*, *8*(1), 15588. https://doi.org/10.1038/ncomms15588

Dietrich, R. A., Delaney, T. P., Uknes, S. J., Ward, E. R., Ryals, J. A., & Dangl, J. L. (1994). *Arabidopsis* mutants simulating disease resistance response. *Cell*, *77*(4), 565–577. https://doi.org/10.1016/0092-8674(94)90218-6

Douchkov, D., Lueck, S., Hensel, G., Kumlehn, J., Rajaraman, J., Johrde, A., Doblin, M. S., Beahan, C. T., Kopischke, M., Fuchs, R., Lipka, V., Niks, R. E., Bulone, V., Chowdhury, J., Little, A., Burton, R. A., Bacic, A., Fincher, G. B., & Schweizer, P. (2016). The barley (*Hordeum vulgare*) cellulose synthase-like D2 gene (*HvCslD2*) mediates penetration resistance to host-adapted and nonhost isolates of the powdery mildew fungus. *New Phytologist*, *212*(2), 421–433. https://doi.org/10.1111/nph.14065

Draper, J. (1997). Salicylate, superoxide synthesis and cell suicide in plant defence. *Trends in Plant Science*, *2*(5), 162–165. https://doi.org/10.1016/S1360-1385(97)01030-3

Duan, X., Wang, X., Fu, Y., Tang, C., Li, X., Cheng, Y., Feng, H., Huang, L., & Kang, Z. (2013). TaEIL1, a wheat homologue of AtEIN3, acts as a negative regulator in the wheat–stripe rust fungus interaction. *Molecular Plant Pathology*, *14*(7), 728–739. https://doi.org/10.1111/mpp.12044

Dugyala, S., Borowicz, P., & Acevedo, M. (2015). Rapid protocol for visualization of rust fungi structures using fluorochrome Uvitex 2B. *Plant Methods*, *11*, 54. https://doi.org/10.1186/s13007-015-0096-0

Facts & Figures on Food and Biodiversity | IDRC - International Development Research Centre. (2010, December 23). IDRC. https://www.idrc.ca/en/research-in-action/facts-figures-food-and-biodiversity

FAO Cereal Supply and Demand Brief. (2022, February 3). Fao.Org. https://www.fao.org/worldfoodsituation/csdb/en/

Feuillet, C., Travella, S., Stein, N., Albar, L., Nublat, A., & Keller, B. (2003). Map-based isolation of the leaf rust disease resistance gene *Lr10* from the hexaploid wheat (*Triticum*

aestivum L.) genome. *Proceedings of the National Academy of Sciences of the United States of America*, *100*(25), 15253–15258. https://doi.org/10.1073/pnas.2435133100

Flor, H. H. (1947). Genetics of pathogenicity in *Melampsora lini*. *Journal of Agricultural Research*, *73*, 241–262.

Fu, D., Uauy, C., Distelfeld, A., Blechl, A., Epstein, L., Chen, X., Sela, H., Fahima, T., & Dubcovsky, J. (2009). A novel kinase-START gene confers temperature-dependent resistance to wheat stripe rust. *Science (New York, N.Y.)*, *323*(5919), 1357–1360. https://doi.org/10.1126/science.1166289

Gao, Y., Wang, Z. Y., Kumar, V., Xu, X. F., Yuan, D. P., Zhu, X. F., Li, T. Y., Jia, B., & Xuan, Y. H. (2018). Genome-wide identification of the *SWEET* gene family in wheat. Elsevier Enhanced Reader. *Gene*, *642*, 284–292. https://doi.org/10.1016/j.gene.2017.11.044

Garnica, D. P., Nemri, A., Upadhyaya, N. M., Rathjen, J. P., & Dodds, P. N. (2014). The Ins and Outs of Rust Haustoria. *PLoS Pathogens*, *10*(9), e1004329. https://doi.org/10.1371/journal.ppat.1004329

Ge, C., Moolhuijzen, P., Hickey, L., Wentzel, E., Deng, W., Dinglasan, E. G., & Ellwood, S. R. (2020). Physiological Changes in Barley mlo-11 Powdery Mildew Resistance Conditioned by Tandem Repeat Copy Number. *International Journal of Molecular Sciences*, *21*(22), 8769. https://doi.org/10.3390/ijms21228769

Götz, S., Arnold, R., Sebastián-León, P., Martín-Rodríguez, S., Tischler, P., Jehl, M.-A., Dopazo, J., Rattei, T., & Conesa, A. (2011). B2G-FAR, a species-centered GO annotation repository. *Bioinformatics (Oxford, England)*, *27*(7), 919–924. https://doi.org/10.1093/bioinformatics/btr059

Götz, S., García-Gómez, J. M., Terol, J., Williams, T. D., Nagaraj, S. H., Nueda, M. J., Robles, M., Talón, M., Dopazo, J., & Conesa, A. (2008). High-throughput functional annotation and data mining with the Blast2GO suite. *Nucleic Acids Research*, *36*(10), 3420–3435. https://doi.org/10.1093/nar/gkn176

Grant, M., Brown, I., Adams, S., Knight, M., Ainslie, A., & Mansfield, J. (2000). The *RPM1* plant disease resistance gene facilitates a rapid and sustained increase in cytosolic calcium that is necessary for the oxidative burst and hypersensitive cell death. *The Plant Journal: For Cell and Molecular Biology*, *23*(4), 441–450. https://doi.org/10.1046/j.1365-313x.2000.00804.x

Green, G. J., & Campbell, A. P. (1979). Wheat cultivars resistant to *Puccinia graminis* f. Sp. *tritici* in western canada: Their development, performance, and economic value. *Can. J. Plant Pathol.*, *1*, 3:11.

Greenberg, J. T., Guo, A., Klessig, D. F., & Ausubel, F. M. (1994). Programmed cell death in plants: A pathogen-triggered response activated coordinately with multiple defense functions. *Cell*, *77*(4), 551–563. https://doi.org/10.1016/0092-8674(94)90217-8

Guevara-Morato, M. Á., de Lacoba, M. G., García-Luque, I., & Serra, M. T. (2010). Characterization of a pathogenesis-related protein 4 (PR-4) induced in Capsicum chinense L3 plants with dual RNase and DNase activities. *Journal of Experimental Botany*, *61*(12), 3259–3271. https://doi.org/10.1093/jxb/erq148

Henningsen, E. C., Omidvar, V., Della Coletta, R., Michno, J.-M., Gilbert, E., Li, F., Miller, M. E., Myers, C. L., Gordon, S. P., Vogel, J. P., Steffenson, B. J., Kianian, S. F., Hirsch, C. D., & Figueroa, M. (2021). Identification of Candidate Susceptibility Genes to *Puccinia*

graminis f. Sp. *Tritici* in Wheat. *Frontiers in Plant Science*, *12*, 638. https://doi.org/10.3389/fpls.2021.657796

Herbers, K., Meuwly, P., Frommer, W. B., Metraux, J. P., & Sonnewald, U. (1996). Systemic Acquired Resistance Mediated by the Ectopic Expression of Invertase: Possible Hexose Sensing in the Secretory Pathway. *The Plant Cell*, *8*(5), 793–803. https://doi.org/10.1105/tpc.8.5.793

Huai, B., Yang, Q., Qian, Y., Qian, W., Kang, Z., & Liu, J. (2019). ABA-Induced Sugar Transporter TaSTP6 Promotes Wheat Susceptibility to Stripe Rust. *Plant Physiology*, *181*(3), 1328–1343. https://doi.org/10.1104/pp.19.00632

Huai, B., Yang, Q., Wei, X., Pan, Q., Kang, Z., & Liu, J. (2020). TaSTP13 contributes to wheat susceptibility to stripe rust possibly by increasing cytoplasmic hexose concentration. *BMC Plant Biology*, *20*(1), 49. https://doi.org/10.1186/s12870-020-2248-2

Huang, S., Sirikhachornkit, A., Su, X., Faris, J., Gill, B., Haselkorn, R., & Gornicki, P. (2002). Genes encoding plastid acetyl-CoA carboxylase and 3-phosphoglycerate kinase of the *Triticum/Aegilops* complex and the evolutionary history of polyploid wheat. *Proceedings of the National Academy of Sciences*, *99*(12), 8133–8138. https://doi.org/10.1073/pnas.072223799

Huerta-Espino, J., Singh, R., Crespo-Herrera, L. A., Villaseñor-Mir, H. E., Rodriguez-Garcia, M. F., Dreisigacker, S., Barcenas-Santana, D., & Lagudah, E. (2020). Adult Plant Slow Rusting Genes Confer High Levels of Resistance to Rusts in Bread Wheat Cultivars From Mexico. *Frontiers in Plant Science, 11*. https://www.frontiersin.org/article/10.3389/fpls.2020.00824

Huerta-Espino, J., & Singh, R. P. (1994). First Report of Virulence to Wheat with Leaf Rust Resistance Gene *Lr19* in Mexico. *Plant Disease, 78*(640). https://doi.org/10.1094/PD-78-0640C

Huerta-Espino, J., Singh, R. P., & Reyna-Martinez, J. (2008). First Detection of Virulence to Genes *Lr9* and *Lr25* Conferring Resistance to Leaf Rust of Wheat Caused by *Puccinia triticina* in Mexico. *Plant Disease, 92*(2), 311. https://doi.org/10.1094/PDIS-92-2-0311A

IWGSC. (2014). A chromosome-based draft sequence of the hexaploid bread wheat (*Triticum aestivum*) genome. https://www.science.org/doi/10.1126/science.1251788

Johal, G. S., Hulbert, S. H., & Briggs, S. P. (1995). Disease lesion mimics of maize: A model for cell death in plants. *BioEssays, 17*(8), 685–692. https://doi.org/10.1002/bies.950170805

Jones, J. D. G., & Dangl, J. L. (2006). The plant immune system. *Nature, 444*(7117), 323–329. https://doi.org/10.1038/nature05286

Jung, H. W., Tschaplinski, T. J., Wang, L., Glazebrook, J., & Greenberg, J. T. (2009). Priming in systemic plant immunity. *Science (New York, N.Y.), 324*(5923), 89–91. https://doi.org/10.1126/science.1170025

Jung, Y. H., Lee, J.-H., Agrawal, G. K., Rakwal, R., Kim, J.-A., Shim, J.-K., Lee, S.-K., Jeon, J.-S., Koh, H.-J., Lee, Y.-H., Iwahashi, H., & Jwa, N.-S. (2005). The rice (*Oryza sativa*) blast lesion mimic mutant, blm, may confer resistance to blast pathogens by triggering multiple defense-associated signaling pathways. *Plant Physiology and Biochemistry: PPB, 43*(4), 397–406. https://doi.org/10.1016/j.plaphy.2005.03.002

Kamlofski, C. A., Antonelli, E., Bender, C., Jaskelioff, M., Danna, C. H., Ugalde, R., & Acevedo, A. (2007). A lesion-mimic mutant of wheat with enhanced resistance to leaf rust. *Plant Pathology, 56*(1), 46–54. https://doi.org/10.1111/j.1365-3059.2006.01454.x

Kassambara, A. (2021). *rstatix: Pipe-Friendly Framework for Basic Statistical Tests* (0.7.0) [Computer software]. https://rpkgs.datanovia.com/rstatix/

Kemen, E., Kemen, A. C., Rafiqi, M., Hempel, U., Mendgen, K., Hahn, M., & Voegele, R. T. (2005). Identification of a Protein from Rust Fungi Transferred from Haustoria into Infected Plant Cells. *Molecular Plant-Microbe Interactions®*, *18*(11), 1130–1139. https://doi.org/10.1094/MPMI-18-1130

Kihara, H. (1944). Discovery of the DD_analyser, one of the ancestors of *Trticum vulgare* (Japanese). *Agriculture and Horticulture (Tokyo)*, *19*, 13–14.

Kolmer, J. A. (1996). Genetics of resistance to wheat leaf rust. *Annual Review of Phytopathology*, *34*, 435–455. https://doi.org/10.1146/annurev.phyto.34.1.435

Kolmer, J. A. (2020, March 6). *Wheat leaf rust: USDA ARS*. Wheat Leaf Rust. https://www.ars.usda.gov/midwest-area/stpaul/cereal-disease-lab/docs/cereal-rusts/wheat-leaf-rust/

Kolmer, J. A., & Anderson, J. A. (2011). First Detection in North America of Virulence in Wheat Leaf Rust (*Puccinia triticina*) to Seedling Plants of Wheat with *Lr21*. *Plant Disease*, *95*(8), 1032. https://doi.org/10.1094/PDIS-04-11-0275

Krasileva, K. V., Vasquez-Gross, H. A., Howell, T., Bailey, P., Paraiso, F., Clissold, L., Simmonds, J., Ramirez-Gonzalez, R. H., Wang, X., Borrill, P., Fosker, C., Ayling, S., Phillips, A. L., Uauy, C., & Dubcovsky, J. (2017). Uncovering hidden variation in polyploid wheat. *Proceedings of the National Academy of Sciences of the United States of America*, *114*(6), E913–E921. https://doi.org/10.1073/pnas.1619268114

Krattinger, S. G., Lagudah, E. S., Spielmeyer, W., Singh, R. P., Huerta-Espino, J., McFadden, H., Bossolini, E., Selter, L. L., & Keller, B. (2009). A putative ABC transporter confers

durable resistance to multiple fungal pathogens in wheat. *Science (New York, N.Y.)*, *323*(5919), 1360–1363. https://doi.org/10.1126/science.1166453

Kusch, S., & Panstruga, R. (2017). mlo-Based Resistance: An Apparently Universal "Weapon" to Defeat Powdery Mildew Disease. *Molecular Plant-Microbe Interactions: MPMI*, *30*(3), 179–189. https://doi.org/10.1094/MPMI-12-16-0255-CR

Levine, M., and Hildreth R.. (1957) A natural occurrence of the aecial stage of *Puccinia rubigo-vera* var. *tritici* in the United States. Phytopathology 47:110-111.

Li, T., & Bai, G. (2009). Lesion mimic associates with adult plant resistance to leaf rust infection in wheat. *Theoretical and Applied Genetics*, *119*(1), 13–21. https://doi.org/10.1007/s00122-009-1012-7

Ling, H.-Q., Zhu, Y., & Keller, B. (2003). High-resolution mapping of the leaf rust disease resistance gene *Lr1* in wheat and characterization of BAC clones from the Lr1 locus. *TAG. Theoretical and Applied Genetics. Theoretische Und Angewandte Genetik*, *106*(5), 875–882. https://doi.org/10.1007/s00122-002-1139-2

Liu, R., Lu, J., Zheng, S., Du, M., Zhang, C., Wang, M., Li, Y., Xing, J., Wu, Y., & Zhang, L. (2021). Molecular mapping of a novel lesion mimic gene (*lm4*) associated with enhanced resistance to stripe rust in bread wheat. *BMC Genomic Data*, *22*(1), 1. https://doi.org/10.1186/s12863-021-00963-6

Lorrain, S., Vailleau, F., Balagué, C., & Roby, D. (2003). Lesion mimic mutants: Keys for deciphering cell death and defense pathways in plants? *Trends in Plant Science*, *8*(6), 263–271. https://doi.org/10.1016/S1360-1385(03)00108-0

Long, D. L., & Kolmer, J.A. (1989). A north american system of nomenclature for *Puccinia recondita* f. sp. *tritici. The American Phytopathological Society*, 79(5), 525-529.

https://www.apsnet.org/publications/phytopathology/backissues/Documents/1989Articles/Phyto79n05_525.PDF

Luo, M.-C., Yang, Z.-L., You, F. M., Kawahara, T., Waines, J. G., & Dvorak, J. (2007). The structure of wild and domesticated emmer wheat populations, gene flow between them, and the site of emmer domestication. *Theoretical and Applied Genetics*, *114*(6), 947–959. https://doi.org/10.1007/s00122-006-0474-0

Maeda, S., Hayashi, N., Sasaya, T., & Mori, M. (2016). Overexpression of BSR1 confers broad-spectrum resistance against two bacterial diseases and two major fungal diseases in rice. *Breeding Science*, *66*(3), 396–406. https://doi.org/10.1270/jsbbs.15157

McCallum, C. M., Comai, L., Greene, E. A., & Henikoff, S. (2000). Targeting Induced Local Lesions In Genomes (TILLING) for Plant Functional Genomics. *Plant Physiology*, *123*(2), 439–442.

Mcfadden, E. S., & Sears, E. R. (1946). The origin of *Triticum spelta* and its free-threshing hexaploid relatives. *Journal of Heredity*, *37*(3), 81–89. https://doi.org/10.1093/oxfordjournals.jhered.a105590

McIntosh, R. A., & Brown, G. N. (1997). Anticipatory breeding for resistance to rust diseases in wheat. *Annual Review of Phytopathology*, *35*, 311–326. https://doi.org/10.1146/annurev.phyto.35.1.311

Mcintosh, R. A., Wellings, C. R., & Park, R. F. (1995). *Wheat Rusts: An Atlas of Resistance Genes*. Melbourne: CSIRO Publishing.

Meyers, B., Kaushik, S., & Nandety, R. (2005). Evolving disease resistance genes. *Current Opinion in Plant Biology*, *8*, 129–134. https://doi.org/10.1016/j.pbi.2005.01.002

Milne, R. J., Dibley, K. E., Schnippenkoetter, W., Mascher, M., Lui, A. C. W., Wang, L., Lo, C., Ashton, A. R., Ryan, P. R., & Lagudah, E. S. (2019). The Wheat *Lr67* Gene from the Sugar Transport Protein 13 Family Confers Multipathogen Resistance in Barley. *Plant Physiology*, *179*(4), 1285–1297. https://doi.org/10.1104/pp.18.00945

Miya, A., Albert, P., Shinya, T., Desaki, Y., Ichimura, K., Shirasu, K., Narusaka, Y., Kawakami, N., Kaku, H., & Shibuya, N. (2007). CERK1, a LysM receptor kinase, is essential for chitin elicitor signaling in *Arabidopsis*. *Proceedings of the National Academy of Sciences*, *104*(49), 19613–19618. https://doi.org/10.1073/pnas.0705147104

Moeder, W., & Yoshioka, K. (2008). Lesion mimic mutants. *Plant Signaling & Behavior*, *3*(10), 764–767.

Moore, J. W., Herrera-Foessel, S., Lan, C., Schnippenkoetter, W., Ayliffe, M., Huerta-Espino, J., Lillemo, M., Viccars, L., Milne, R., Periyannan, S., Kong, X., Spielmeyer, W., Talbot, M., Bariana, H., Patrick, J. W., Dodds, P., Singh, R., & Lagudah, E. (2015). A recently evolved hexose transporter variant confers resistance to multiple pathogens in wheat. *Nature Genetics*, *47*(12), 1494–1498. https://doi.org/10.1038/ng.3439

Mortazavi, A., Williams, B., McCue, K., & Wold, B. (2008). Mapping and Quantifying mammalian transcriptomes by rna-seq. *Nature Methods*, *5*(7), 621–628.

Mu, X., Li, J., Dai, Z., Xu, L., Fan, T., Jing, T., Chen, M., & Gou, M. (2021). Commonly and Specifically Activated Defense Responses in Maize Disease Lesion Mimic Mutants Revealed by Integrated Transcriptomics and Metabolomics Analysis. *Frontiers in Plant Science*, *12*. https://www.frontiersin.org/article/10.3389/fpls.2021.638792

Neugebauer, K., Bruce, M., Todd, T., Trick, H.N., Fellers, J.P. 2018. Wheat differential gene expression induced by different races of *Puccinia triticina*. PLoS One. 13(6):e0198350. https://doi.org/10.1371/journal.pone.0198350.

Olivera, P. D., Rouse, M. N., & Jin, Y. (2018). Identification of New Sources of Resistance to Wheat Stem Rust in *Aegilops spp*. In the Tertiary Genepool of Wheat. *Frontiers in Plant Science, 9*. https://www.frontiersin.org/article/10.3389/fpls.2018.01719

Ozkan, H., Brandolini, A., Shafer-Pregl, R., & Salamini, F. (2002). AFLP Analysis of a Collection of Tetraploid Wheats Indicates the Origin of Emmer and Hard Wheat Domestication in Southeast Turkey. *Molecular Biology and Evolution*, *19*(10), 1797–1801.

Petersen, G., Seberg, O., Yde, M., & Berthelsen, K. (2006). Phylogenetic relationships of *Triticum* and *Aegilops* and evidence for the origin of the A, B, and D genomes of common wheat (*Triticum aestivum*). *Molecular Phylogenetics and Evolution*, *39*(1), 70–82. https://doi.org/10.1016/j.ympev.2006.01.023

Petre, B., Saunders, D. G. O., Sklenar, J., Lorrain, C., Win, J., Duplessis, S., & Kamoun, S. (2015). Candidate Effector Proteins of the Rust Pathogen *Melampsora larici-populina* Target Diverse Plant Cell Compartments. *Molecular Plant-Microbe Interactions®*, *28*(6), 689–700. https://doi.org/10.1094/MPMI-01-15-0003-R

Piffanelli, P., Zhou, F., Casais, C., Orme, J., Jarosch, B., Schaffrath, U., Collins, N. C., Panstruga, R., & Schulze-Lefert, P. (2002). The Barley MLO Modulator of Defense and Cell Death Is Responsive to Biotic and Abiotic Stress Stimuli. *Plant Physiology*, *129*(3), 1076–1085. https://doi.org/10.1104/pp.010954

Poland, J. A., Brown, P. J., Sorrells, M. E., & Jannink, J.-L. (2012). Development of High-Density Genetic Maps for Barley and Wheat Using a Novel Two-Enzyme Genotyping-by-Sequencing Approach. *PLOS ONE*, *7*(2), e32253. https://doi.org/10.1371/journal.pone.0032253

Pritchard, J. K., Stephens, M., & Donnelly, P. (2000). Inference of population structure using multilocus genotype data. *Genetics*, *155*(2), 945–959. https://doi.org/10.1093/genetics/155.2.945

Qiu, J.-W., Schürch, A. C., Yahiaoui, N., Dong, L.-L., Fan, H.-J., Zhang, Z.-J., Keller, B., & Ling, H.-Q. (2007). Physical mapping and identification of a candidate for the leaf rust resistance gene *Lr1* of wheat. *Theoretical and Applied Genetics*, *115*(2), 159–168. https://doi.org/10.1007/s00122-007-0551-z

Rafiqi, M., Gan, P. H. P., Ravensdale, M., Lawrence, G. J., Ellis, J. G., Jones, D. A., Hardham, A. R., & Dodds, P. N. (2010). Internalization of Flax Rust Avirulence Proteins into Flax and Tobacco Cells Can Occur in the Absence of the Pathogen. *The Plant Cell*, *22*(6), 2017–2032. https://doi.org/10.1105/tpc.109.072983

Rahman, A., Kuldau, G. A., & Uddin, W. (2014). Induction of Salicylic Acid–Mediated Defense Response in Perennial Ryegrass Against Infection by *Magnaporthe oryzae*. *Phytopathology*®, *104*(6), 614–623. https://doi.org/10.1094/PHYTO-09-13-0268-R

Rao, M. V., Lee, H., Creelman, R. A., Mullet, J. E., & Davis, K. R. (2000). Jasmonic Acid Signaling Modulates Ozone-Induced Hypersensitive Cell Death. *The Plant Cell*, *12*(9), 1633–1647.

Roelfs, A. P., Singh, R. P., & Saari, E. E. (1992). *Rust Diseases of Wheat: Concepts and Methods of Disease Management*. CIMMYT.

Rstudio Team. (2022). *Rstudio: Integrated Development Environment for R* (2022.2.1.461) [Computer software]. Rstudio, PBC. http://www.rstudio.com/

Saghai-Maroof, M. A., Soliman, K. M., Jorgensen, R. A., & Allard, R. W. (1984). Ribosomal DNA spacer-length polymorphisms in barley: Mendelian inheritance, chromosomal location, and population dynamics. *Proceedings of the National Academy of Sciences of the United States of America*, *81*(24), 8014–8018.

Samborski, D. J. (1985). Wheat Leaf Rust. *Diseases, Distribution, Epidemiology, and Control (Academic Press)*, 39–59.

Saur, I. M. L., Bauer, S., Lu, X., & Schulze-Lefert, P. (2019). A cell death assay in barley and wheat protoplasts for identification and validation of matching pathogen AVR effector and plant NLR immune receptors. *Plant Methods*, *15*(1), 118. https://doi.org/10.1186/s13007-019-0502-0

Schafer, J. F., & Roelfs, A. P. (1985). Estimated relation between numbers of urediniospores of *Puccinia graminis* f. Sp. *tritici* and rates of occurrence of virulence. *Phytopathology, 75*, 749–750. Scopus.

Schwessinger, B., & McDonald, M. (2017, December 7). *High quality DNA from Fungi for long read sequencing e.g. PacBio, Nanopore MinION*. Protocols.Io. https://www.protocols.io/view/high-quality-dna-from-fungi-for-long-read-sequenci-k6qczdw

Shao, Z.-Q., Xue, J.-Y., Wu, P., Zhang, Y.-M., Wu, Y., Hang, Y.-Y., Wang, B., & Chen, J.-Q. (2016). Large-Scale Analyses of Angiosperm Nucleotide-Binding Site-Leucine-Rich Repeat Genes Reveal Three Anciently Diverged Classes with Distinct Evolutionary Patterns. *Plant Physiology*, *170*(4), 2095–2109. https://doi.org/10.1104/pp.15.01487

Simons, K.J., Fellers, J.P., Trick, H.N., Zhang, Z., Tai, Y-S., Gill, B.S., Faris, J.D. 2006. Molecular characterization of the major wheat domestication gene *Q*. Genetics 172: 547–555.

Skou, J. (1982). *Callose Formation Responsible for the Powdery Mildew Resistance in Barley with Genes in the ml-o Locus*. https://doi.org/10.1111/J.1439-0434.1982.TB00009.X

Soleiman, N., Solís, I., Soliman, M., Sillero, J., Villegas, D., Alvaro, F., Royo, C., Serra, J., Ammar, K., & Martinez-Moreno, F. (2016). Short communication: Emergence of a new race of leaf rust with combined virulence to *Lr14a* and *Lr72* genes on durum wheat. *Spanish Journal of Agricultural Research*, *14*, e10SC02. https://doi.org/10.5424/sjar/2016143-9184

Stanford, A., Bevan, M., & Northcote, D. (1989). Differential expression within a family of novel wound-induced genes in potato. *Molecular and General Genetics MGG*, *215*(2), 200–208. https://doi.org/10.1007/BF00339718

Su, J., Yang, L., Zhu, Q., Wu, H., He, Y., Liu, Y., Xu, J., Jiang, D., & Zhang, S. (2018). Active photosynthetic inhibition mediated by MPK3/MPK6 is critical to effector-triggered immunity. *PLoS Biology*, *16*(5), e2004122. https://doi.org/10.1371/journal.pbio.2004122

Sun, Y., Li, L., Macho, A. P., Han, Z., Hu, Z., Zipfel, C., Zhou, J.-M., & Chai, J. (2013). Structural Basis for flg22-Induced Activation of the *Arabidopsis* FLS2-BAK1 Immune Complex. *Science*. https://doi.org/10.1126/science.1243825

Szabo, L. J., & Bushnell, W. R. (2001). Hidden robbers: The role of fungal haustoria in parasitism of plants. *Proceedings of the National Academy of Sciences*, *98*(14), 7654–7655. https://doi.org/10.1073/pnas.151262398

Takahashi, A., Kawasaki, T., Henmi, K., ShiI, K., Kodama, O., Satoh, H., & Shimamoto, K. (1999). Lesion mimic mutants of rice with alterations in early signaling events of defense. *The Plant Journal: For Cell and Molecular Biology*, *17*(5), 535–545. https://doi.org/10.1046/j.1365-313x.1999.00405.x

Tamaoki, D., Seo, S., Yamada, S., Kano, A., Miyamoto, A., Shishido, H., Miyoshi, S., Taniguchi, S., Akimitsu, K., & Gomi, K. (2013). Jasmonic acid and salicylic acid activate a common defense system in rice. *Plant Signaling & Behavior*, *8*(6), e24260. https://doi.org/10.4161/psb.24260

Thomazella, D. P. de T., Seong, K., Mackelprang, R., Dahlbeck, D., Geng, Y., Gill, U. S., Qi, T., Pham, J., Giuseppe, P., Lee, C. Y., Ortega, A., Cho, M.-J., Hutton, S. F., & Staskawicz, B. (2021). Loss of function of a DMR6 ortholog in tomato confers broad-spectrum disease resistance. *Proceedings of the National Academy of Sciences*, *118*(27). https://doi.org/10.1073/pnas.2026152118

van Schie, C. C. N., & Takken, F. L. W. (2014). Susceptibility Genes 101: How to Be a Good Host. *Annual Review of Phytopathology*, *52*(1), 551–581. https://doi.org/10.1146/annurev-phyto-102313-045854

Wang, F., Wu, W., Wang, D., Yang, W., Sun, J., Liu, D., & Zhang, A. (2016). Characterization and Genetic Analysis of a Novel Light-Dependent Lesion Mimic Mutant, lm3, Showing Adult-Plant Resistance to Powdery Mildew in Common Wheat. *PLOS ONE*, *11*(5), e0155358. https://doi.org/10.1371/journal.pone.0155358

Wang, S., Lei, C., Wang, J., Ma, J., Tang, S., Wang, C., Zhao, K., Tian, P., Zhang, H., Qi, C., Cheng, Z., Zhang, X., Guo, X., Liu, L., Wu, C., & Wan, J. (2017). SPL33, encoding an

eEF1A-like protein, negatively regulates cell death and defense responses in rice. *Journal of Experimental Botany*, *68*(5), 899–913. https://doi.org/10.1093/jxb/erx001

Wang, Z., Li, X., Wang, X., Liu, N., Xu, B., Peng, Q., Guo, Z., Fan, B., Zhu, C., & Chen, Z. (2019). Arabidopsis Endoplasmic Reticulum-Localized UBAC2 Proteins Interact with PAMP-INDUCED COILED-COIL to Regulate Pathogen-Induced Callose Deposition and Plant Immunity. *The Plant Cell*, *31*(1), 153–171. https://doi.org/10.1105/tpc.18.00334

Wegulo, S. N., & Byamukama, E. (2012, November). *Rust Diseases of Wheat* [Extension]. NebGuide. https://extensionpublications.unl.edu/assets/pdf/g2180.pdf

Wickham, H., Averick, M., Bryan, J., Chang, W., McGowan, L. D. A., François, R., Grolemund, G., Hayes, A., Henry, L., Hester, J., Kuhn, M., Pedersen, T. L., Miller, E., Bache, S. M., Müller, K., Ooms, J., Robinson, D., Seidel, D. P., Spinu, V., … Yutani, H. (2019). Welcome to the tidyverse. *Journal of Open Source Software*, *4*(43), 1686. https://doi.org/10.21105/joss.01686

Wickham, H., François, R., Henry, L., & Müller, K. (2022). *dplyr: A Grammar of Data Manipulation*. https://dplyr.tidyverse.org, https://github.com/tidyverse/dplyr

Williams, N. D., J. D. Miller and D. L. Klindworth, 1992. Induced mutations of a genetic suppressor of resistance to wheat stem rust. *Crop Sci.* 32**:** 612–616

Wright, S. a. I., Azarang, M., & Falk, A. B. (2013). Barley lesion mimics, supersusceptible or highly resistant to leaf rust and net blotch. *Plant Pathology*, *62*(5), 982–992. https://doi.org/10.1111/ppa.12007

Yalpani, N., Silverman, P., Wilson, T. M., Kleier, D. A., & Raskin, I. (1991). Salicylic acid is a systemic signal and an inducer of pathogenesis-related proteins in virus-infected tobacco. *The Plant Cell*, *3*(8), 809–818.

Yamaguchi, Y., Huffaker, A., Bryan, A. C., Tax, F. E., & Ryan, C. A. (2010). PEPR2 Is a Second Receptor for the Pep1 and Pep2 Peptides and Contributes to Defense Responses in *Arabidopsis*. *The Plant Cell*, *22*(2), 508–522. https://doi.org/10.1105/tpc.109.068874

Yamaguchi, Y., Pearce, G., & Ryan, C. A. (2006). The cell surface leucine-rich repeat receptor for AtPep1, an endogenous peptide elicitor in *Arabidopsis*, is functional in transgenic tobacco cells. *Proceedings of the National Academy of Sciences*, *103*(26), 10104–10109. https://doi.org/10.1073/pnas.0603729103

Yao, Q., Zhou, R., Fu, T., Wu, W., Zhu, Z., Li, A., & Jia, J. (2009). Characterization and mapping of complementary lesion-mimic genes *lm1* and *lm2* in common wheat. *Theoretical and Applied Genetics*, *119*(6), 1005–1012. https://doi.org/10.1007/s00122-009-1104-4

Yin, Z., Chen, J., Zeng, L., Goh, M., Leung, H., Khush, G. S., & Wang, G.-L. (2000). Characterizing Rice Lesion Mimic Mutants and Identifying a Mutant with Broad-Spectrum Resistance to Rice Blast and Bacterial Blight. *Molecular Plant-Microbe Interactions®*, *13*(8), 869–876. https://doi.org/10.1094/MPMI.2000.13.8.869

Yong, Y., Qiujun, L., Xinyu, C., Weifang, L., Yuwen, F., Zhengjin, X., Yuanhua, W., Xuming, W., Jie, Z., Chulang, Y., Chengqi, Y., Qiong, M., & Jianping, C. (2021). Characterization and Proteomic Analysis of Novel Rice Lesion Mimic Mutant with Enhanced Disease Resistance. *Rice Science*, *28*(5), 466–478. https://doi.org/10.1016/j.rsci.2021.07.007

Yuan, B., Shen, X., Li, X., Xu, C., & Wang, S. (2007). Mitogen-activated protein kinase OsMPK6 negatively regulates rice disease resistance to bacterial pathogens. *Planta*, *226*, 953–960. https://doi.org/10.1007/s00425-007-0541-z

Yuchun, R. A. O., Ran, J. I. A. O., Sheng, W. A. N. G., Xianmei, W. U., Hanfei, Y. E., Chenyang, P. A. N., Sanfeng, L. I., Dedong, X., Weiyong, Z. H. O. U., Gaoxing, D. A. I., Juan, H. U., Deyong, R. E. N., & Yuexing, W. A. N. G. (2021). SPL36 Encodes a Receptor-like Protein Kinase that Regulates Programmed Cell Death and Defense Responses in Rice. *Rice*, *14*, 34. https://doi.org/10.1186/s12284-021-00475-y

Zeilmaker, T., Ludwig, N. R., Elberse, J., Seidl, M. F., Berke, L., Van Doorn, A., Schuurink, R. C., Snel, B., & Van den Ackerveken, G. (2015). DOWNY MILDEW RESISTANT 6 and DMR6-LIKE OXYGENASE 1 are partially redundant but distinct suppressors of immunity in *Arabidopsis*. *The Plant Journal*, *81*(2), 210–222. https://doi.org/10.1111/tpj.12719

Zeng, L.-R., Qu, S., Bordeos, A., Yang, C., Baraoidan, M., Yan, H., Xie, Q., Nahm, B. H., Leung, H., & Wang, G.-L. (2004). Spotted leaf11, a Negative Regulator of Plant Cell Death and Defense, Encodes a U-Box/Armadillo Repeat Protein Endowed with E3 Ubiquitin Ligase Activity. *The Plant Cell*, *16*(10), 2795–2808. https://doi.org/10.1105/tpc.104.025171

Zhang, Q., Zhang, X., Zhuang, R., Wei, Z., Shu, W., Wang, X., & Kang, Z. (2020). TaRac6 Is a Potential Susceptibility Factor by Regulating the ROS Burst Negatively in the Wheat–*Puccinia striiformis* f. Sp. *tritici* Interaction. *Frontiers in Plant Science*, *11*, 716. https://doi.org/10.3389/fpls.2020.00716

Zhang, X., Tian, B., Fang, Y., Tong, T., Zheng, J., & Xue, D. (2019). Proteome analysis and phenotypic characterization of the lesion mimic mutant bspl in barley. *Plant Growth Regulation*, *87*(2), 329–339. https://doi.org/10.1007/s10725-018-00474-y

Zhang, Z., Lenk, A., Andersson, M. X., Gjetting, T., Pedersen, C., Nielsen, M. E., Newman, M.-A., Hou, B.-H., Somerville, S. C., & Thordal-Christensen, H. (2008). A Lesion-Mimic Syntaxin Double Mutant in *Arabidopsis* Reveals Novel Complexity of Pathogen Defense Signaling. *Molecular Plant*, *1*(3), 510–527. https://doi.org/10.1093/mp/ssn011

Zhao, S., Shang, X., Bi, W., Yu, X., Liu, D., Kang, Z., Wang, X., & Wang, X. (2020). Genome-Wide Identification of Effector Candidates With Conserved Motifs From the Wheat Leaf Rust Fungus *Puccinia triticina*. *Frontiers in Microbiology*, *11*. https://www.frontiersin.org/article/10.3389/fmicb.2020.01188

Zhou, J., Peng, Z., Long, J., Sosso, D., Liu, B., Eom, J.-S., Huang, S., Liu, S., Vera Cruz, C., Frommer, W. B., White, F. F., & Yang, B. (2015). Gene targeting by the TAL effector PthXo2 reveals cryptic resistance gene for bacterial blight of rice. *The Plant Journal: For Cell and Molecular Biology*, *82*(4), 632–643. https://doi.org/10.1111/tpj.12838

Zierold, U., Scholz, U., & Schweizer, P. (2005). Transcriptome analysis of mlo-mediated resistance in the epidermis of barley. *Molecular Plant Pathology*, *6*(2), 139–151. https://doi.org/10.1111/j.1364-3703.2005.00271.x

Appendix A - Supplemental Tables

Supplemental Table 1

3-way ANOVA results for time course microscopy in 1995 against Thatcher

3-way ANOVA 1dpi Tc v 1995					
Effect	Dfn	Dfd	F	p p<.05	ges
Variety	1	228	5.266	0.023	*.023
Rep	1	228	0.107	0.743	0.000471
Leaf	2	228	2.663	0.072	0.023
Variety:Rep	1	228	0.967	0.326	0.004
Variety:Leaf	2	228	0.681	0.507	0.006
Rep:Leaf	2	228	0.251	0.778	0.002
Variety:Rep:Leaf	2	228	2.902	0.057	0.025

3-way ANOVA 3dpi Tc v 1995					
Effect	Dfn	Dfd	F	p p<.05	ges
Variety	1	228	11.975	0.000644	0.05
Rep	1	228	1.957	0.163	0.009
Leaf	2	228	1.079	0.342	0.009
Variety:Rep	1	228	1.22	0.271	0.005
Variety:Leaf	2	228	5.047	0.007	0.042
Rep:Leaf	2	228	0.656	0.52	0.006
Variety:Rep:Leaf	2	228	2.26	0.107	0.019

3-way ANOVA 5dpi Tc v 1995					
Effect	Dfn	Dfd	F	p	p<.05
Variety	1	228	40.867	9.1E-10	0.152
Rep	1	228	7.26	0.008	0.031
Leaf	2	228	1.608	0.203	0.014
Variety:Rep	1	228	0.137	0.712	0.0006
Variety:Leaf	2	228	2.188	0.114	0.019
Rep:Leaf	2	228	2.445	0.089	0.021
Variety:Rep:Leaf	2	228	5.236	0.006	0.044

Supplemental Table 2

3-way ANOVA results for time course microscopy in 2048 against Thatcher

3-way ANOVA 1dpi Tc v 2048					
Effect	Dfn	Dfd	F	p p<.05	ges
Variety	1	228	18.335	0.0000273	0.074

Rep	1	228	0.166	0.684	0.000729
Leaf	2	228	7.494	0.705	0.063
Variety:Rep	1	228	0.664	0.416	0.003
Variety:Leaf	2	228	8.076	0.000409	0.066
Rep:Leaf	2	228	0.696	0.499	0.006
Variety:Rep:Leaf	2	228	1.32	0.269	0.011

3-way ANOVA 3dpi Tc v 2048					
Effect	Dfn	Dfd	F	p p<.05	ges
Variety	1	228	4.625	0.033	0.02
Rep	1	228	1.072	0.302	0.005
Leaf	2	228	7.086	0.001	0.059
Variety:Rep	1	228	0.514	0.474	0.002
Variety:Leaf	2	228	1.732	0.179	0.015
Rep:Leaf	2	228	1.377	0.255	0.012
Variety:Rep:Leaf	2	228	0.818	0.0442	0.007

3-way ANOVA 5dpi Tc v 2048					
Effect	Dfn	Dfd	F	p	p<.05
Variety	1	228	13.3558	0.000289	0.056
Rep	1	228	0.697	0.405	0.003
Leaf	2	228	1.427	0.242	0.012
Variety:Rep	1	228	4.052	0.045	0.017
Variety:Leaf	2	228	1.851	0.159	0.016
Rep:Leaf	2	228	0.646	0.525	0.006
Variety:Rep:Leaf	2	228	3.307	0.038	0.028

Supplemental Table 3

3-way ANOVA results for time course microscopy in 1995 against Thatcher

3-way ANOVA 1dpi Tc v 2348					
Effect	Dfn	Dfd	F	p p<.05	ges
Variety	1	228	4.018	0.046	0.017
Rep	1	228	0.198	0.656	0.00087
Leaf	2	228	0.757	0.47	0.007
Variety:Rep	1	228	0.794	0.374	0.003
Variety:Leaf	2	228	1.451	0.236	0.013
Rep:Leaf	2	228	2.096	0.125	0.018
Variety:Rep:Leaf	2	228	0.608	0.545	0.005

3-way ANOVA 3dpi Tc v 2348					
Effect	Dfn	Dfd	F	p p<.05	ges

Variety	1	228	18.335	0.0000273	0.074
Rep	1	228	0.166	0.684	0.000729
Leaf	2	228	7.494	0.000705	0.062
Variety:Rep	1	228	0.665	0.416	0.003
Variety:Leaf	2	228	8.076	0.000409	0.066
Rep:Leaf	2	228	0.696	0.499	0.006
Variety:Rep:Leaf	2	228	1.32	0.269	0.011

3-way ANOVA 5dpi Tc v 2348					
Effect	Dfn	Dfd	F	p p<.05	ges
Variety	1	228	56.818	1.12E-12	0.199
Rep	1	228	4.94	0.027	0.021
Leaf	2	228	0.402	0.67	0.004
Variety:Rep	1	228	0.336	0.563	0.001
Variety:Leaf	2	228	0.196	0.822	0.002
Rep:Leaf	2	228	1.578	0.209	0.014
Variety:Rep:Leaf	2	228	1.596	0.205	0.014

Supplemental Table 4

Total reads at each step of RNAseq expression analysis. Paired reads indicate the number of reads present after inputting paired sequences into CLC. Trimmed reads indicate the number of reads present after using the "trim reads" function in CLC. Unique expression reads and total expression reads are values obtained after conducting RNA-seq analysis against the Chinese Spring reference transcripts.

Reads	Paired Reads	Trimmed Reads	Unique Expression Reads	Total Expression Reads
Tc	122,958,108	122,957,912	31,931,108	48,020,281
1995 M6	132,197,652	132,197,246	35,827,259	52,857,226
1995R1	123,374,894	123,374,468	34,489,339	50,574,315
1995R2	123,544,614	123,544,402	34,596,141	50,857,948
1995R3	110,414,914	110,414,738	29,903,202	44,405,704
1995S1	113,822,218	113,822,018	29,378,334	43,467,206
1995S2	119,518,044	119,517,850	30,832,223	46,496,583
1995S3	122,533,092	122,532,908	32,128,349	47,318,308
2048 M6	37,962,996	37,960,294	9,602,532	14,113,352
2048R1	35,761,030	35,758,496	9,389,490	13,522,123
2048R2	39,031,256	39,028,554	10,057,070	14,616,204
2048R3	74,275,640	74,270,036	19,109,602	27,624,321
2048S1	30,885,762	30,883,502	7,454,242	11,058,499
2048S2	37,717,303	37,714,528	9,051,012	13,367,632

2048S3	35,330,254	35,327,674	8,607,939	12,676,569
2348 M6	92,912,212	92,911,486	25,208,288	37,112,348
2348R1	78,102,422	78,072,468	21,608,025	29,902,709
2348R2	80,857,280	80,826,366	23,066,955	31,473,998
2348R3	85,961,696	85,960,962	22,051,303	33,204,848
2348S1	74,004,136	73,976,446	20,261,582	27,432,461
2348S2	74,728,248	77,698,816	20,980,165	28,246,990
2348S3	86,749,408	86,748,802	23,415,367	34,393,918